December 2015

INDOOR ENVIRONMENTAL QUALITY (IEQ) AND BUILDING ENERGY OPTIMIZATION THROUGH MODEL PREDICTIVE CONTROL (MPC)

Korbaga Fantu Woldekidan
Syracuse University

ABSTRACT

This dissertation aims at developing a novel and systematic approach to apply Model Predictive Control (MPC) to improve energy efficiency and indoor environmental quality in office buildings. Model predictive control is one of the advanced optimal control approaches that use models to predict the behavior of the process beyond the current time to optimize the system operation at the present time. In building system, MPC helps to exploit buildings' thermal storage capacity and to use the information on future disturbances like weather and internal heat gains to estimate optimal control inputs ahead of time.

In this research the major challenges of applying MPC to building systems are addressed. A systematic framework has been developed for ease of implementation. New methods are proposed to develop simple and yet reasonably accurate models that can minimize the MPC development effort as well as computational time.

The developed MPC is used to control a detailed building model represented by whole building performance simulation tool, EnergyPlus. A co-simulation strategy is used to communicate the MPC control developed in Matlab platform with the case building model in EnergyPlus. The co-simulation tool used (MLE+) also has the ability to talk to actual building management systems that support the BACnet communication protocol which makes it easy to implement the developed MPC control in actual buildings.

A building that features an integrated lighting and window control and HVAC system with a dedicated outdoor air system and ceiling radiant panels was used as a case

building. Though this study is specifically focused on the case building, the framework developed can be applied to any building type.

The performance of the developed MPC was compared against a baseline control strategy using Proportional Integral and Derivative (PID) control. Various conventional and advanced thermal comfort as well as ventilation strategies were considered for the comparison. These include thermal comfort control based on ASHRAE comfort zone (based on temperature and relative humidity) and Predicted Mean Vote (PMV) and ventilation control based on ASHRAE 62.1 and Demand Control Ventilation (DCV). The building energy consumption was also evaluated with and without integrated lighting and window blind control. The simulation results revealed better performance of MPC both in terms of energy savings as well as maintaining acceptable indoor environmental quality. Energy saving as high as 48% was possible using MPC with integrated lighting and window blind control.

A new critical contaminant - based demand control ventilation strategy was also developed to ensure acceptable or higher indoor air quality. Common indoor and outdoor contaminants were considered in the study and the method resulted in superior performance especially for buildings with strong indoor or outdoor contaminant sources compared to conventional CO_2 - based demand control ventilation which only monitors CO_2 to vary the minimum outdoor air ventilation rate.

INDOOR ENVIRONMENTAL QUALITY (IEQ) AND BUILDING ENERGY OPTIMIZATION THROUGH MODEL PREDICTIVE CONTROL (MPC)

by
Korbaga Woldekidan

B.Sc., BahirDar University, 2001
M.Sc., Addis Ababa University, 2004

Dissertation
Submitted in partial fulfillment of the requirements for the degree of
Doctor of Philosophy in Mechanical and Aerospace Engineering
in the Graduate School of Syracuse University

December 2015

AKNOWLEDGEMENTS

First of all I would like to thank my almighty God for giving me the health and courage to finish this long journey.

I want to use this opportunity to express my sincere gratitude to my advisor Prof. Jianshun Zhang for the continuous support of my PhD study and related research, for his patience, motivation, and immense knowledge. His guidance helped me in all the time of research and writing of this thesis. I could not have imagined having a better advisor and mentor for my PhD study. And also I would like to thank my dissertation committee members and faculty in the Department of Mechanical and Aerospace Engineering.

A special thanks to my family. Your prayer was what sustained me thus far. I would also like to thank all my friends especially the Ethiopian community in Syracuse. You make life far from home much easier.

At last but not least, I would like to thank my wife Selam and my boys Biruk and Christian. You are the love of my life and having you by my side is the reason for my success and I love you so much.

TABLE OF CONTENTS

LIST OF TABLES

LIST OF FIGURES

1 INTRODUCTION

1.1 Background and Problem Definition

Overall, buildings account for 41 percent of all primary energy consumption in U.S. and are responsible for nearly 40% of greenhouse gas emissions (USDOE 2011). In commercial buildings, HVAC systems account for 43% of the primary energy use followed by lighting which accounts for 14% (USDOE 2011). The above figures are clear indications of the energy intensiveness of building systems and the associated savings possible from improvement of the building HVAC and lighting systems.

Various energy - saving measures can be taken to reduce energy consumption both during design and operation phases of a building system. Some of the measures include architectural considerations, construction type and material selection, use of onsite renewable energy resources, use of more energy - efficient equipment and making the operation of the equipment more efficient through advanced maintenance and control strategies. The focus of this dissertation is to investigate advanced control strategies that can handle the multi - variable nature of the various interacting HVAC and lighting systems.

Buildings consist of numerous dynamically interacting components that are nonlinear and complex. The potential energy savings from advanced building control systems relies on better manipulation and control of these components. To help automatic condition monitoring and better control of these components, most modern buildings are equipped with Building automation system (BAS). BAS is equipped with sensors deployed in various section of the building to enable building operators to have better

control and performance monitoring of the various systems including HVAC, lighting and water system.

For complex systems like HVAC that consist of various subsystems with diverse dynamic response characteristics at various time-scales, a hierarchical control approach is recommended ((G.Dieck-Assad, 1987), (R.Garduno-Ramirez, 2001)). A Hierarchical control strategy involves an outermost supervisory control layer which assigns the set-points for the plant operation parameters such as which component should operate (on/off states) and at what conditions it must operate (temperatures, pressures, mass flow rates, power levels, etc.). The inner layer, consisting of component - level feedback controllers, will try to achieve these set-points by adjusting underlying actuators such as control valves, compressors and pumps.

In a conventional control system, the supervisory-level controllers that comprises a group of logics are used to take actions based on the preset conditions and/or rules, or the commands from the operators while local controllers which are sets of PID and simple on-off controllers are used to track set points form supervisory controllers. These conventional controllers don't consider the interactions between different system and subsystems and also they don't have a means to automatically respond to building dynamics resulted from changes in weather condition, internal load schedule, IAQ requirements and the like. This inability can create thermal discomfort during transient periods and also compromise system efficiency.

Intelligent buildings information obtained from BAS can be used to get optimal control variables both in the supervisory and local control level. These optimal control variables can be communicated to the actual physical systems through direct digital controls (DDC). In this regard, a common communication protocol called Building Automation and Control Network (BACnet) that can be used by various DDC

controllers from different vendors. BACnet creates a capability to read/write data and commands from a single platform without using proprietary codes of each manufacturer.

Thanks to availability of sensors and processing advancement of computers, the dynamics of the building can be modeled and predicted in a good accuracy and can be used to help optimal controllers to take a smart decision. In this regard Model predictive controllers (MPC) show superior performance compared to other conventional controllers and can be used for building HVAC and lighting control system. In the past decades, various studies have been done to implement MPC in building systems. But most of the implementations have been based on very simplified building models and they are more of proof - of - concepts than actual evaluation of the strategy.

In this dissertation a more detailed MPC is developed and its advantages for various building control strategies are investigated. To decrease computational time that could result from the non-linearity of the various systems and components involved, simplified and yet sufficiently accurate models are developed to capture the dynamics of the building envelope as well as the HVAC system. The case building is represented by its detailed physical model developed in EnergyPlus simulation software and a co-simulation strategy is used to integrate the MPC with the building model developed in EnergyPlus. MLE+ (Willy et al. 2012), an open source Matlab/Simulink tool box is used for co-simulation. MLE+ can also be used for actual implementation of the MPC in the real building using its capability to communicate with actual control points in the Building Management System (BMS) through BACnet.

1.2 Objectives

The ultimate objective of this dissertation is to develop a whole - building MPC that can minimize energy consumption while maintaining acceptable indoor air quality and comfort conditions.

Specific objectives of the project include:

- Identify major influencing parameters and develop a reduced - order building and HVAC component models that can predict state variables in a reasonable accuracy with less computation time for model predictive controller;
- Develop a method for MPC controller that considers thermal, lighting and pollution load dynamics.
- Estimate the potential benefits of using MPC for building control compared to conventional control systems using detailed EnergyPlus Model.

1.3 Research Methodology

The following methods are implemented in the course of the research to achieve the objectives mentioned.

- Model development and parameter identification: simplified models are used for the MPC and corresponding model parameters are identified using trended data measured from the case building.
- Detailed simulation model development: EnergyPlus model is developed as a virtual test bed to check performance of MPC prior to implementation in the actual building.

- MPC development and co-simulation: The MPC controller is developed based on simplified and yet sufficiently accurate models in MATLAB environment and a co-simulation tool, MLE+, is used to communicate with EnergyPlus. The co-simulation strategy enables communication between controller and the building at each time step and creates a feedback loop for the controller.
- Evaluation of the control strategy: The benefit of the developed advanced controller is compared against baseline buildings according to ASHRAE recommendations. Combination of various control strategies are investigated.

1.4 Dissertation Outline

This dissertation is organized in seven chapters. The remaining chapters are summarized below.

Chapter 2: Literature Review: Intensive literature review is made in building envelope and Indoor Environmental Quality (IEQ) modeling, model - based control methods and model predictive control (MPC).

Chapter 3: A Framework for Model Predictive Control for Building Environmental Systems: This chapter introduces implementation of MPC in an intelligent building. Optimization methods used and case building specific objective and constraint functions are discussed in detail. Finally techniques used for implementation of the MPC in real building as well as in virtual building (Using detailed EnergyPlus Model) are discussed.

Chapter 4: Component Models for MPC: The models used in MPC are discussed in detail in this chapter. The components discussed are specific to the case building which is using an HVAC system that has a dedicated outdoor air HVAC system and

radiant ceiling panels. Methods are also developed to simplify the building envelope model. Simplified parametric equations that can be used to estimate effect of solar radiation on building heat and lighting gain are also developed.

Chapter 5: Evaluation of MPC: Comparison of various control strategies with their MPC versions are given in this chapter. It shows the potential benefit of MPC compared to conventional control systems.

Chapter 6: A Novel Energy - Efficient Demand - Based Ventilation System for critical contaminant and overall IAQ control: a new demand - controlled ventilation strategy based on the critical contaminant is developed and its performance is evaluated compared to conventional control strategies.

Chapter 7: Conclusion and Discussion: This chapter summarizes the major findings of the research as well as recommendations for future related works.

2 LITRATURE REVIEW

The impacts of energy consumption and CO_2 emission in the building environment is forcing governments to give more attention to strategies that enable building systems to operate in an energy - efficient manner and ultimately save energy and reduce associated emissions. From time to time, more and more strict rules are in place that have to be considered by building designers and operators during various phases of the building from site selection to final building operation to reduce building energy use. Among them rules set by ASHRAE 90.1 and European Energy Performance of Buildings Directive (EPBD) are worth mentioning.

For the past three decades, a wide variety of approaches have been developed for improving energy efficiency in buildings. In recent years, Model Predictive Control (MPC) strategy for building HVAC system is getting increasing attention. Development and integration of HVAC system MPC requires thorough understanding of the HVAC system working principles, interactions of the building envelope to the surrounding environment both internally and externally as well as thermal comfort and IEQ requirements.

The literature review section introduces the different approaches used for modelling different systems involved in the MPC and discusses the researches done in optimal controllers in general and MPC in particular. Finally a summary of the literature review findings is given emphasizing on the research gaps in the area.

2.1 Building Envelope System

Building envelope system separates and protects the indoor environment of the building from the outdoor environment and the building dynamics is greatly affected by it. The accuracy of the models used for building envelope highly affect the

performance of the model-based control system. Various approaches exist to model building envelope systems. The heat balance method (HBM) is the standard ASHARE load calculation method (ASHRAE 2009) in which system of equations that include zone air heat balance and a set of outside and inside heat balances at each surface are solved simultaneously at each time step. Another method for load calculation is Radiant Time Series (RTS) method (Spittler, Fisher, and Pedersen 1997) which is a simplified version of HBM where the energy storage and release in the zone is approximated by a predetermined zone response called Radiant Time Factors (RTFs). RTS method effectively replaces all other simplified non heat balance methods such as cooling load temperature difference, solar cooling load, cooling load factor method (CLTD,SCL,CLF), the transfer function method (TFM) and the total equivalent temperature difference/time averaging method (TETD/TA). In both methods, simplifying assumptions are made in solving wall heat conduction problems:

- Heat conduction is assumed to be one dimensional. Two dimensional effects due to corners and non-uniform boundary conditions are ignored.
- Materials are assumed to be homogeneous and have constant thermal properties.

Based on the above assumptions, the governing equations of conductive heat transfer problems can be given by diffusion and Fourier equations as

$$\frac{\partial^2 T(x,\tau)}{\partial x^2} = \frac{1}{\alpha}\frac{\partial T(x,t)}{\partial t} \qquad 1$$

$$q'' = -K\frac{\partial T(x,\tau)}{\partial x} \qquad 2$$

Where q'' is heat flux (w/m^2), T is temperature (K), K is thermal conductivity (W/m^{2}K), t is time (sec), x is thickness (m) and α is thermal diffusivity (m^2/s).

Although the above transient problem can be solved analytically, the problem gets complicated when it involves multilayered constructions and numerical methods are advocated in such instances. Different numerical solutions exist in literature which include lumped parameter methods, frequency response method, finite difference/finite element methods and Z transform methods (McQuiston, Parker, and Spittler 2000).

The rate of change of zone air temperature, humidity and pollutant concentration can be given by the following differential equations that account for the different sources and sinks:

$$C_a\dot{T} = Q_{vent} + Q_{wall} + Q_{opaque} + Q_{window} + Q_{internal} + Q_{inf} \quad (3)$$

$$\rho V_r \frac{dw_r}{dt} = \dot{m}_{sys}(w_{sys} - w_r) + \dot{m}_{inf}(w_o - w_r) + \frac{q_l}{h_{fg}} \quad (4)$$

$$\frac{dC}{dt} = \frac{\dot{V}_{sys}(C_{sys} - C_r)}{V_r} + \frac{\dot{V}_{inf}C_o}{V_r} + S_r - k_d \quad (5)$$

where C_a is air capacitance (kJ/K), T is room temperature (K), Q is heat lost/gain (kW), V is volume(m^3), w is humidity ratio (kg of water/kg of air), $\dot{m}$ is mass flow rate (kg/s), $\dot{V}$ is volumetric flow rate (m^3/s), q_l is zone latent heat gain (kW), h_{fg} is heat of vaporization for water (kJ/kg), C is contaminant concentration (kg/m^3), S is contaminant generation(kg/m^{3}s) , k_d is contaminant decay rate (kg/m^{3}s) and the subscripts *vent* is mechanical ventilation, *wall* is external and partition walls, *opaque*

is opaque surfaces other than walls, *internal* is internal heat sources, *inf* is infiltration, *r* is room and *sys* is HVAC system.

2.2 Indoor Environmental Quality (IEQ)

According to Center of Disease Control and Prevention (CDC), IEQ is defined as "the quality of a building's environment in relation to health and wellbeing of those who occupy space within it." The topic of IEQ is getting more attention recently after various researchers showed the relation between IEQ, human health and performance. The major factors affecting IEQ are air quality, thermal condition, acoustic condition and visual condition ((Wong, Mui, and Hui 2008) (Lai and Yik 2009)). Various researchers attempted to quantify the relation between each factor and overall occupant thermal comfort. In this regard Frontczak and Wargocki (Frontczak and Wargocki 2011) did comprehensive literature review and came up with a summary as shown in Figure 1 which gives quantification by various researchers. The allowable range of these IEQ factors are discussed in the following sections.

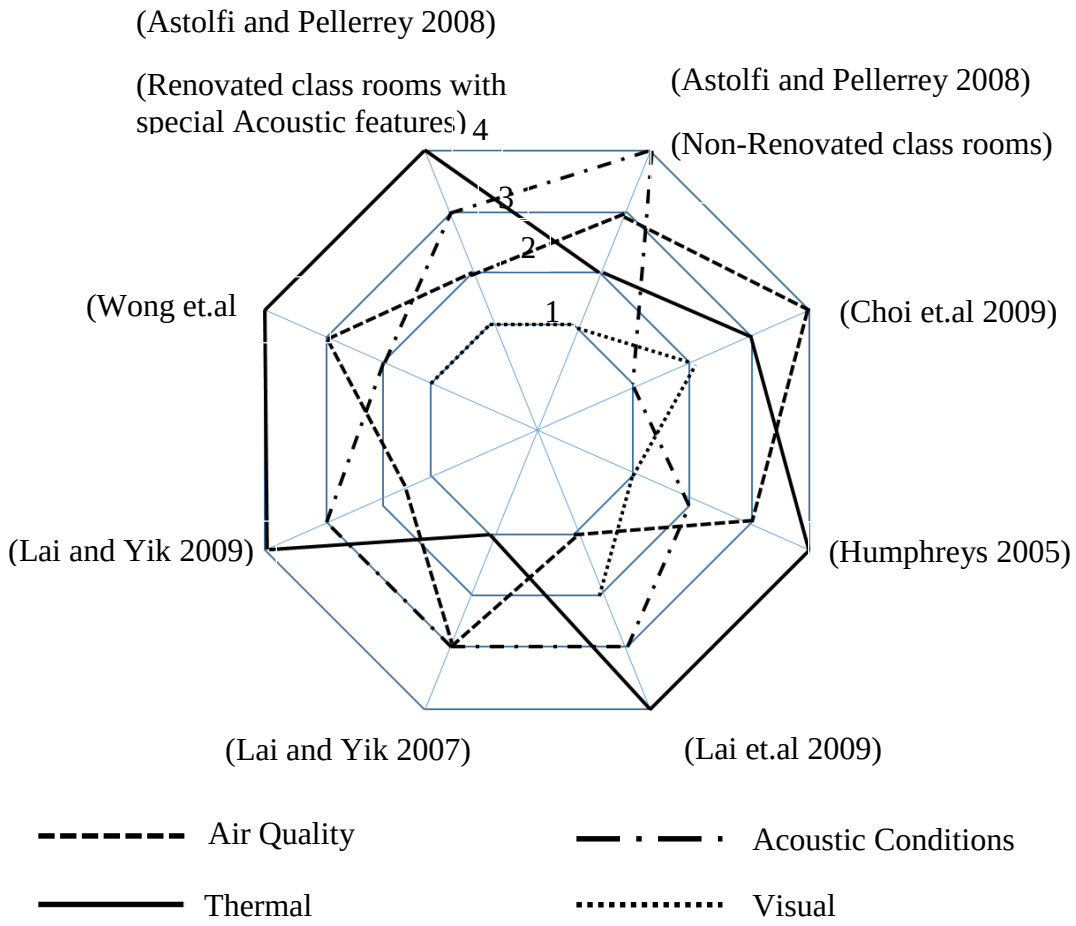

Figure 1: Ranking of effect of IEQ factors on overall occupant satisfaction according to previous researchers. (Higher number indicates higher ranking) [source: (Frontczak and Wargocki 2011)]

2.2.1 Air Quality

A precise definition of air quality is subjective and based on ASHRAE it can be defined as "air in which there are no known contaminants at harmful concentrations as determined by cognizant authorities and with which a substantial majority (80% or more) of the people exposed do not express dissatisfaction"(ASHRAE Standard 62.1 2007). In a real environment, several pollutants co-exist. Various studies have shown associations between indoor air quality and human performance in addition to the potential health risk due to poor air quality. Research by Fisk (Fisk 2002) estimated

the potential gain of productivity from improved indoor air quality to be between 20 to 160 Billion Dollars in US considering only office workers. To achieve acceptable IAQ, combinations of the following actions are essential: contaminant source control, proper ventilation, humidity management and adequate filtration. Source control of contaminants can be achieved by either reducing the possible source of the contaminant in the building or by filtering the incoming air to the building. Regarding proper ventilation various strategies have been implemented in the past several years. ASHRAE 62.1 sets the minimum ventilation rate needed for buildings during occupied hours. In the ASHRAE 62.1 2004 version, determination of minimum outdoor ventilation rate is changed to be based on both occupancy level and floor area from its previous version that sets minimum outdoor ventilation rate based on either occupancy or floor area.

Most traditional ventilation systems provide fixed minimum outdoor ventilation rate based on design occupancy level and this could result in loss of energy or discomfort when the building operates in off - design conditions. A more advanced control strategy called Demand Controlled Ventilation (DCV) varies ventilation rate based on occupancy. Various researchers showed superiority of DCV over conventional strategy.((Emmerich, Mitchell, and Beckman 1994), (N. Nassif 2011) (S. Wang and Xu 2002), (Josephine and Xingbin Lin 2011)). Most DCV systems use indoor CO_2 concentration level as a means to control ventilation rate due to its direct association with presence of occupants. Even though CO_2 as a pollutant is not that hazardous except at very elevated concentration (5000 ppm), studies suggested that indoor concentration of 700 ppm above outdoor CO_2 concentration is believed to create unacceptable level of human body odor and is used as the permissible CO2 limit according to ASHRAE62.1.

Some of the commonly available indoor air contaminants with their acceptable indoor concentration are given in Table 1

Table 1: Properties of common indoor air contaminants

	Indoor Generation Rate	Permissible Indoor Concentration	Deposit Rate
CO_2	$\frac{0.0028 * A_D * M * RQ}{0.23 * RQ + 0.77}$ (l/sec/person)[1]	700 ppm[3][6]	0
Formaldehyde	61 μg/hr.m² [2]	0.027 ppm[4]	0
Toluene	36 μg/hr.m² [2]	0.07 ppm[5]	0
PM2.5	0	35 μg/m³	0.2 (hr^{-1})[7]

[1](ASHRAE-Fundamental, 2005) [2] (EPA-BASE, 2006) [3] (ASHRAE-62.1:2004) [4] (ASHRAE ADDENDA: 62.1-2004, 2006) [5] (OEHHA, 1999)
[6] 700 ppm is concentration difference between indoor and outdoor CO_2 concentration
[7] (Henderson, Milford, and Miller 2005)

Where A_D is Dubies Body surface area (m^2), M is metric of metabolic rate, RQ is respiration quotient (0.83 for an adult engaged in a light activity)

2.2.2 Thermal Conditions

As previously shown in Figure 1, most researchers agree that thermal comfort has a great influence on the productivity and satisfaction of indoor building occupants. The majority of heating, ventilation and air conditioning systems for thermal comfort are based either on a single temperature control loop or, in some cases, on a temperature and relative humidity control loop. However, thermal comfort is a more complex concept and more parameters are needed to provide thermal satisfaction to occupants.

Many researchers tried to develop different models and indices to quantify thermal comfort. Some of the models and indices include comfort model according to ISO7730 (ISO 7730 2005), ASHRAE winter and summer comfort zones, PMV-PPD (predicted mean vote-Predicted percentage dissatisfied) model and Two-Node model (ASHRAE 2009).

2.2.3 Visual Conditions

Visual condition is described by parameters such as luminance distribution, illuminance level, glare, color of light etc. Illuminating Engineering Society of North America (IESNA) recommends different illuminance level depending on the purpose of the building. For typical office 300-500 lux is recommended at working height of 0.8m. Lighting is usually provided to a building system through electric lighting and solar illuminance. These two sources of lighting also affect the cooling/heating pattern of the HVAC system because of the associated thermal load with them. In the past decades different researches have been conducted to provide lighting in optimal way so that the associated thermal load to HVAC systems is minimum while providing the required illuminance level. The researchers include from application of simple shading device to use of more advanced windows like nematic curvilinear aligned phase (NCAP) where it is possible to get variable solar transmission and reflection through a voltage controlled scattering mechanism (Van Konynenburg, Marsland, and McCoy 1989). Recently more modern buildings are starting to use integrated automatic window blinds and couple of researchers tried to come up with optimal control of the blind angle and electric lighting ((Reinhart 2004), (LaVerne and Gregory D.Salhoff 1998), (Tzempelikos and Athienitis 2007),(Biao Sun et al. 2013)).

2.3 Model Based Control

Traditional building control systems are typically designed with the sole objective of meeting the thermal demands. Such controllers include simple on-off and Proportional-Integral-Derivative (PID) controllers. These controllers are readily available, simple and easy to implement but they have the following limitations (Chandan 2010):

- Non-Optimality: the primary target is to meet set point conditions and these controller don't respond to energy efficiency requirements with changing working conditions.
- Control interface: these controllers don't have a means to communicate between each other and the decision of one controller can affect the other which often compromise energy efficiency and life time of components involved.
- Instability: Since local controllers guarantees only the stability of the corresponding subsystem, there is a possibility that the overall system can run to instability. Extensive tuning is needed to determine parameters under which the system is stable.

The above inherent problems of traditional controllers invoke the use of model - based/optimal control system in areas involving many local controllers like building systems. Model - based control problems include a cost function and differential equations/models describing the path of the control variables that minimize the cost function. The history of model - based controllers can be traced back to end of 1970s in the process industries (Richalet et al. 1978). In the building sector, many of the efforts related to control were focused on local controllers((Goswami 1986); (Rishel 2003); (Moore and Fisher 2003) etc.) until recently where growing energy consumptions and associated costs evoked the building professionals to pay more attention to integerated optimal control systems. In the last two decades more research on model - based control for building system has been done thanks to growing scale of BAS and availability of data from the BAS.

The models used for model - based controllers can be broadly classified as physical model, gray box model and Black box model. Physical model - based approach uses sets of quantitative mathematical relationships based on governing physical principles or sets of qualitative relationships derived from knowledge of underlying physics. When modelled accurately, physical model - based approach gives the most accurate result. The drawbacks of this approach are: it is computationally expensive; it requires many inputs; some of the inputs might not be readily available and it need significant development effort (Katipamula and Brambley 2005). In black box models, relationships are established between input and output data without any prior knowledge of the system operating mechanism. The accuracy of black box model highly depend of the richness of the training data to represent the entire working range of the system. Though simple, black box models need a large set of trended data to drive the input - output relationship and no extrapolation is allowed outside the training data. Grey box model is a combination of simplified physical model and black box model where unknown parameters of the model are estimated using system identification based on experimental/measured data. In general these models have a simple form and have a great potential to use in online control applications (Katipamula and Brambley 2005). Based on literature review summary on advanced controller design for building system by Yu (Yu 2012), among the paper published from 1991 to 2005 , 36% are first principle physical model - based, 15% are black box model - based , 42% are grey box model - based while 7% are model free. Some of the research papers reviewed in optimal control are summarized below.

Nassief et al. (Nabil Nassif, Kajl, and Sabourin 2005) presented amodel - based optimal control of VAV air conditioning system. In this research, a simplified optimization process for assigning set points based on VAV model and monitored

data was proposed and evaluated. The considered set points were supply air temperature, supply duct static pressure and chilled water temperature. The research showed that 16.2% saving was possible compared to the existing rule based control strategy.

Chaw et al. (Chow et al. 2002) developed optimal control strategy for absorption chiller system. Neural network (black box model) was used for modeling the chiller while genetic algorithm was used to find global optimum operation point. A system based approach which include the chiller and the building system and their associated variables is used. Chilled water and cold water flow rate were considered as control variables. Three optimal control strategies were considered in the study: case-1: constant chilled and cooling flow rates; case-2: variable cooling flow rate and constant chilled water flow rate and case-3: variable chilled and cold water flow rate. The results of these cases were compared with the bench mark .i.e. operation based on nominal values. The results show that there is a considerable saving in all the three cases with case - 3 excelling the first two due to the fact that there is more flexibility for the control variables. Compared to the bench mark, there was 14.2% saving using case - 2 and 19.2% saving using case - 3.

Wang and Jin (S. Wang and Jin 2000) used grey box mode to develop optimal control for VAV air conditioning system. The control strategy was based on the response of the entire system for changes in control variables. Recursive least square (RLS) technique was used for parameter identification of the grey box model while genetic algorithm was used for solving the nonlinear optimization problem. TRNSYS was used as a platform for dynamic simulation of the building and the control system. The optimal control results were compared against the base line condition in which Air handling Unit (AHU) temperature set-point, outdoor ventilation rate set-point and

chilled water temperature set-point were set to be constant. The simulation was performed for sunny and cloudy summer and winter conditions and the results showed that besides improvement in thermal comfort there was an energy saving of up to 25 % (sunny winter days)

In summary apart from considerable effort needed for model development, model - based controllers have superior performance compared to conventional controllers both in terms of energy saving and providing thermal comfort. Though the choice of the model to be used depends on the complexity of the system and information availability, grey box models tends to be a good choice for building system.

2.4 Model-Based Predictive Control

Model - based predictive control is an advanced type of model - based control where at each sampling time, starting at the current state, an open-loop optimal control problem is solved over a finite horizon. The ability to handle hard constraints on control and state variables simply and effectively makes MPC one of the control strategies that have a substantial impact in industrial control problems (D.Q.Mayne 2001). In general MPC involves three basic elements: Process and disturbance model; Optimization and application of Receding horizon principle. Process and disturbance models help to predict the behavior of the future output of the process on the basis of control inputs and disturbances applied to the process. Beside they also help to calculate input signals to the process that can minimize the objective function.

The third element of MPC is the Receding horizon principle. After computation of the optimal control sequence, only the first control sample will be implemented and subsequently the horizon is shifted one sample step forward and the optimization is repeated with the new information from measurements.

Because of the ability of MPC to integrate weather forecast, occupancy information and utility price variation in determining optimal operation, it is getting more attention in building control system. In the last decades there have been several attempts made to utilize MPC in HVAC system. Yahioui et al. (Yahiaoui et al. 2006) developed an MPC strategy for operation of building cooling system. In the research runtime MPC control strategy is developed using a TCP/IP communication protocol to integrate controller designed in Matlab/Simulink environment and building model developed in ESP-r simulation software. The result showed a 20% energy saving and 9.97 percent improvement in Coefficient of performance compared to baseline operating condition in which the plant is operated manually by using the policy defined by the plant manager based on operators' experience.

Anthony et al. (Anthony and Francesco 2011) used bilinear model predictive control to optimize operation of HVAC system for a five zone building. The HVAC system considered was a variable air volume (VAV) with reheat. Zone air mass flow rate, zone supply air temperature, outdoor air damper opening and air temperature leaving cooling coil were considered as control variables. The first order energy balance that gives zone temperature dynamics was discretized using trapezoidal method. Sequential quadratic programming was used to solve the non-convex optimization problem which was resulted due to nonlinear constraints. The control performance of the MPC developed was able to exhibit aspects of heuristic HVAC control such as economizer control, supply temperature reset, demand response, precooling and load shifting.

Yuan et al. (Yuan and Perez 2006) demonstrated performance of MPC for multiple zone ventilation and temperature control. The research focused on addressing the issue of poor indoor air quality (IAQ) due to over ventilation and/or under ventilation

associated with conventional ventilation control schemes. The research considered a single duct variable air volume (VAV) system for the case study. The MPC generates optimized control inputs for zone air flow, zone reheat and AHU supply temperature set point. ASHRAE 62.1 ventilation requirement was used as a constraint during the optimization process. The case building was simulated for four different weather conditions and the result showed that the IAQ was maintained in all the cases and the study recommended MPC to be a good candidate for ventilation and temperature control of multi-zone buildings.

Gruber et al. (Gruber, Gwerder, and Tödtli 2001) developed predictive control for building heating application with the objective of providing optimal hot water temperature. A Prediction horizon of three days was used and the algorithm computes new set point values every 20 minutes. A linearized room model is used in the controller model while weather data of the previous 24 hours is used to replace forecast for the coming 24hours. The controller was tested with simulation using historical data before implemented in a field test. Though the paper doesn't mention the actual benefit compared to conventional one, it stated that it was at least as good as a very well-tuned conventional controller.

Chen (Chen 2002) compared advantage of using generalized predictive control (GPC) over the conventional controllers, PID and Bang-Bang controllers for floor radiant heating system of a full-scale out door test room. Recursive least square algorithm was implemented for parameter identification of the full scale room. The research compared the three control approaches based on tuning effort, response speed, offset band, on-off cycling and requirement of system identification. The results demonstrated that the behavior of GPC was superior to the other two in every aspect except that it requires system identification.

Fierie et al.(Freire, Oliveira, and Mendes 2008) applied MPC for building indoor thermal comfort control problem. The model used a simplified model to represent heating and/or cooling from HVAC system. The controller is checked for thermal comfort based predicted mean vote (PMV) (nonlinear model) and comfort zone defined by a psychometric chart (linear model). The study also compared the performance of the controller by first considering optimization of thermal comfort alone and later including energy consumption minimization in addition to thermal comfort. PMV approach showed a better performance in terms of thermal comfort and energy consumption due to its ability to adapt to individual parameters.

Mahdavi (Mahdavi 2008) developed predictive simulation based lighting and shading control for a building. The controller make use of real-time sensing and lighting simulation. Position of window blind and status of the luminaires were used as control variables. Parametric equations were developed based on experiments to relate lighting gain and illuminance level at reference points located at different locations inside the building. The model - based control evaluates set of candidate control states based on lighting simulation which resulted in values for pertinent performance indicators. The research claimed that the calibrated models can be used as virtual sensors and also help to monitor values that are not possible to measure by physical sensors like glare indices.

2.5 Summary of Literature Review

Building systems in general are a complicated where interaction between various subsystems exist in various levels. The different efforts done in optimization of different subsystems showed performance improvement. It is also evident that there is still a big room for performance improvement. Though the papers discussed above

touched most of the sensitive areas in building system, below are list of things that are not well addressed so far.

- Most of the researchers used first principle based building models which are suitable for single zone and simple geometry buildings, but are difficult to apply in real buildings, which typically have multiple zones and irregular shapes. On the other hand developing detailed model may require high level mathematical skill and high computation cost which may not be viable for building control operation. Thus an intermediate solution is needed that can close the gap between the two extremes (simplified and detailed modeling approaches).
- The interactions between solar radiation and building system have considerable impact on the building HVAC system operation. Most of the researchers so far used either experimental value for the test case or assumed heat load due to solar gains which is not practical in real predictive control development. The heat transfer mechanism of solar radiation into a building system is complex, and a systematic approach is needed so that it can be implemented in actual building control system.
- The ventilation strategies used to improve indoor air quality so far doesn't consider presence of multiple contaminants. The most recent energy - efficient ventilation strategy, i.e. demand - based controlled ventilation (DCV) changes ventilation rate based on indoor CO_2 level. This could result in poor indoor air quality in cases where there is strong contaminant source of indoor or outdoor origin. Thus a new control strategy that considers other critical contaminants is needed.

- Maintaining acceptable illuminance level at a reference plane involves determination of illuminance from solar radiation and electric lighting at the reference plane. This requires complex analysis which is a function of building geometry, position of the source window and electric lighting relative to the reference plane. In addition, visible transmittance of window materials is a function of solar incident angle and sky clearness which involves tracking of the sun throughout the day. This complex analysis is not convenient for control purpose due to the fact that it needs considerable development effort. Thus simplified models that can be easy to implement in optimal control algorithms are needed.

3 A FRAMEWORK FOR MODEL PREDICTIVE CONTROL OF BUILDING ENVIROMENTAL SYSTEMS

According to Intelligent building institute (IBI) of US, An Intelligent building is defined as" *one that provides a productive and cost effective environment through optimization of its four basic components: structure, systems, services and management and the interrelationships between them*". With technology rapidly changing, the efforts towards the goal of intelligent building are supported by use of digital computers for diagnostic and control, advanced actuators and sensors for accurate sensing and controlling, and use of distributed network for better communication and integration of systems. Intelligent Buildings take advantage of these technological advancements for devising mechanisms to operate the building in its most optimal condition. Availability of building automation systems in most modern buildings pave the way of developing efficient modern control strategies

As previously stated in the introduction section, traditional controllers like PID and simple on off controllers doesn't consider building dynamics and are not smart enough to consider interaction of different components supporting the building system. This deprive the building system the chance to save energy and in extreme cases, it can create discomfort conditions especially during transient periods where there are drastic changes in indoor or outdoor conditions.

In a complex system like building where there are different systems and subsystems interacting, an integrated approach should be taken both during design and operation phase so that the building meets its objective of providing better working environment with minimum energy and maintenance cost. One of the integral approaches that secure better environment control with less energy consumption is use of a model -

based optimal controller. In this research, a model - based predictive control strategy is used to find optimum set points for the HVAC and lighting system operation.

3.1 Model Predictive Control

Model-based Predictive Control (MPC) is an advanced method of process control which relies on dynamic model of the process. Control design method based on MPC is getting more and more popular in most industries and it is also an active area of research. One of the reason behind its popularity is its ability to yield high performance without human intervention for a long period of time (Carols E., David M., and Manfred 1989). MPC controller design involves the following three basic elements. Even if MPC can have different forms depending on the type of the process that needs to be controlled, all MPC controllers have the following common features:

Process/Prediction model:

The core of MPC is the process model which is used to predict how the process changes over time when it interacts with the internal and external disturbances. These models helps to evaluate the system response for different control inputs and decide the best combination of control inputs that gives optimal performance. The performance of MPC highly depends on how close these models predict the actual process.

The process model can be given in a general form using Equation 6 as

$$\boldsymbol{x(k+1) = g(x(k), y(k), u(k), d(k))} \qquad \mathbf{6}$$

where x(k) is the state variable, u(k) is the control input signal , d(k) is a vector containing all known signals ,such as the reference signal and known (or measurable) disturbances, y(k) is the measurement and k represent current time step. For a

multiple input multiple output (MIMO) system each one of the above parameters represent a vector of inputs and outputs. Given a predicted input sequence, the corresponding sequence of the state predictions is generated by simulating the model forward over the prediction horizon of N sampling intervals. These predicted sequences can be stacked into vectors as:

$$\mathrm{u}_k = \begin{bmatrix} u(k|k) \\ u(k+1|k \\ . \\ . \\ . \\ u(k+N-1|k) \end{bmatrix} \qquad \mathrm{x}_k = \begin{bmatrix} x(k|k) \\ x(k+1|k) \\ . \\ . \\ . \\ x(k+N-1|k) \end{bmatrix}$$

Where *u(k+i|k)* and *x(k+i|k)* denote input and state vectors at time *k+i* that are predicted at time *k*, and *x(k+i|k)* are state variables that evolve according to the model defined in Equation 6 with initial condition at the beginning of the prediction horizon defined as *x(k|k)=x(k).*

Optimization:

The optimization problem associated with the process model discussed above can be represented by a cost function in a discretized form as (Camacho and Bordons 2003):

$$\boldsymbol{J(k)} = \sum_{\boldsymbol{i=0}}^{\boldsymbol{N}} \boldsymbol{\varphi}\big(\boldsymbol{x(k+i|k)}, \boldsymbol{y(k+i|k)}, \boldsymbol{u(k+i|k)}, \boldsymbol{d(k+i|k)}\big) \qquad \mathbf{7}$$

Subjected to

$$\boldsymbol{x^L} \leq \boldsymbol{x(k)} \leq \boldsymbol{x^u} \qquad \mathbf{8}$$

$$\boldsymbol{y^L} \leq \boldsymbol{y(k)} \leq \boldsymbol{y^u} \qquad \mathbf{9}$$

$$\boldsymbol{u^L} \leq \boldsymbol{y(k)} \leq \boldsymbol{y^u} \qquad \mathbf{10}$$

$$\boldsymbol{x(k_o)} = \mathbf{X_o} \qquad \mathbf{11}$$

Where φ is the cost function, X_o is vector of initial state variables, X_f is vector of final state variables, N is prediction horizon, and superscripts l and u stands for lower and upper limit

Receding horizon principle: Predictive control uses the so-called receding horizon principle. At each time step k of the optimization process, optimal control input sequence $u^*(k) = \{u(k|k), u(k|k+1), \ldots\ldots u(k+N-1|k)\}$ is computed based on the governing principles defined by the component models of the MPC controller and only the first element of the input sequence, $u^*(k) = u(k|k)$ is executed while the remaining elements of the sequence are discarded. Once the y (k+1) values are known, the prediction horizon will be shifted by one time step and the entire process will be repeated to find the new sets of control inputs, $u^*(k+1) = \{u(k+1|k+1), \ldots\ldots u(k+N-1|k+1)\}$ and again only the first control input, $u^*(k+1) = u(k+1|k+1)$ will be executed while the remaining are discarded. This process will be repeated throughout the optimization process. The prediction horizon remains the same length despite the repetition of the optimization at future time instants. The strategy of shifting the prediction horizon is what is termed as receding horizon principle and it is shown in Figure 2. At each time step (k), known values of state and output variables from the previous time step (k-1) are used and this procedure introduces feedback into the MPC law, thus providing a degree of robustness to modeling errors and uncertainty.

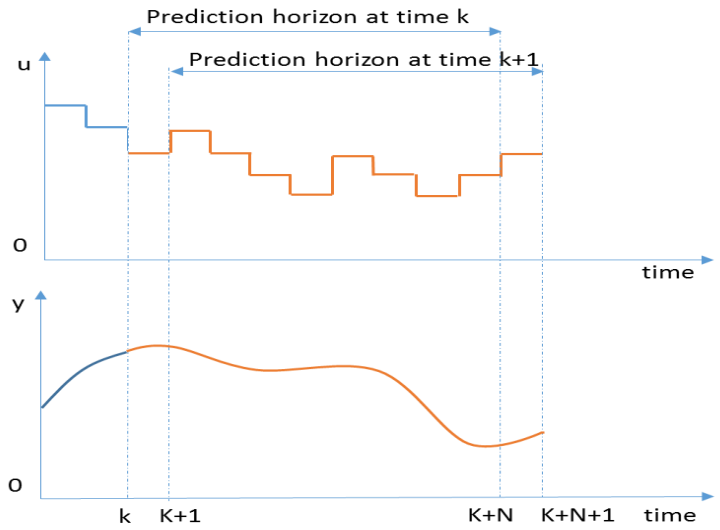

Figure 2: Receding horizon principle

3.2 Application of MPC to the Case Building

The general implementation of MPC in a building system is summarized in Figure 3. The figure shows the core of MPC including the physical models, objective function, constraint function and an optimization engine. The Prediction models predict the variation of various disturbances that affect the building system over time. These disturbances include weather, occupancy, lighting, outdoor contaminant, utility rate etc. The physical model predict the response of the building system for these disturbances and estimates the comfort levels and the energy requirements for various control inputs. The "Optimization" engine find the optimal solution (control inputs in this case) that satisfy the constraints set by the constraint function. Once these control inputs are determined, they will be send to the actual building and the current state variables of the real building (sensor values) will be returned to the MPC control as a feedback for the next time step. The details of MPC controller are discussed in detail below

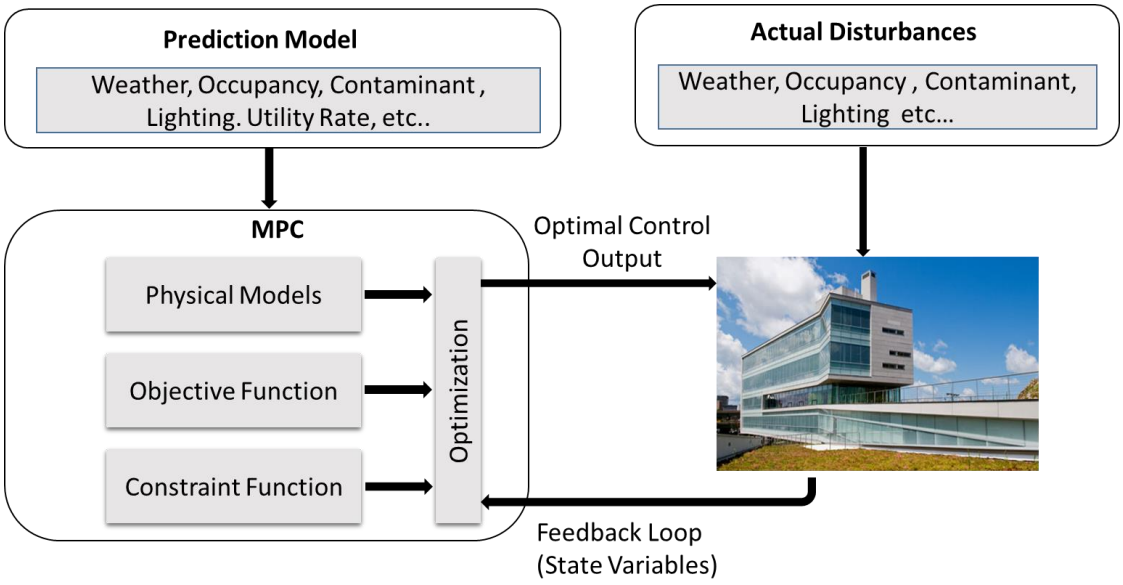

Figure 3. Application of MPC on a real building

3.2.1 Objective Function

In MPC the objective function serves two purposes: stability and performance targeting. Choosing a structure for objective function that forms a Lyapunov function for the closed loop system will guarantee stability. But for a slow dynamics systems, such as building, the requirement is generally relaxed and it is possible to select the cost function solely based on performance(Široký et al. 2011).

In this study the objective function is formulated to be the total energy required to maintain the building in its acceptable IEQ. The considered IEQ parameters are thermal comfort, contaminant concentration and lighting level. The control inputs (variables) used to achieve these IEQ parameters are zone radiant panel chilled water/hot water flow, zone supply air mass flow rate, supply air temperature and window blind angle. Although the objective function has a general form that can be used by any building system, the parameters considered can vary from building to building depending on the HVAC system implemented. The scope of this research is to apply MPC in a case building that has an HVAC system which uses combination of

dedicated outdoor air system and radiant ceiling panels. The specific features of the case building will be discussed in chapter 4. The energy costs associated with maintaining the mentioned IEQ parameters can be merged and defined as the objective function given by:

$$\min_{u} J(k) = \sum_{k=0}^{N} e(cooling/heating) + e(supply\ fan) + e(chilled\ water/hot\ water\ pump) + e(lighting) \quad 12$$

Where $e(cooling/heating)$ is the total energy cost consumed by cooling/heating coil and ceiling radiant panels ($), $e(supply\ fan)$ is total energy cost consumed by supply/return air fans ($), $e(chilled\ water/hot\ water\ pump)$ is the energy cost associated with chilled water pump, ceiling radiant panels chilled water pumps and hot water pump ($) and $e(lighting)$ is the energy cost for lighting ($). The above stated energy cost functions are dictated by the set of linear and nonlinear models which will be discussed in chapter 4.

3.2.2 Constraints

The constraints considered can be broadly classified into IEQ constraints and operational constraints. The IEQ constraints are those constraints that should be satisfied by the HVAC and lighting system to give the required values of the defined IEQ parameters. On the other hand operational constraints are those constraints that arise due to the physical limits of the involved components.

IEQ constraints include thermal comfort level, contaminant concentration level and lighting level. As previously discussed in the literature review, there are various measurement scales for thermal comfort. In this study the performance of the control system is checked based on two thermal comfort scales: PMV and comfort zone

according to ISO7730 (Figure 4). Comfort zone according to ISO7730 is used instead of the one recommended by ASHRAE because of the fact that it uses flat upper and lower limit which makes it easy to be implemented in control algorithms. Table 2 summarizes the ranges of recommended values for the considered IEQ parameters.

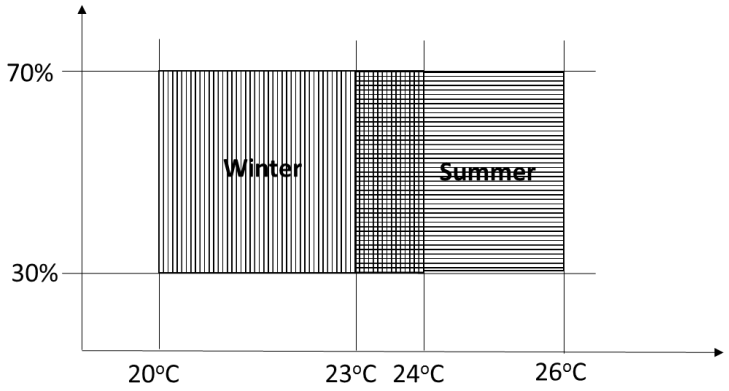

Figure 4: RH/T for comfort zone according to ISO7730

Table 2. Ranges of allowable values for IEQ parameters

IEQ Parameters	Min	Max
Thermal Comfort		
Predicted mean vote(PMV)	-0.5	0.5
Temperature (^{o}C) -Winter	20	24
-Summer	23	26
Relative Humidity (RH) (%)	30	70
Lighting(lux)	500	-
CO_2(ppm)	0	1200
Formaldehyde(ppm)	0	0.027
Toluene(ppm)	0	0.07
PM2.5($\mu g/m^3$)	0	35

The operational constraints enforce the computed optimal control sequences to consider the physical limits imposed by the capacity of the components supporting the HVAC and Lighting system of the building. Some of these constraints also depend on the arrangement of components in the AHU as shown in the Figure 5. Operational constraints help the optimization engine to exclude values out of the valid region and

narrow the search region and thus improve computation time. In this study the following operational constraints are considered.

- The ceiling radiant panels surface temperature should be above dew point temperature of the room/zone air to avoid condensation
- The temperature of the air leaving the cooling coil should be less than or equal to the temperature of air leaving the enthalpy wheel
- The temperature of the air leaving the heating coil should be greater than or equal to the temperature of the air leaving the desiccant wheel
- Supply air temperature should be greater than or equal to cooling coil outlet temperature
- Summation of the cooling load should be less than or equal to the total capacity of the heat pumps cooling capacity
- Summation of the heating load should be less than or equal to the capacity of the total heat pumps heating capacity
- The temperature of the air leaving the cooling coil should be greater than or equal to the cooling coil inlet chilled water temperature
- The temperature of the air leaving the heating coil should be less than or equal to the heating coil inlet temperature.
- The air supplied to each zone and the chilled/hot water supplied to ceiling radiant panels existing in each zone should not exceed their design capacities as given in Table 3.

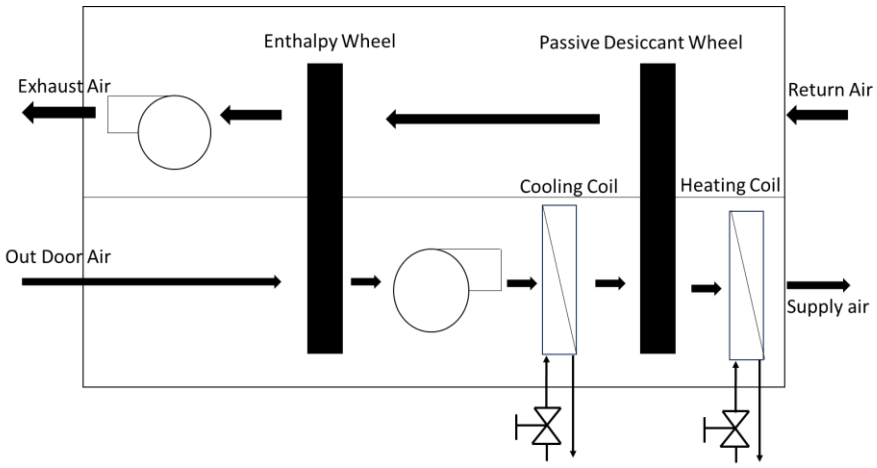

Figure 5. Arrangement of components in the Air Handling Unit (AHU) of the case building.

Table 3: Ranges of zone flow rates for air and cold/hot water

Variables	Zone 1		Zone 2		Zone 3		Zone 4		Zone 5	
	min	max	min	max	min	max	min	max	min	max
Air mass flow rate(kg/s)	0	0.8	0	1.4	0	0.8	0	1.1	0	1.1
Radiant panel										
Cold water flow rate(kg/s)	0	1.796	0	3.034	0	2.243	0	1.796	0	2.894
Hot water floe rate(kg/s)	0	1.182	0	1.682	0	0.955	0	1.182	0	2.061

3.2.3 Disturbances

Controlled as well as uncontrolled disturbances which affect the operation of the building system are considered in this study. Internal heat gain from equipments and lighting are assumed to be controlled disturbances while outdoor air conditions (dry bulb temperature and relative humidity), solar radiation, occupant schedule and indoor and outdoor contaminant concentrations are assumed to be uncontrolled disturbances. MPC requires prediction of these disturbances for the period of the control horizon and the possible benefit that can be obtained from MPC relies on how well these disturbances are predicted and used by the model to estimate optimized control input for the system. If no occupant sensors are used for lighting control, the lighting and equipment schedules are often static and easy to predict. In this study constant profiles

suggested by ASHRAE 90.1 are used for week days and weekends for lighting and equipment schedules. For the weather variables, typical metrological year 3 (TMY3) (Wilcox and Marion 2008) data are used. To avoid possible errors due to prediction, advanced methods like Kalman filter can be used (Cassola and Burlando 2012). In this study weather predictions are assumed to be perfect.

Internal heat gains due to occupants follow schedules of occupants of the building. Occupant detectors are widely used in most intelligent buildings for security purposes and advanced ventilation strategies like demand controlled ventilation. In MPC accurate prediction of occupants can bring a huge difference in the overall energy saving. The study done by Frauke (Frauke 2011) showed that the possible saving for a sample building with MPC controller using homogeneous occupancy was up to 34% while a saving of up to 50% was possible using alternating occupancy. The simplest and most commonly used occupancy models are set of predefined static coefficients that multiply the design maximum occupancy. Developing occupancy prediction model is beyond the scope of this study and a static occupancy profile recommended by ASHRAE 90.1 for an office building is used Figure 6 . More advanced prediction models that can be used for demand based control strategies exist in literatures including linear regression models (Claridge and Abushakra 2001) and Markov Chain Models((Erickson, Carreira-Perpiñán, and Cerpa 2011), (Lu et al. 2010)). It should be noted that the occupancy model is not integral part of the MPC and can be changed whenever a good model is available in the future.

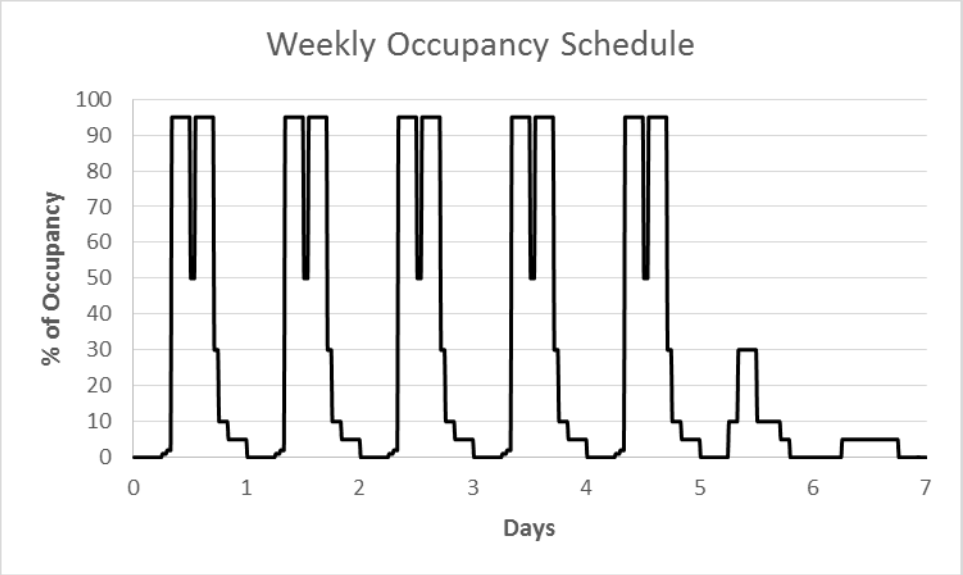

Figure 6: Assumed weekly occupant schedule.

Four contaminants, CO2, Toluene, formaldehyde and PM2.5, are considered in this research. Similarly simplified assumptions are used to account for the disturbances related to dynamic variation of the contaminants. For Formaldehyde and Toluene , geometric mean values based on EPA-BASE study (EPA_BASE 2006) are assumed to represent outdoor concentration and indoor generation rates. CO_2 and PM2.5 are relatively difficult to predict because of their high hourly and seasonal variations. Some researchers tried to predict outdoor concentration of these contaminants using statistical models (Shih and Tsokos 2008) and hidden semi Markov models (Dong et al. 2009) . A constant outdoor CO_2 concentration of 500ppm is assumed while previous year measured outdoor PM2.5 data is used as prediction for current outdoor PM 2.5 concentration. Indoor PM 2.5 generation rate is assumed to be negligible and not considered. Assuming occupants to be the major source of indoor CO2, indoor CO2 generation can be estimated using:

$$V_{CO_2} = \frac{0.028\ x\ A_D\ x\ M\ xRQ}{0.23\ x\ RQ + 0.77} \quad (13)$$

Where V_{CO2} is CO_2 generation rate (l/sec/person), A_D is Dubies Body surface area (m^2), M is metric of metabolic rate, RQ is respiration quotient (0.83 for an adult engaged in a light activity). Thus the total CO2 concentration prediction follows the occupancy prediction profile since it depends on the number of occupants. The acceptable concentration limits for these contaminants are summarized in Table 1.

3.2.4 Optimization Problem

One of the major challenge associated with MPC is the optimization problem that has to be solved at each time step. For a given set of problem, there always exist different optimization techniques with different structures and characteristics. One optimization technique is superior to the others in a specific area where it is targeted for during its development. The choice of the optimization technique is a critical step during MPC design and it should consider the nature of the problem in hand. The whole building system dynamics consists various system with different time scale (like room air and wall surface temperature) which make the problem a stiff problem. The fact that it is a stiff nonlinear problem makes the computation difficult and require more commutation time.

In general nonlinear optimization techniques could be categorized as local and global optimization techniques. The major difference between the two is that global techniques gives one optimal value (global solution) for the cost function irrespective of the starting point (initial guess) of the optimization while local optimization technique could result more than one solution depending on the starting point of the optimization. Some of the global optimization techniques include simulated

annealing, branch and bound, genetic algorithms etc. on the other hand some of the local optimization techniques include direct search method and gradient based techniques. Though global optimization techniques are known for best solution, finding the global solution for big systems like building could take considerable amount of time and thus the associated computational cost and memory demand is high. Since MPC is online control strategy by nature, the computation time is very critical. The optimization should converge before the set time for new control input which usually depend on the nature of the building.

In this research local optimization techniques are used to avoid the risk of taking more computation time than the control input set time. To minimize the chance of finding infeasible local optimum points, rule based strategies are used for assigning initial guess values which are in the feasible range. The rules used are based on the time of the day, occupancy hours, and also based on the season: cooling or heating. The logics used are presented below

Night time, heating

$$\dot{m}_{hw_{rp},i} = \dot{m}_{hw_{rp},i,min}\,, \dot{m}_{as,i} = \dot{m}_{as,i,min},\ T_{a,s} = T_{oa}\,, Ba_i = 0 \qquad (14)$$

Occupied time, heating

$$\dot{m}_{hw_{rp},i} = \dot{m}_{hw_{rp},i,max}\,, \dot{m}_{as,i} = \dot{m}_{as,i,max},\ T_{a,s} = T_{hw}\,, Ba_i = 45 \qquad (15)$$

Night time, cooling

$$\dot{m}_{chw_{rp},i} = \dot{m}_{cw_{rp},i,min}\,, \dot{m}_{as,i} = \dot{m}_{as,i,min}, T_{a,s} = T_{oa}\,, Ba_i = 90 \qquad (16)$$

Occupied time, cooling

$$\dot{m}_{chw_{rp},i} = \dot{m}_{chw_{rp},i,max}\,, \dot{m}_{as,i} = \dot{m}_{as,i,max},\ T_{a,s} = T_{chw}\,, Ba_i = 45 \qquad (17)$$

Where $\dot{m}$ is mass flow rate (kg/s), *T* is temperature (K), *Ba* is blind angle (deg) and subscripts *rp* is radiant panel, *a* is air, *oa* is outdoor air, *chw* is chilled water, *hw* is hot water, *i* is zone number, *min* is minimum limit and max is maximum limit. Once the mode of operation is changed to occupied mode, the optimal control inputs from the previous time step are used as an initial guess for the next time step. This is owing to the fact that there will be no abrupt change in the building operation in two consecutive time steps. This will considerably decrease the search region for the optimization problem and as a result reduce the computation time substantially.

Constrained Optimization by Linear Approximation (COBYLA) is used as an optimization method in this research because of its ability to support arbitrary nonlinear equality and inequality constraints. In addition it is a derivative free optimization technique which considerably reduce the engineering effort needed for MPC development. This method solves the optimization problem by generating successive linear approximation of the objective and constraint functions by linear interpolation at n+1 points in the space of the variables and optimize these approximations in a trust region at each time step. To reduce the computation time, the original problem is modified using Augmented Lagarangian (AUGLAG) method before solved in COBYLA. AUGLAG combines the nonlinear objective function and constraint function in to one function by adding a penalty function for any possible violation of constraints. Opti tool box (Jonathan and David 2012), a free Matlab tool box which contains various optimization algorithm including COBYLA is used as a simulation platform.

3.3 Optimal Control Implementation

The performance of the MPC depends on the accuracy of the models used for capturing the working physics of each involved components as well as the optimization technique used for computing. MPC by nature is open loop for the given time step and thus it is essential to verify the accuracy of the controller before implementation. In this research the actual building is represented by its detailed physical model developed in EnergyPlus simulation software and a co-simulation strategy is used to communicate between the MPC and the EnergyPlus model. MLE+ (Willy et al. 2012), an open source Matlab/Simulink tool box is used for co-simulation. MLE+ can also be used for actual implementation of the MPC in the real building using its capability to communicate with actual control points in the Building Management System (BMS) through BACnet. The EnergyPlus model and the MLE + co-simulation strategy are discussed below in more detail.

3.3.1 EnergyPlus Model Highlights:

EnergyPlus simulation software is one of the most advanced and matured software available for energy and thermal load analysis of whole building system(EnergyPlus 2011). In this research the EnergyPlus model is used as a virtual test bed to evaluate effects of various control strategies on energy consumption and IEQ of the building. The developed EnergyPlus model contains five major loops namely: air loop, chilled water loop, hot water loop, radiant ceiling cooling loop and condenser loop.

Air loop: This loop contains dedicated outdoor air system in the supply side and zone air system in the demand side. The dedicated outdoor air system contains desiccant wheel, enthalpy wheel, cooling coil, heating coil and fan. The zone air system is assumed to be variable air volume (VAV) with no reheat at the terminal. The

dedicated outdoor air system supplies air that is needed for maintaining the required indoor air quality and moisture content in each zone.

Chilled water loop: The chilled water loop contains cooling coil and a liquid to liquid heat exchanger in the demand side and seven ground water heat pumps in the supply side. The liquid to liquid heat exchanger is used to provide the right cold water temperature for the radiant ceiling panel system which is above each zone's dew point temperature to avoid condensation.

Hot water loop: The hot water loop contains 4 ground water heat pump and one auxiliary boiler in the supply side of the loop and heating coil and radiant panel system in the demand side of the loop. The heating loop supports all the heating demand of the building. During normal operations the heat pumps will be working sequentially to support the required load. In the cases where the heat pumps are unable to meet the building heating demand the auxiliary boiler will be enabled in addition to the four heat pumps.

Ceiling radiant panel cooling loop: This loop is responsible for providing the cold water required for ceiling radiant panel cooling system. It contains liquid to liquid heat exchanger in the supply side and ceiling radiant panels in the demand side. As previously discussed in the chilled water loop section, this loop is introduced to avoid the risk of condensation at the ceiling radiant panels.

Condenser loop: The condenser loop contains heat pumps in the demand side and ground heat exchanger and auxiliary cooling tower in the supply side. The case building implement a system called hybrid GSHP that use heat exchanger and cooling tower to minimize unnecessary heat exchanger size that could be resulted due to unbalance in annual heat rejection and extraction.

The above mentioned major loops in the building model are summarized in Figure 7.

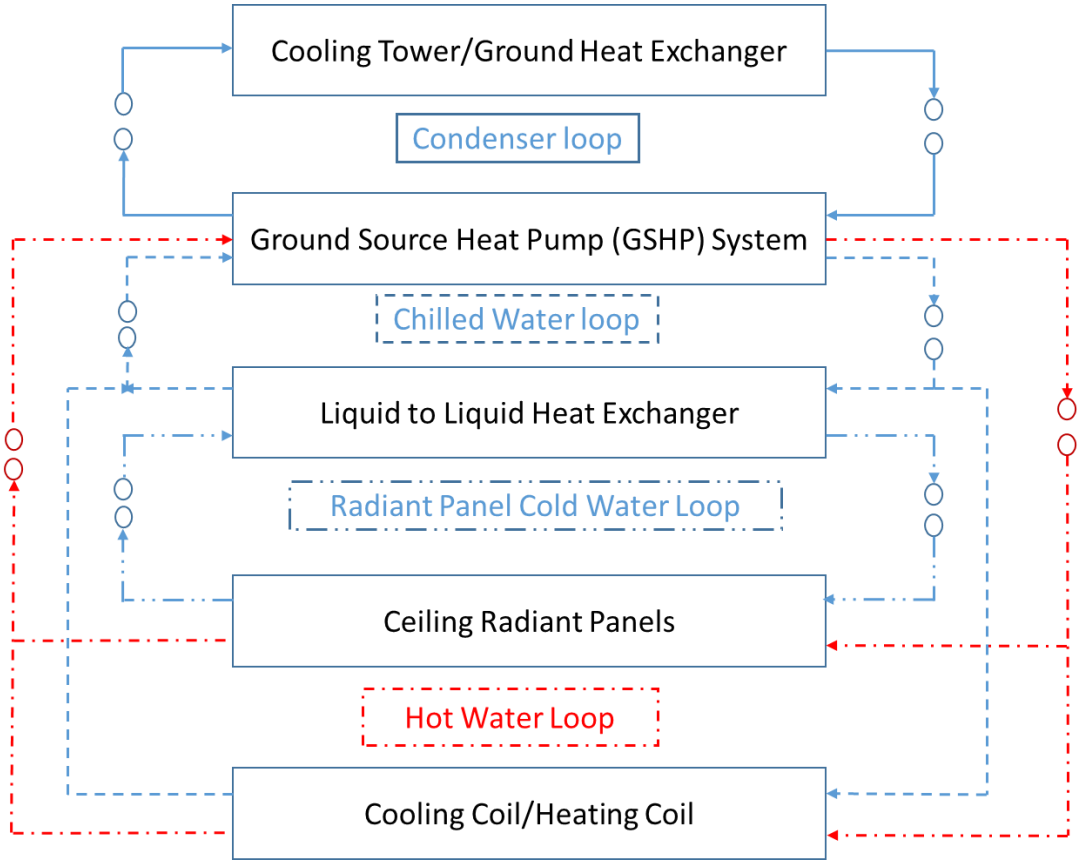

Figure 7. EnergyPlus model major loops

3.3.2 Co-simulation Strategy

Conventionally, EnergyPlus is used for offline energy simulation (Pang et al. 2011).To engage EnergyPlus in a real time energy analysis and to help growing demand of simulation for improved building energy performance, building control virtual test bed (BCVTB) is developed by Lawrence Berkley national laboratory. BCVTB is a software environment that allows coupling of different simulation programs for co-simulation(Wetter 2012). Although Matlab can be interfaced with EnergyPlus using BCVTB, interactive execution and debugging of Matlab code is not possible since it is called by BCVTB as a client(Willy et al. 2012). To this end, MLE+ is developed to better communicate EnergyPlus with Matlab/Simulink with all

the functionalities of execution and debugging enabled(Willy et al. 2012). In this research MLE+ is used for co-simulation of the MPC controller developed in Matlab and detailed building model developed in EnergyPlus. This approach is tested in previous researches and proved to be successful.(Nghiem and Pappas 2011). MLE+ also has a capacity to communicate with the actual building with the help of BACnet.

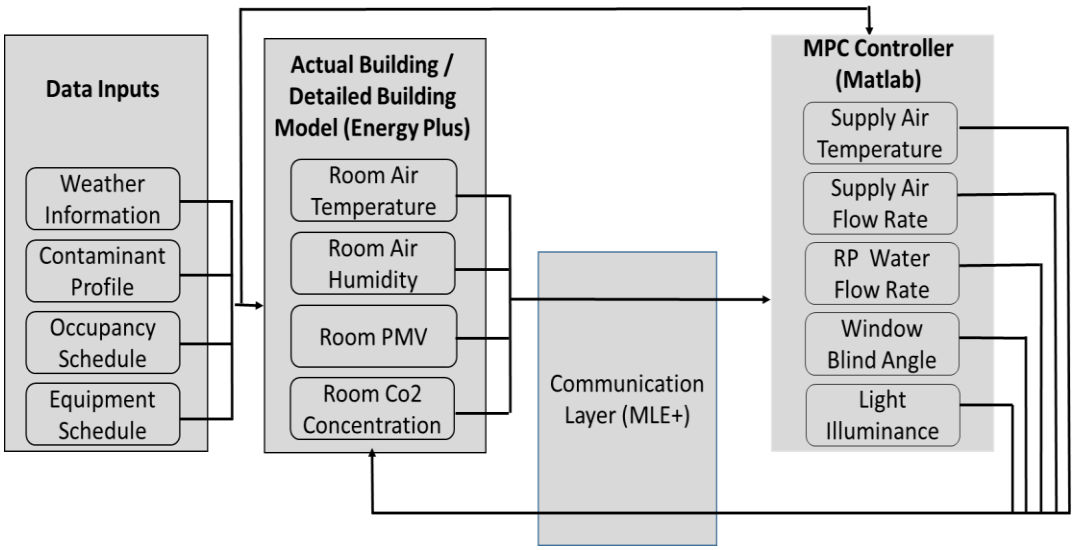

Figure 8: Communication framework between EnergyPlus and Matlab

Parameter exchange between EnergyPlus and MLE+

During co-simulation, EnergyPlus and Matlab exchange sets of parameters at each time step using MLE+ as a bridge. The parameters exchanged between MPC controller and EnergyPlus model are shown in Figure 3.7. At each time step, MPC sends supply air flow rate, supply air temperature, ceiling radiant panels chilled/hot water flow rate, window blind slat angle and lighting dimming level set points to the EnergyPlus while room conditions (air temperature, contaminant level, Relative humidity, PMV and lighting level) are send to MPC as a feedback to correct the controller for the next time step.

4 COMPONENT MODELS FOR MPC

4.1 Introduction

As mentioned in the previous chapters, one unique feature of optimal controllers in general and MPC in particular is the use of models to predict how the system evolves with time when it is subjected to variations in operating conditions or environment. The performance of MPC highly relies on the accuracy of the models used. The models used for MPC can be broadly divided in to quantitative, qualitative and process or history based models (Katipamula and Brambley 2005).

Quantitative (detailed physics) models require detail information about the component to be modeled and more senor inputs are needed to capture the operating condition. In practice very limited information is available about HVAC components even from manufacturer catalogues. The number of available sensors in a building management system is also very limited and the available sensors are those which are used for control purpose and overall energy usage measurement. In addition to that most of the detailed physics models are nonlinear models and are computationally expensive to solve.

In process history based approach, the model needs lots of training data and are usually specific to the system on which the models are trained for. The model is only valid for the range of operation within the training data and it is not possible to extrapolate the result for a value out of training data range (Srinivas Katipamula M. R., 2005). This could result instability in the control system when the system operate in some extreme conditions which are out of the normal operation range.

Qualitative models (reduced - order physics - based model) use combinations of simplified physics and rule based approach to estimate the operating condition of a

system. For models used for development of MPC for a building, qualitative models are preferable for the following core reasons.

- Qualitative models require less information about the components to be modeled as well as less sensor data for condition monitoring. Building systems are known for their less sensor density unlike other systems like process industries (Zimmermann, Lu, and Lo 2011).
- Use of simplified models can reduce the number of nonlinear and differential equations that would be resulted from detailed physics model. Solving nonlinear equations numerically involve numerous iterations and as a result the computation time can grow to minutes and even hours.
- Due to inherent characteristics of MPC controllers to use measured response of the system (room temperature, Relative humidity etc.) as an input for next time step, the propagation of model errors that arise from simplifications can be minimized.

In this chapter the models used in the MPC are discussed. The component models discussed are specific to an HVAC system that has a dedicated outdoor air system and ceiling radiant panels for heating and cooling, which is the scope of this research.

4.2 Case Building Definition

Syracuse Center of Excellence (COE) head quarter building is used as a case building in this research. The Building is LEED Platinum Certified and it is used as a test bed for environmental and energy technologies and building innovations. The facility includes high-end technologies which enable to carry out advanced research and developments. The various features of the building include - Total Indoor Environmental Quality [TIEQ] Lab, green roof, geothermal system, lighting control

systems, natural ventilation and personal ventilation systems, advanced building heat recovery/reuse systems and integrated control system for improving indoor air.

4.2.1 Building Envelope System Definition

The COE building has five floors and each floor has different zones with different activities and floor area. The building is relatively narrow with extensive windows, providing a high level of occupant comfort with ample natural lights and opportunities for views and natural ventilation. The south façades of the building features highly insulated glass with integrated electronically controlled blinds that provide solar heat and glare control, capable of operation at 15 degree increment in blind's angle. In this research the case building is simplified to five zones and the internal loads associated with each zone are summarized in Table 4.

Table 4: Design capacities for COE building

Floor name	Floor area (m^2)	Max occupancy	Lighting (kW)	Equipment (kW)
1st floor	630	61	14.7	3
2nd floor	960	120	25.7	4.5
3rd floor	622	158	23.6	6.8
4th floor	653	97	29.5	9.8
5th floor	666	61	27.7	13

4.2.2 HVAC System Definition

The HVAC system of the case building is a dedicated outdoor air (DOAS) - with radiant ceiling panel system. This kind of system has been successfully utilized in different parts of the world and the following factors are believed to be reasons behind its growing demand in building industries: enable independent control of temperature and humidity, provide more effective ventilation and prevent virus and bacteria transmission among different zones(Ge, Xiao, and Xu 2011). The two major subsystems of DOAS-CC system: Air system and water system are discussed below.

4.2.2.1 Air System

Unlike "All air system" whereby supply air is responsible for maintaining the required indoor air quality (IAQ) as well as thermal comfort, supply air in DOAS-CC system is mainly used for providing the required indoor air quality (IAQ) and moisture control. Building thermal load in DOAS-CC system is taken care by radiant ceiling panels. The AHU unit of the case building is equipped with enthalpy wheel and passive desiccant wheel. Both enthalpy wheel and desiccant wheel exchange heat and moisture between return air and fresh air but enthalpy wheel is mainly used for heat recovery while desiccant wheel is used for dehumidification. Use of desiccant wheel avoids the need to lower down the air temperature below dew point temperature for dehumidification and can reduce the cooling demand by up to 30% compared to conventional systems (Casas and Schmitz 2005).

4.2.2.2 Water System

The hot/cold water required for heating/cooling is coming from seven Ground Source Heat Pumps (GSHP) installed in the facility. The facility uses the so called 'hybrid GSHP' system which have supplemental heat rejecters (cooling tower) to reject excess heat on a seasonal or diurnal basis, thereby reducing the required size of the Ground Loop Heat Exchanger (GLHE) and, hence, the first cost of the system.
One of the issues associated with use of ceiling radiant panels is the risk of having surface condensation on panel surfaces especially if low temperature chilled water is used. To avoid this, the temperature of chilled water supplied to radiant panels is increased to 62^{o}F from heat pump supply temperature of 50^{o}F using an intermediate heat exchanger.

4.2.3 Lighting and Integrated Window Blind System

The case building uses fluorescent and LED lightings, which are controlled by daylight harvesting system and have an auto dimming capability. It also have an auto shut off capacity based on occupancy sensors. The building also have windows with integrated electronically controlled blinds in its south façade. The blind control provides glare and solar heat control and the blind angle can be controlled in 15^{o} increment. The daylight harvesting system and window control system work in parallel and provide lighting saving and also control the heat gain from these sources.

4.3 Building Envelope and Air Model

In this section, models that are used to predict IEQ in terms of temperature, relative humidity, PMV, contaminant concentration, and lighting are discussed. These models will help to quantify the effect of indoor and outdoor disturbances in IEQ and ultimately enable the MPC to take appropriate and optimized action so that the HVAC and lighting system respond accordingly.

4.3.1 Thermal Load Model

Building envelope is exposed to different boundary conditions both from inside and outside. These boundary conditions are changing every time due to different controlled and uncontrolled disturbances which in turn keeps the building system in transient condition for most of the time. Thermal dynamics of the building system is highly affected by thermal mass/capacitance of the building materials and inside air. As discussed in the literature review section, there are various methods to estimate dynamics of building system. Heat balance method, one of the methods recommended by ASHRAE(ASHRAE 2009) is used in this research. Since building is a complex

system, a complete theoretical approach is impractical for MPC application. The following assumptions are considered for simplifying the problem.

- Air in the zone is fully mixed. Temperature distribution is uniform and the dynamics can be expressed in a lumped capacitance model
- The heat transfer through structures is one dimensional
- The density of the air is assumed to be constant and is not influenced by changes in temperature and relative humidity.

The building indoor air temperature is affected by convective heat gains from surrounding envelope structures and air exchange between the boundaries and it is given by

$$\boldsymbol{\rho_a V_a Cp_a \frac{dT}{dt} = Q_{vent} + Q_{opaque} + Q_{window} + Q_{internal} + Q_{inf} + Q_{rad}} \quad 18$$

Where Q_{vent} is heat gain/loss due to mechanical ventilation (W), Q_{opaque} is convective heat gain/loss through opaque wall structure (external wall, partitions, ceiling and floor) (W), Q_{window} is convective heat gain/ loss through window (W), $Q_{internal}$ is convective heat gain due to internal sources (people, lighting and equipment etc.) (W), Q_{inf} is convective heat gain/loss due to infiltration (W), Q_{rad} is convective heat gain/loss through radiant systems (W), ρ_a is density of air (kg/m^3), V_a is volume of air (m^3), Cp_a is specific heat capacity of air.

Each of these sources contributing to total heat gain of the building are discussed below.

Heat gain/loss due to mechanical ventilation.

In most buildings, mechanical ventilation serves two purposes; providing thermal comfort by offsetting the sensible and latent heat gains and diluting indoor air contaminants. The heat introduced in to the building though mechanical ventilation can be given by:

$$\boldsymbol{Q_{vent} = \dot{m}_s c_p (T_s - T_r)} \qquad 19$$

Where m_s is mass flow rate of supply air (kg/s), c_p *is* Specific heat of air (J/kg.k), T_s is Supply air temperature (k), T_r is room air temperature (k).

Heat gain/loss through structures

All the structures surrounding the building, external wall, partitions, ceilings and floors share the same heat transfer mechanism. Interaction of these structures with surrounding atmosphere is given in Figure 9

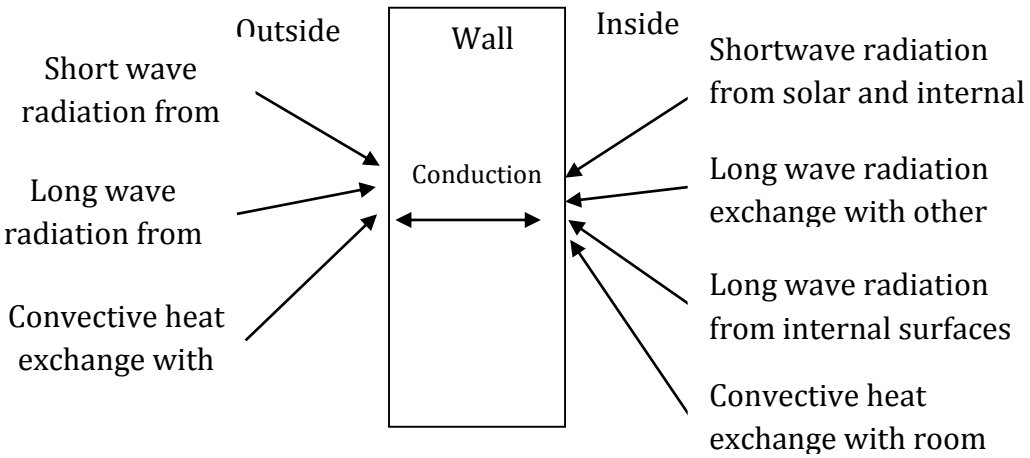

Figure 9. Wall heat interactions with inside and outside boundaries.

The thermal capacitance and resistance involved in the heat balance of a building thermal system is analogous to the capacitance and resistance as it is in an electric network. An extensive number of literatures are available on modeling heat transfer through the wall and work by Gouda (Gouda, Danaher, and Underwood 2002) showed that 3 resistor and 2 capacitor model (3R2C) is sufficient to capture heat interaction of two spaces separated by a wall. Similar approach as shown in Figure 10 is used for wall model. Advanced simulation software including EnergyPlus and Transys also use this method.

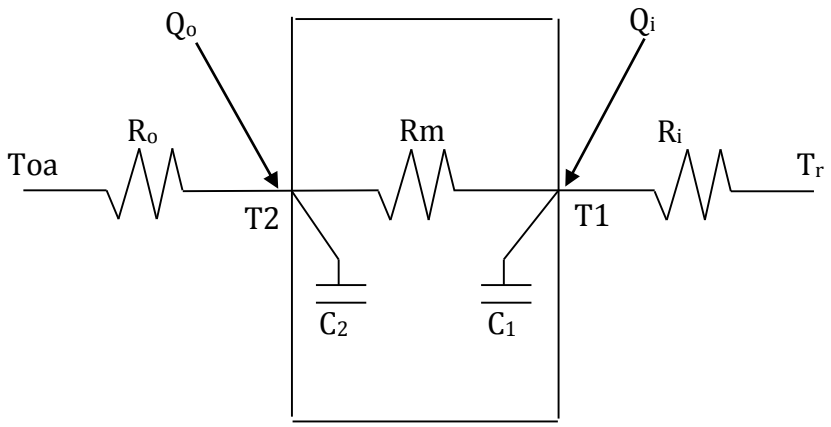

Figure 10. Wall thermal resistance capacitance (3R2C) model

The time varying nature of fluxes, coupled with thermal inertia of the wall create a transient hear conduction problem in the interior and exterior side of the wall. Rate of change of temperature on these surfaces is represented by first order equations as:

$$C_2\dot{T}_2 = Q_o + \frac{T_{oa} - T_2}{R_o} + \frac{T_1 - T_2}{R_m} \quad (20)$$

$$C_1\dot{T}_1 = \frac{T_2 - T_1}{R_m} + \frac{T_r - T_1}{R_i} + Q_i \quad (21)$$

Where C_2 is thermal capacitance of the external layer (J/K), C_1 is thermal capacitance of the internal layer (J/K), Q_o is summation of short wave and long wave radiations absorbed by external surface (W), Q_i is summation of shortwave and long wave radiations absorbed by internal surface (W), T_o is outdoor air temperature (^{o}k),T_2 is external surface temperature (^{o}k), T_1 is internal surface temperature (^{o}k), Tr is room air temperature (^{o}K), R_o is outdoor air resistance (^{o}k/W), R_i is indoor air resistance (^{o}k/W) and R_m is lumped construction material resistance (^{o}k/W)

Heat gain/loss through window

Because of the fact that window's capacitance is very small, the portion of heat stored in a window is often neglected. For clear windows, the heat transferred in to the building due to temperature difference between indoor and outdoor air temperatures can be calculated as:

$$Q_{win} = \frac{T_{oa} - T_r}{R} \quad (22)$$

Where Tr is room temperature (ok), Toa is outdoor air temperature (ok), R is overall resistance (ok/W), R incudes effect of conductivity of the window material and indoor and outdoor convective heat transfer coefficients.

When a shade/ blind is attached to the window the heat transfer mechanism will be more complicated and has to consider the effect of solar radiation absorbed by the shade. For window with internal shades, the absorbed portion of the solar radiation can be assumed to be immediately convected to the zone air (EnergyPlus 2012). The

heat gain associated with windows is discussed in more detail in 'Window Model' section.

Heat gain/loss through infiltration/exfiltration.

ASHRAE **(ASHRAE 2009)** recommends various models from simplified to more detailed ones for capturing infiltration/exfiltration phenomena. Infiltration flow calculation based on design flow rate (Coblenz and Achenbach 1963) is used in this research and it is shown in equation 23. As listed in

Table **5**, various simulation software use similar equation by modifying the parameters in equation 23 .

$$\boldsymbol{Infiltration = I_{design} . (A + B. |T_z - T_{oa}| + C . Wind\ Speed + D . windspeed^2)} \quad \textbf{23}$$

Pacific Northwest national laboratory (PNNL) recommends use of DOE-2 model for infiltration calculation with input design infiltration rate(I_{design}) of 0.001024$m^3/s/m^2$ of above grade exterior wall surface area (Gowri, Winiarski, and Jarnagin 2009) and the same model is used in this research.

Table 5: Infiltration model coefficients [Source:(EnergyPlus 2012)]

Model Name	Constant Coefficient (A)	Temperature Coefficient (B)	Wind Speed Coefficient (Linear Term) (C)	Wind Speed Coefficient (Quadratic Term) (D)	Reference Wind Speed
Constant Infiltration (Energy Plus Default)	1	0	0	0	NA
DOE-2 Infiltration Methodology	0	0	0.224	0	10 mph
Blast Infiltration Methodology	0.606	0.03636	0.1177	0	7.5 mph

Heat gain/loss through ceiling radiant panel.

The ceiling radiant panel exchange heat to the surrounding through convection and radiation. The convective portion of the heat exchange directly affect the room air temperature while the radiation portion is absorbed by surrounding surfaces before it affects the room air temperature and thus only the convective portion is included in the room air heat balance. The heat transfer mechanism of the ceiling radiant panels is discussed in more detail in **"Radiant Panel**" section.

4.3.2 Indoor Air Moisture Model

Indoor air moisture content is one of the major factors affecting the thermal comfort. Latent heat gain from internal sources, air exchange through infiltration/exfiltration and mechanical ventilation affect the room air moisture content. The change in humidity ratio can be modeled by first order equation as:

$$\rho V_r \frac{dw_r}{dt} = \dot{m}_{sys}(w_{sys} - w_r) + \dot{m}_{inf} \cdot (w_o - w_r) + \frac{q_l}{h_g} \qquad 24$$

Where ρ density of air (kg/m^3), V is room/zone volume (m^3), w is humidity ratio (kg/kg), $\dot{m}$ is supply air mass flow rate (kg/s), q_l is room latent heat gain (W), h_g is specific latent heat of vaporization (J/kg). Subscript r is room, o is outdoor, sys is mechanical system and inf is infiltration.

4.3.3 Indoor Air Contaminant Model

Recently indoor air quality is getting more attention due to its impact on health and performance of the occupants. Various regulation and standards are in place to limit the concentration of indoor air contaminants in acceptable range. The building HVAC system should be able to clean the air as well as dilute the indoor air contaminant concentration to the level required by the set standards. Assuming mass flow rate of

supply and return air to be the same in each zone, indoor air contaminant concentration over time can be estimated by

$$\rho V_r \frac{dC_r}{dt} = \dot{m}_{sys}(C_{sys} - C_r) + \dot{m}_{inf} C_o - \dot{m}_{exf} C_r + S_r - k_d C_r \quad (25)$$

Where C is contaminant concentration (kg/m3), $\dot{m}$ is mas flow rate (kg/s), S_r is room contaminant source generation (kg/m^3/s), k_d is contaminant rate of deposition on surface (kg/s), ρ is density of air (kg/m^3), V_r is room air volume (m^3) and subscript *sys* is mechanical ventilation, *inf* is infiltration, *exf is* exfiltration, *r* is room and *o* is outdoor

4.3.4 Thermal Comfort Model

According to ASHRAE, thermal comfort is defined as the condition of mind that expresses satisfaction with the thermal environment. Fanger (Fanger 1973) has developed an index called Predicted mean vote (PMV) based on votes of a large group of people. PMV value ranges from +3 for very hot condition to -3 for very cold condition. ASHRAE 55 (ASHRAE Standard 55-2013 2013) recommends a PMV value between +0.5 and -0.5 for acceptable thermal comfort. Similar index which is commonly used as an index for thermal comfort is predicted percentage of dissatisfied (PPD). ASHRAE recommends PPD less than 10% for acceptable thermal comfort.

$$PMV = (0.028 + 0.3033e^{-0.036M}) * \left\{ \begin{array}{c} (M-W) - 3.05e^{-3}[5733 - 6.99(M-W) - Pa] \\ -0.42[(M-W) - 58.15] - 1.7 * 10^{-5} M * \\ (5867 - Pa) \\ -0.0014M(34 - T_a) - \\ 3.96e^{8} f_{cl}[(T_{cl} + 273)^4 - (T_r + 273)^4] \\ -f_{cl} h_c (T_{cl} - T_a) \end{array} \right\} \quad (26)$$

$$T_{cl} = 35.7 - 0.028(M - W) - 0.155I_{cl}[3.96 * 10^{-8} f_{cl}\{(T_{cl} + 273)^4 - (T_r + 273)^4\} + f_{cl} h_{cl}(T_{cl} - T_a)] \quad (27)$$

$$h_c = \begin{cases} 2.38(T_{cl} - T_a)^{0.25} & for\ 2.38(T_{cl} - T_a)^{0.25} > \sqrt{V_{ar}} \\ 12.1\sqrt{V_{ar}} & for\ 2.38(T_{cl} - T_a)^{0.25} < \sqrt{V_{ar}} \end{cases} \quad (28)$$

$$f_{cl} = \begin{cases} 1.00 + 0.2I_{cl} & for\ I_{cl} < 0.5Clo \\ 1.05 + 0.1I_{cl} & for\ I_{cl} > 0.5Clo \end{cases} \quad (29)$$

$$PPD = 100 - 95e^{-0.03353PMV^4 - 0.2179PMV^2} \quad (30)$$

Where M is metabolism (W/m^2, 1 met=58.15W/m^2), W is external work (W/m^2), T_a is dry bulb temperature (^{o}C), T_r is radiant temperature (^{o}C), Pa is partial water vapor pressure (Pa), f_{cl} is ratio of clothed body area to nude body area, T_{cl} is surface temperature of clothing, I_{cl} is thermal resistance of clothing (clo, 1clo=0.155m^2 K/W), and h_c is conventional heat transfer coefficient (W/m^{2}K)

4.3.5 Window Model

Window system provides direct route for entry of solar radiation in to a building envelope. This introduction of solar radiation affects the IEQ in terms of lighting and temperature. The heat gain associated with solar radiation helps the HVAC system by decreasing heating load during winter while it puts extra cooling load to the system during summer. In regards to lighting, the solar gain improves the illuminance level of the building envelope and could potentially save associated energy costs for electric lighting.

Most modern buildings have a blind that can be manually or automatically adjusted to address both lighting and thermal issues. In this research a window model - based

on (ISO 15099:2003, n.d.) is used to quantify the thermal and visible transmittance of the window for various blind angle. In addition parametric equations are developed to account for the effect of geometry on the distribution of thermal radiation and illuminance in various building surfaces surrounding the window. The parametric equations minimize the effort to develop model - based control system for window as well as whole building system that would otherwise be difficult using detailed models because of its computationally intensive nature. To sections below presents the models that are used for capturing the effect of blind angle on thermal and visible transmittance.

4.3.5.1 Window Thermal Model

The amount of thermal radiation transmitted to the building depends on the direct and diffuse radiation incident on the window surface. The overall diffuse and direct transmittance of the window glazing system are affected by optical properties of the layers making up the glazing system, i.e. glass and blind optical properties. Transmittance of glass layer is affected only by the incident angle while blind transmittance properties are affected by geometry, incident angle and reflectance of the blind slat.

Glass transmittance

Dependence of optical properties of glass on incident angle depends on whether the glass is coated or uncoated. A fourth order regression fit (EnergyPlus 2012) is used to determine reflectance and transmittance as follows:

$$\bar{\tau}(\emptyset) = \bar{\tau}_0 + \bar{\tau}_1 \cos(\emptyset) + \bar{\tau}_2 cos^2(\emptyset) + \bar{\tau}_3 cos^3(\emptyset) + \bar{\tau}_4 cos^4(\emptyset) \quad 31$$

$$\bar{\rho}(\emptyset) = \bar{\rho}_0 + \bar{\rho}_1 \cos(\emptyset) + \bar{\rho}_2 cos^2(\emptyset) + \bar{\rho}_3 cos^3(\emptyset) + \bar{\rho}_4 cos^4(\emptyset) \quad 32$$

Table 6: polynomial coefficients used to determine glass optical properties

	0	1	2	3	4
$\bar{\tau}_{clr}$	-0.0015	3.355	-3.84	1.46	0.0288
$\bar{\rho}_{clr}$	0.999	-0.563	2.043	-2.532	1.054
$\bar{\tau}_{brz}$	-0.002	2.813	-2.341	-0.0573	0.599
$\bar{\rho}_{brz}$	0.997	-1.868	6.513	-7.862	3.225

If the glass has normal transmittance >0.645 it will be considered as clear and its optical properties can be given by

$$\boldsymbol{T}(\emptyset) = \boldsymbol{T}(\mathbf{0})\bar{\boldsymbol{\tau}}_{\boldsymbol{clr}}(\emptyset) \quad 33$$

$$\boldsymbol{R}(\emptyset) = \boldsymbol{R}(\mathbf{0})\left(\mathbf{1} - \bar{\boldsymbol{\rho}}_{\boldsymbol{clr}}(\emptyset)\right) + \bar{\boldsymbol{\rho}}_{\boldsymbol{clr}}(\emptyset) \quad 34$$

If a glass has normal transmittance <0.645, it will be considered as coated and its optical properties are given by

$$\boldsymbol{T}(\emptyset) = \boldsymbol{T}(\mathbf{0})\bar{\boldsymbol{\tau}}_{\boldsymbol{brz}}(\emptyset) \quad 35$$

$$\boldsymbol{R}(\emptyset) = \boldsymbol{R}(\mathbf{0})\left(\mathbf{1} - \bar{\boldsymbol{\rho}}_{\boldsymbol{brz}}(\emptyset)\right) + \bar{\boldsymbol{\rho}}_{\boldsymbol{brz}}(\emptyset) \quad 36$$

Where $T(0)$ is the transmittance of glass at normal incidence, $R(0)$ is reflectance of glass at normal incidence.

Blind transmittance

Depending on the relative magnitude between slat angle and incidence angle, some portion of the incident direct radiation will be directly transmitted while the remaining portion is reflected and diffused to the zone. The blind optical properties are

calculated based on the approach presented by Simmler (Simmler, Fischer, and Winkelmann 1996). To simplify the model, the following assumptions are made.

- The slat is flat
- The slats are perfect diffuser
- Thickness of the slat is ignored

Figure 11 represents the slat geometry divided in to different segments, s_i for a specific incident angle and slat angle.

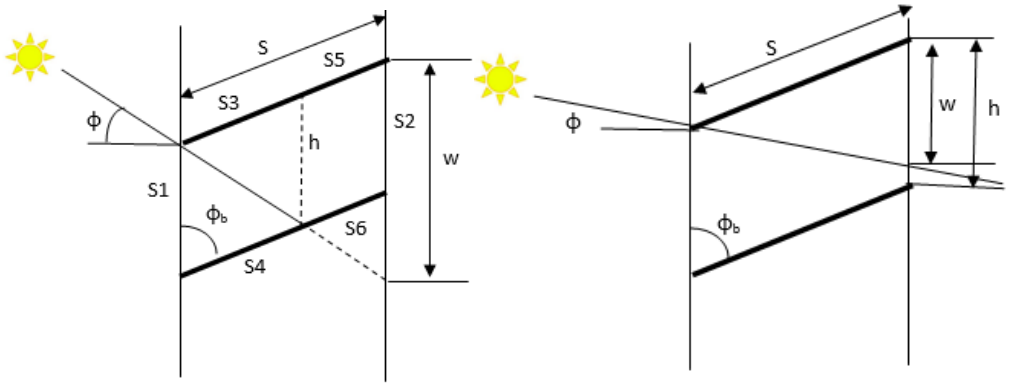

(a) (b)

Figure 11: (a)side view of blind cell with reflection (b) side view of blind cell showing direct transmittance without reflection [source:(EnergyPlus 2012)]

Direct to direct blind transmittance:

The portion of the direct radiation passing through the window without deflection (Figure 11 b) can be given by:

$$\tau_{bl,f}^{dir,dir} = 1 - \frac{|w|}{h}, \quad |w| \leq h \tag{37}$$

Where

$$w = S\frac{\cos(\emptyset_b - \emptyset)}{\cos(\emptyset)} \tag{38}$$

Where φ_b is blind slat angle (deg) and φ is incident angle (deg)

Direct to diffuse blind transmittance and reflectance:

The direct to diffuse blind transmittance is determined using radiosity method that involves the total radiant flux in to the cell from s_i (J_i), the irradiance on the cell side of s_i (G_i) and the source flux from the cell side of s_i (Q_i)

For different segments of the cell shown in Figure 11 the above three quantities are inter related as :

$$J_1 = Q_1 \quad (39)$$

$$J_2 = Q_2 \quad (40)$$

$$J_3 = Q_3 + \rho^b_{dif,dif} G_3 + \tau_{dif,dif} G_4 \quad (41)$$

$$J_4 = Q_4 + \tau_{dif,dif} G_3 + \rho^f_{dif,dif} G_4 \quad (42)$$

$$J_5 = Q_5 + \rho^b_{dif,dif} G_5 + \tau_{dif,dif} G_6 \quad (43)$$

$$J_6 = Q_6 + \tau_{dif,dif} G_5 + \rho^f_{dif,dif} G_6 \quad (44)$$

$$G_i = \sum_{j-1}^{6} J_j F_{ji} \ , i = 1..6 \quad (45)$$

Where F_{ji} is the view factor between s_j and s_i, $\rho^b_{dif,dif}$ is blind back side diffuse to diffuse reflectance, $\rho^f_{dif,dif}$ blind front side diffuse to diffuse reflectance, $\tau_{dif,dif}$ blind diffuse to diffuse transmittance.

The above equations can be rewritten in matrix form as

$$Q' = XJ' \quad (46)$$

Where X is a six by six matrix and

$$J' = \begin{bmatrix} J_1 \\ J_2 \\ J_3 \\ J_4 \\ J_5 \\ J_6 \end{bmatrix} \qquad Q' = \begin{bmatrix} Q_1 \\ Q_2 \\ Q_3 \\ Q_4 \\ Q_5 \\ Q_6 \end{bmatrix}$$

Using $Q_1=Q_2=Q_5=Q_6=0$ and

$$for\ \emptyset_s \leq \emptyset + \frac{\pi}{2} (beam\ heats\ front\ of\ slats) \begin{cases} Q_3 = \tau_{dir,dif} \\ Q_4 = \rho^f_{dir,dif} \end{cases}$$

$$for\ \emptyset_s > \emptyset + \frac{\pi}{2} (beam\ heats\ back\ of\ slats) \begin{cases} Q_3 = \rho^b_{dir,dif} \\ Q_4 = \tau_{dir,dif} \end{cases}$$

The matrix can be solved for J', $J' = X^{-1}Q'$ and the front direct to diffuse transmittance and reflectance of the blind can be given by:

$$\boldsymbol{\tau^{dir,dif}_{bl,f} = G_2 = \sum_{j=3}^{6} J_j F_{j2}} \qquad \textbf{47}$$

$$\boldsymbol{\rho^{dir,dif}_{bl,f} = G_1 = \sum_{j=3}^{6} J_j F_{j1}} \qquad \textbf{48}$$

Diffuse to diffuse transmittance and reflectance of blind

Diffuse to diffuse optical properties are determined by assuming uniformly distributed diffuse radiation in each slat. Thus the cell shown in Figure 11 is divided in to two segments of equal length i.e. $s_3=s_4$ and $s_5=s_6$. For front side properties a unit source, $Q_1=1$ is assigned while all other Q_i are zero. Using similar methodology used for finding direct to diffuse transmittance and reflectance, the diffuse to diffuse transmittance and reflectance are given by

$$\tau_{bl,f}^{dif,dif} = G_2 = \sum_{j=1}^{6} J_j F_{j2} \quad (49)$$

$$\rho_{bl,f}^{dif,dif} = G_1 = \sum_{j=1}^{6} J_j F_{j1} \quad (50)$$

Glazing system transmittance

The overall optical property of the window glazing system can be found by considering the individual layers comprising the glazing system. For window glazing system with internal blind, the system transmittance for direct and diffuse radiation which depends on the incident angle and slat angle can be given as:

$$\begin{aligned} T_{f,sys}^{dir,all}(\emptyset,\emptyset_s) = T_{gl,ex}^{dir}(\emptyset)\Bigg(\tau_{bl,f}^{dir,dir}(\emptyset_s)\Bigg(T_{gl,in}^{dir}(\emptyset) \\ + \frac{T_{gl,int}^{dif} R_{gl,int,f}^{dir} \rho_{bl,b}^{dir,dif}}{1 - R_{gl,int,f}^{dif} \rho_{bl,b}^{dif}} + \frac{T_{gl,int}^{dif} R_{gl,int,f}^{dir} R_{gl,ext,b}^{dif}}{1 - R_{gl,int,f}^{dir} R_{gl,ext,b}^{dif}}\Bigg) \\ + \tau_{bl,f}^{dir,dif}(\emptyset_s)\Bigg(T_{gl,int}^{dif} \\ + \frac{\rho_{bl,f}^{dir,dif}(\emptyset_s) R_{gl,ext,b}^{dif} R_{gl,int,f}^{dif}}{1 - \rho_{bl,f}^{dif} R_{gl,b}^{dif} R_{gl,int,f}^{dif}}\Bigg)\Bigg) \end{aligned} \quad (51)$$

$$T_{f,sys}^{dif,dif} = \frac{\tau_{bl,f}^{dif,dif} T_{gl,ext}^{dif} T_{gl,int}^{dif}}{1 - R_{gl,int,f}^{dif} \rho_{bl,b}^{dif} R_{gl,ext,b}^{dif}} \quad (52)$$

4.3.5.2 Window Illuminance Model

Utilization of sunlight can save considerable amount of electric energy needed for lighting purpose. The lighting provided at the reference working plane should have a comfortable illuminance level. The window blind angles can be adjusted using

optimal controllers to provide the required illuminance level while considering the associated heat gain in an optimized manner.

An experimental model by Athenitis (Athienitis and Tzempelikos 2002) is used to predict the visible transmittance of the window blind. The model determines visibility transmittance as a function of sky condition (clear and overcast), blind slat angle (ϕ_s) and angle of incidence (ϕ). The model combines beam and diffuse radiations together but it is experimentally investigated that it doesn't cause much error since separate models are developed for clear and cloudy conditions. For cloudy days the visibility transmittance is given by:

$$\tau_v^{diffuse}(\emptyset_s) = \frac{4.5 * 10^{12} {\emptyset_s}^{-6}}{e^{\frac{335}{\emptyset_s}} - 1} \quad (53)$$

For clear sky incidence angle has significant effect on visible transmittance and visible transmittance is given by

$$\tau_v^{clear}(\emptyset_s, \emptyset) = 0.55 e^{\frac{-(\emptyset_s - 80)^2}{1900}} (-4.917 * 10^{-7}\emptyset^4 + 0.00009\emptyset^3 - 0.00567\emptyset^2 + 0.13\emptyset - 0.0437) \quad (54)$$

Accordingly the daylight transmitted to a building during overcast sky during a particular time and day of the year is given by (Murdoch 1985)

$$E_{overcast}(n, t) = E_w^{ov}(n, t)\tau_v^{diffuse}(\emptyset_s) \quad (55)$$

Where

$$E_w^{ov}(n, t) = 500\left(0.3 + 21 \sin\left(\alpha(n, t)\right)\right)(1 + \rho_g) \quad (56)$$

$\alpha(n,t)$ is solar altitude for a particular day n at a particular time t, ρ_g is ground reflectance.

For clear sky days the daylight transmitted through window consists of: direct sunlight(E_{wsun}), diffuse light from sky(E_{wsky}) and reflected light from ground(E_{wg}) and is given by (Murdoch 1985)

$$\boldsymbol{E_{clear}(n,t) = \tau_v^{clear}(n,t)\left(E_{wg}(n,t) + E_{wsky}(n,t) + E_{wsun}(n,t)\right)} \quad 57$$

Where

$$\boldsymbol{E_{wg}(n,t) = F_{w-g}\rho_g\left(E_{h,sky}(n,t) + E_{h,sun}(n,t)\right)} \quad 58$$

$$\boldsymbol{E_{wsky}(n,t) = F_{w-sky}E_{h,sky}(n,t)} \quad 59$$

$$\boldsymbol{E_{w,sun} = E_0 f(n) e^{-c.m(n,t)} \cos(\alpha(n,t))} \quad 60$$

Where ρ_g is ground reflectance, $F_{w\text{-}g}$ is window to ground view factor, $F_{w\text{-}sky}$ is window to sky view factor,

$$\boldsymbol{f(n) = 1 + 0.033\cos\left(360.\frac{n}{365}\right)} \quad 61$$

is a correction factor to account for elliptical shape of the earth's orbit around the sun, $E_{h,sky}$ and $E_{h,sun}$ are horizontal illuminance due to sky and solar horizontal illuminance given by:

$$E_{h,sun} = E_0 f(n) e^{-c.m(n,t)} \sin(\alpha(n,t)) \quad (62)$$

$$E_{h,sky}(n,t) = 800 + 15500[\sin(\alpha(n,t))]^{1/2} \quad (63)$$

Where E_0=127500lx is the average illuminance on a surface perpendicular to the sun's rays outside the earth's atmosphere(CIE 85 1989), c is the optical atmospheric extinction coefficient (0.21 for clear sky), and $m(n,t) = {}^{1}/_{\sin(\alpha(n,t))}$ is the relative optical air mass.

4.4 HVAC Component and Terminal Unit Models

4.4.1 Fan

Fan is responsible for pushing air to the required place at the required pressure. In HVAC system it is the second most energy consuming unit next to chiller/compressor (Westphalen and Koszalinski 1999). Its dynamics is much faster and quasi steady models can predict the performance in a reasonable accuracy. The Performance of a VFD fan can be estimated by simple polynomial based curve fit model that account for part load (EnergyPlus 2012). The relationship between airflow rate and fan power consumption is expressed as:

$$f_{flow} = {}^{\dot{m}}/_{\dot{m}_{design}} \quad (64)$$

$$f_{pl} = c_1 + c_2 f_{flow} + c_3 f_{flow}^2 + c_4 f_{flow}^3 + c_5 f_{flow}^4 \quad (65)$$

$$\dot{Q}_{tot} = {}^{f_{pl}\dot{m}_{design}\Delta P}/_{(e_{tot}\rho_{air})} \quad (66)$$

Where $\dot{Q}_{tot}$ is Fan power (W), $\dot{m}$ is air mass flow rate (kg/s), $\dot{m}_{design}$ is design (maximum) air flow (kg/s), ΔP is fan design pressure increase (Pa), e_{tot} is fan total efficiency, ρ_{air} is density of air (kg/m^3), c_1-c_5 are fan performance coefficients.

Due to unavailability of measured fan power data from the case building BMS, default parameters recommended by Commercial Energy Service Network (COMNET 2010) are used to characterize fan part load curve, fpl. The corresponding values used are listed in Table 7.

Table 7. Fan curve default values

Fan Type	C1	C2	C3	C4	C5
VFD Fan	0.0013	0.1470	0.9506	-0.099	0

4.4.2 Pump

Similar to fan, the performance of a VFD pump can be predicted using a polynomial-based curve fit that is based on part load ratio of the pump.

$$\boldsymbol{PLR = \dot{V} / \dot{V}_{des}} \quad (67)$$

$$\boldsymbol{Fraction\ Full\ Load\ Power = C_1 + C_2 PLR + C_3 PLR^2 + C_4 PLR^3} \quad (68)$$

$$\boldsymbol{P_{pump} = Fraction\ Full\ Load\ Power * P_{pump,des}} \quad (69)$$

Where PLR is pump part load ratio, P_{pump} is pump power consumption (W), $P_{pump,des}$ is design pump power Consumption(W), $\dot{V}$ is water flow rate (m^3/s), $\dot{V}_{des}$ is design pump capacity (m3/s) ,$C_1 - C_4$ is Pump performance coefficients.

4.4.3 Radiant Panel

The simulation model of the ceiling radiant panel is based on the steady state heat and mass equations given in the work of Conroy and Mumma (Conroy and Stanley 2001). The model calculate the cooling capacity of the ceiling radiant panel (q_o) using an iterative approach by assuming and correcting radiant panel surface temperature (T_c) for the given boundary conditions. In principle, radiant panels respond transiently to a change in room loads. However, the response time constant in a metal chilled panel is very short (<5 min) and this justifies the use of quasi-steady radiant panel model for model - based controllers and hourly analysis procedures (Jeong and Mumma 2004a). In this research an analytical method proposed by Mumma (Jeong and Mumma 2004b) is used and discussed below. More detail clarifications could be found in the reference.

The convective and radiative heat transfer from the radiant panel due to temperature difference between the panel surface temperature (Tp) and the room temperature (Tr) is given by (ASHRAE 2012)

$$\boldsymbol{q_r = h_r * (AUST - T_p)} \quad 70$$

$$\boldsymbol{q_{c,c} = h_{c,c} * (T_r - T_p)} \quad 71$$

$$\boldsymbol{q_{c,h} = 0.87(t_p - t_r)^{0.25}(t_p - t_r)} \quad 72$$

Where the convective and radiative heat transfer coefficients (h_r and $h_{c,c}$) are given by

$$\boldsymbol{h_r = 5e^{-8} * ((AUST + 273)^2 + (Tp + 273)^2) * ((AUST + 273) + (Tp + 273))} \quad 73$$

$$h_{c,c} = f_c + 2.13\left(T_r - T_p\right)^{0.31} \quad (74)$$

$$f_c = 0.28021 - 0.13931 * \Delta T \quad (75)$$

$$AUST = T_a - 3Z \quad (76)$$

$$Z = \frac{7}{(T_{oa} - 45)} \quad (77)$$

Where $q_{c,c}$ is convective heat transfer during cooling (W/m^2), $q_{c,h}$ is convective heat transfer during heating (W/m^2), qr is radiative heat transfer (W/m^2), h_r is radiative heat transfer (W/m^2K) and is based on ASHRAE fundamental, AUST is area weighted average temperature of all indoor surfaces of walls, ceiling, floor, window, door etc. (excluding active panel surfaces) , $h_{c,c}$ is convective heat transfer coefficient during cooling (W/m^2K) (Jeong and Mumma 2004b)

Convective and radiation heat transfer equations shown above (Equation 70 and Equation 71) assumed known panel surface temperature (T_{pm}) which is not a measured value. Thus an initial guess is used which is later updated by equation 85 for a defined convergence criteria between the initial guess and computed value of T_{pm}. The approach for determining T_{pm} is discussed below.

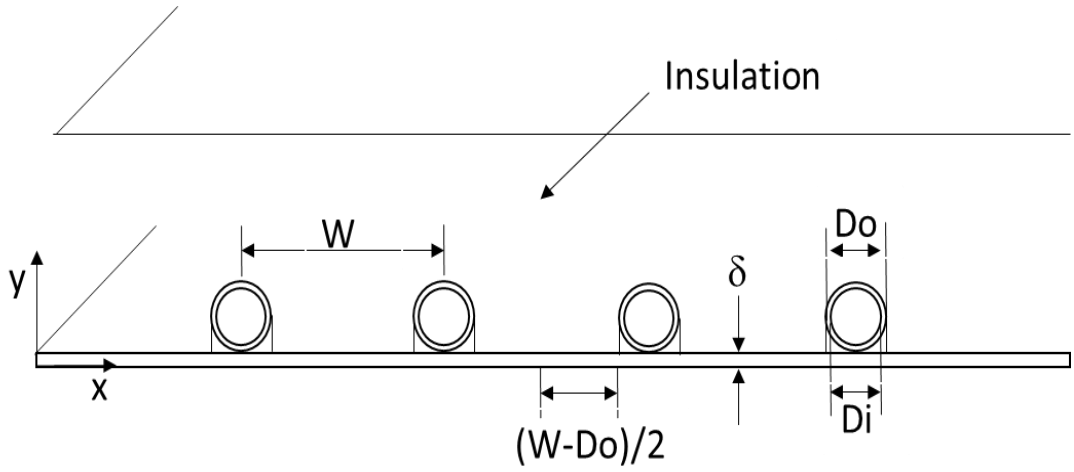

Figure 12. Cross section of top insulated ceiling radiant panel. [source:(Jeong and Mumma 2004b)]

The radiant panel effectiveness, i.e. ratio of actual heat transfer to the ideal heat transfer when the entire panel surface is at the base temperature T_b (the temperature immediately below the tubes) is given by

$$F = \frac{\boldsymbol{tanh}(\boldsymbol{m}(\boldsymbol{w}-\boldsymbol{D_o})/\boldsymbol{2})}{(\boldsymbol{m}(\boldsymbol{w}-\boldsymbol{D_o})/\boldsymbol{2})} \quad , \qquad \boldsymbol{m} = \sqrt{\boldsymbol{U_o}/\boldsymbol{k}\,.\,\boldsymbol{\delta}} \tag{78}$$

where U_o overall heat transfer coefficient (W/m^2K), k panel material conductivity (W/mK), δ panel thickness (m), D_o panel tube outer diameter (m), W panel tube spacing (m)

The ratio between overall heat transfer coefficient between fluid and room to overall heat transfer coefficient between fin and room, F' is given by

$$\boldsymbol{F'} = \frac{\boldsymbol{1}/\boldsymbol{U_o}}{\boldsymbol{w}\left[\frac{\boldsymbol{1}}{\boldsymbol{U_o}[\boldsymbol{D_o}+(\boldsymbol{w}-\boldsymbol{D_o})\boldsymbol{F}]}+\frac{\boldsymbol{1}}{\boldsymbol{h_i}\boldsymbol{\pi}\boldsymbol{D_i}}\right]} \tag{79}$$

Where the forced heat transfer coefficient inside the tube (h_i) for a give hydraulic diameter (D_h) and fluid conductivity (k_f) is given by

$$\boldsymbol{h_i = \frac{Nu_D k_f}{D_h}, \quad Nu_D = 0.023 \, . Re_D^{4/5} . \, Pr^{0.4}} \tag{80}$$

The temperature of the fluid leaving the can be derived using mass and energy balance in the direction of flow and is given by

$$\frac{T_{fo} - T_r}{T_{fi} - T_r} = exp\left(-\frac{U_o \, . A_p \, . \, F^{'}}{\dot{m} C_p}\right) \tag{81}$$

Where T_{fi} is fluid inlet temperature, A_p panel area, C_p is specific heat capacity (kJ/kg k), $\dot{m}$ is mass flow rate to the panel (kg/s), F' is panel efficiency factor

The panel heat removal factor (FR) which relates the actual heat gain by the panel to the heat gain by the panel if the entire surface of the panel were at the fluid inlet temperature (T_{fi}) is given by

$$F_R = \frac{\dot{m} C_p (T_{fo} - T_{fi})}{A_p U_o (T_a - T_{fi})} \tag{82}$$

The heat transfer (q_o) form the panel can be given in terms of the fluid inlet temperature as well as panel mean surface temperature (T_{pm}) can be given in Equation 83 and Equation 84

$$q_o = F_R U_o (T_a - T_{fi}) \tag{83}$$

$$q_o = U_o (T_a - T_{pm}) \tag{84}$$

The above two equations (83 and 84) can be equated and solved for the mean surface temperature (T_{pm}) as given in equation 85.

$$T_{pm} = T_{fi} + \frac{\dot{m}C_p\left(T_{fo} - T_{fi}\right)}{A_p F_r U_o} \cdot (1 - F_R) \qquad 85$$

4.4.4 Heating /Cooling Coil

The cooling /heating coil model is used to predict the required amount of chilled water/hot water and the related heat transfer to the air. In this research the task of dehumidification is assumed to be entirely done by the existing passive desiccant wheel downstream of the cooling coil and thus the working state of cooling coil is completely dry .i.e. no condensation exists at the cooling coil. Thus similar model can be used for both heating and cooling coil. A simplified parametric equation developed by Wang (Y.-W. Wang et al. 2004) is used. The heat extracted from or rejected to the air by the coil during cooling or heating is given by:

$$\boldsymbol{Q = \frac{c_1 m_a^{0.8}}{1 + c_2\left(\frac{m_a}{m_w}\right)^{0.8}}\left(T_a - T_w\right)} \qquad 86$$

Where Q is heat transfer from the coil to the air (W), m_a is mass flow rate of air (kg/sec), m_w is mass flow rate of chilled/hot water, T_a is temperature of incoming air (^oC), Tw is inlet temperature of chilled/ hot water (^oC), C_1, C_2 are parameters that accounts for heat transfer coefficients in the air and water side. Detailed definitions and derivation of these parameters can be found in (Y.-W. Wang et al. 2004). Actual trended values from the building management system (BMS) is used to determine the values of C1 and C2 and after parameter identification the model result

is compared with actual result and is shown in Figure 13. It is evident from the plot that the predicted values are in 95% confidence interval range for most of the time.

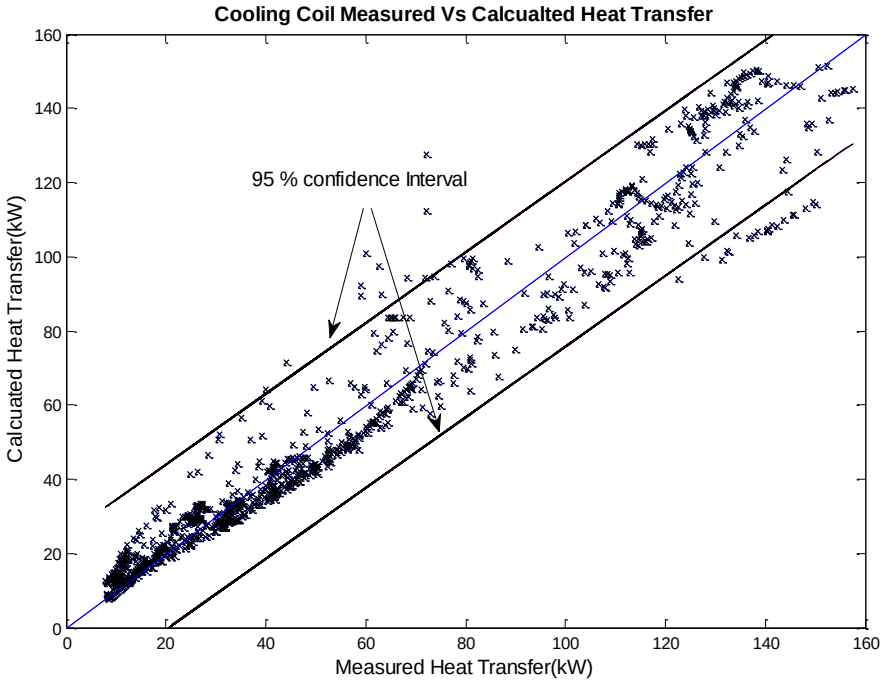

Figure 13. Comparison of measured and calculated cooling coil heat transfer

In the event where chilled/ hot water flow rate is not available from Building Management System(BMS) , Pressure difference across the coil , Δp can be used to determine mass flow rate(Y.-W. Wang et al. 2004).

$$\dot{m}_{chw} = \frac{-a_1 + \sqrt{a_1^2 - 4a_2(a_0 - \Delta p)}}{2a_2} \quad 87$$

Where a_0, a_1 and a_2 are model parameters to be determined through catalogue data or online testing.

4.4.5 Enthalpy Wheel

An Enthalpy Wheel is a type of energy recovery ventilator (ERV) whereby energy is transferred form exhaust air to incoming air through the use of a rotating air permeable heat exchanger. During winter, the system pre-heat and humidity the incoming outdoor air while it dehumidify and pre-cool the incoming outdoor air. The

heat exchangers are generally made of porous materials to increase surface area which aids in energy transfer.

A general model of the enthalpy heat recovery wheel which is provided in the documentation of EnergyPlus**(EnergyPlus 2012)**. The model is based on sensible and latent effectiveness obtained from balanced flow (similar supply and return flow rates) at 75% and 100% of the nominal flow rate. These data are available from manufacturer catalogue and can also be found in Air conditioning, Heating and Refrigeration Institute (AHRI) certified product directory. The values for the case building SEMCO TE-18 model enthalpy wheel are shown in **Table 8**

$$\boldsymbol{\varepsilon_s = \varepsilon_{s,75\%} + (\varepsilon_{s,100\%} - \varepsilon_{s,75\%})\left(\frac{HX_{flowratio} - 0.75}{1 - 0.75}\right)} \quad 88$$

$$\boldsymbol{\varepsilon_l = \varepsilon_{l,75\%} + (\varepsilon_{l,100\%} - \varepsilon_{l,75\%})\left(\frac{HX_{flowratio} - 0.75}{1 - 0.75}\right)} \quad 89$$

Where $\varepsilon_{s,75\%}$ is sensible effectiveness at 75% flow, $\varepsilon_{s,100\%}$ is sensible effectiveness at 100% flow, , $\varepsilon_{l,75\%}$ is latent effectiveness at 75% , $\varepsilon_{l,100\%}$ is latent effectiveness at 100% flow, $HX_{flowratio}$ is the ratio of the average volumetric flow rate ((supply flow + exhaust flow)/2) to the nominal supply flow rate, ε_l is latent effectiveness at the operating condition and ε_s is sensible effectiveness at the operating condition.

Table 8. SEMCO TE-18 sensible and latent effectiveness

Air flow	100%		75%	
	ε_s	ε_l	ε_s	ε_l
Heating	79	79	84	83
Cooling	79	78	84	82

The supply air condition in terms of temperature and humidity ratio can be determined using the heat exchanger effectiveness and stream flow conditions as:

$$T_{1,out} = T_{1,in} + \varepsilon_s \left(\frac{\dot{m}c_{p,min}}{\dot{m}c_{p,1}} \right) (T_{2,in} - T_{1,in}) \quad 90$$

$$\omega_{1,out} = \omega_{1,in} + \varepsilon_l \left(\frac{\dot{m}c_{p,min}}{\dot{m}c_{p,1}} \right) (\omega_{2,in} - \omega_{1,in}) \quad 91$$

$$\dot{m}c_{p,min} = min(\dot{m}_1 c_{p,1}, \dot{m}_2 c_{p,2}) \quad 92$$

Where T is air temperature(°C), ṁ is air mass flow rate(kg/sec) , ω is humidity ration(kg water/kg air), $\dot{m}c_p$ is heat capacity rate (W/K) and the Subscripts 1 is for supply flow, 2 is for exhaust flow, in is inlet and out is outlet.

4.4.6 Passive Desiccant Wheel

Passive desiccant wheel works on the principle of sorption by which a desiccant removes moisture form the air. Unlike the enthalpy recovery wheel, the partition and the rotation speed of an active dehumidification unit are designed to drive the moisture and heat removal along the isenthalpic line. The process is illustrated in Figure 14. The process air passes through ¾ of the desiccant wheel and the regeneration air passes through 1/4 of the wheel. The operation and dynamic modeling is much more complex than enthalpy recovery wheel.

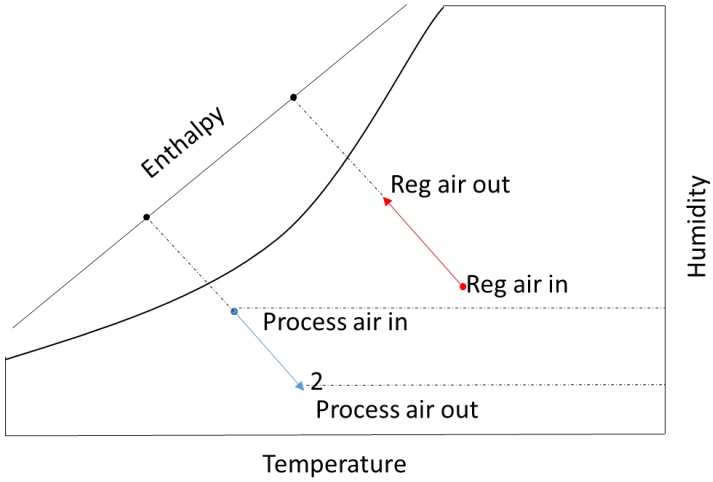

Figure 14. Desiccant wheel dehumidification process

Out let temperature and humidity of the process air can be estimated using inlet conditions of process air and regeneration air as shown below(EnergyPlus 2012).

$$R_{T,out} = B_1 + B_2.R_{w,in} + B_3 R_{T,in} + B_4\left(R_{w,in}/R_{T,in}\right) + B_5.P_{w,in} + B_6 P_{T,in} + B_7\left(P_{w,in}/P_{T,in}\right) + B_8.RFV \quad (93)$$

$$R_{w,out} = C_1 + C_2.R_{w,in} + C_3 R_{T,in} + C_4\left(R_{w,in}/R_{T,in}\right) + C_5.P_{w,in} + C_6 P_{T,in} + C_7\left(P_{w,in}/P_{T,in}\right) + C_8.RFV \quad (94)$$

Where R is regeneration air, P is process air , RFV is face velocity of regeneration air (m/s), B_1---B_7 , C_1---C_7 are parameters to be determined from measured data and subscripts *T* is temperature (^oC), ω is humidity ratio (kg water/kg air) , *in* is incoming air and *out* is outgoing air.

Face velocity of regeneration air (RFV) can be calculated as

$$\mathbf{RFV} = \dot{\mathbf{m}}_{\mathbf{reg,in}} \Big/ \boldsymbol{\rho}_{\mathbf{a}}\mathbf{A}_{\mathbf{face}} \qquad 95$$

Where $\dot{m}_{reg,in}$ is mass flow rate of regeneration air (kg/s), ρ_a is density of air (kg/m3), A_{face} is heat exchanger face area (m^2) which is given by

$$\mathbf{A}_{\mathbf{face}} = \mathbf{V}_{\mathbf{face,nom}} \Big/ \dot{\mathbf{v}}_{\mathbf{face,nom}} \qquad 96$$

Where $V_{face,nom}$ is nominal air volume flow rare specified for the heat exchanger (m^3/s) $\dot{v}_{face,nom}$ is nominal air face velocity specified for the heat exchanger (m/s). Assuming adiabatic condition with the surrounding air and balanced air flow between regeneration and process side, the process side outlet temperature and humidity can be determined by applying energy and mass balance and is given by

$$\boldsymbol{T_{p,out} = T_{p,in} - \left(R_{T,out} - R_{T,in}\right)} \qquad 97$$

$$\boldsymbol{w_{p,out} = w_{p,in} - \left(w_{T,out} - w_{T,in}\right)} \qquad 98$$

Nonlinear regression analysis is performed to determine the parameters in Equation 93 and Equation 94. The results show that the model predict the temperature and relative humidity in an acceptable accuracy.

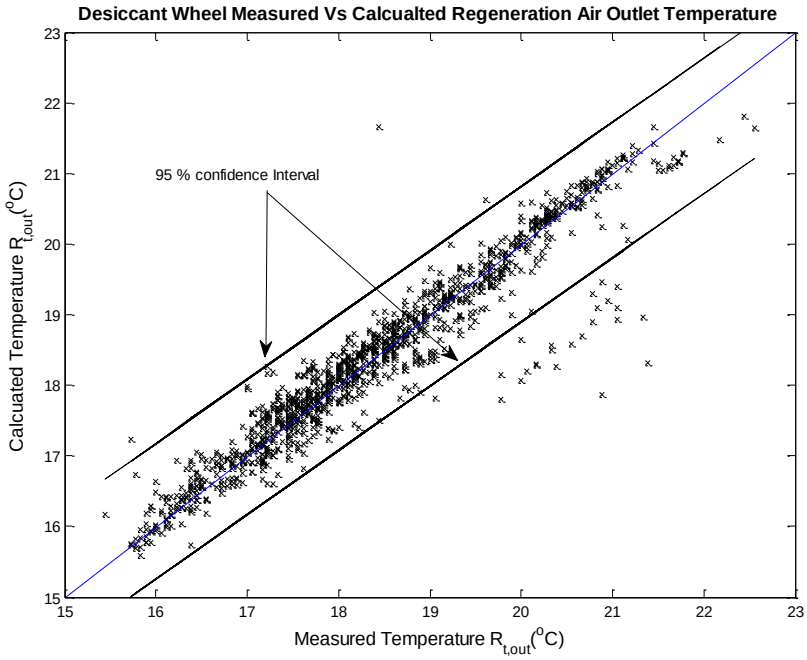

Figure 15. Comparison of measured and predicted desiccant wheel outlet temperature

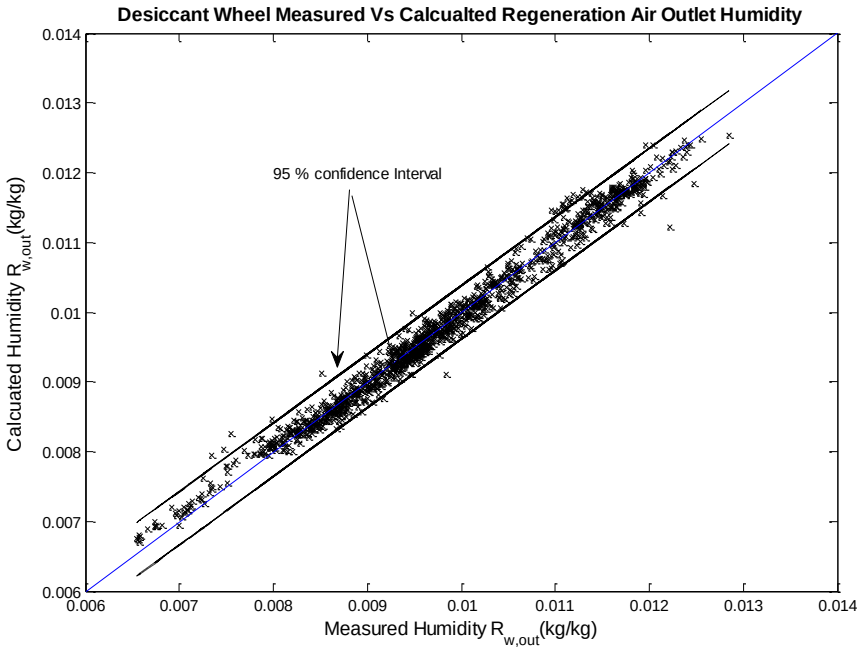

Figure 16. Measured and predicted desiccant wheel outlet humidity ratio

4.5 Development of Simplified Models for MPC

One of the issues in model - based control system is to find a reliable and yet simplified model for predicting the response of the system for various controlled and

uncontrolled disturbances. The model for whole building energy analysis and control involves varies complicated differential and analytical equations. Inclusion of these equations in model - based control system increase the computation time and development effort which makes it infeasible for model - based control design. In the past various efforts have been made to simplify building models from heat transfer point of view((Deng et al. 2010),(Antoulas and Sorensen 2001)).

In this research efforts have been made to develop simplified models that can capture building envelope heat gain as well as lighting resulting from solar radiation. To minimize the number of equations to be solved for wall heat gain, walls in each zone with the same construction material are lumped together and the corresponding heat gains are determined for the lumped wall. Detailed model results from EnergyPlus are used to develop simplified parametric equations to capture the effect of building geometry in the corresponding heat gain and are discussed in detail below.

4.5.1 Lumped Wall Model

The construction of Building wall involves different layers of construction material with different thermal resistance and heat capacity. To simplify the conductive heat transfer from outdoor to indoor or vice versa lumped mass approach is used by most simulation tools. One of the widely used lumped mass model is ASHRAE thermal network model with three resistances and two capacitance (3R2C) to represent the entire wall assembly(ASHRAE 2009).

In this research we lumped walls of similar construction material existing in different orientation of a particular zone. This will greatly reduce the number of ODE equations to solve and significantly reduce the computation time especially when the building has a large number of zones. The parameters that will be affected due to wall lumping

are convective heat transfer coefficients and short wave/long wave radiations absorbed by individual surfaces. For internal surfaces, constant internal convective coefficients suggested by Walton (Walton 1983) are used. Though outdoor convective heat transfer is changing through-out the day mainly due to local wind speed, constant outdoor convective heat transfer of 20 W/m^2k is used (IDAE 2009). To see effect of constant outdoor convective heat transfer on the outdoor wall surface temperature, the same wall is simulated using constant h_o and h_o obtained using DOE-2 Model. The result is shown in Figure 17 and it is evident from the figure that effect of using constant h_o on the surface wall temperature is negligible. This is because of the fact that the main factor affecting the wall surface temperature is the shortwave/long wave radiation absorbed on the surface and the convective heat gain has little effect.

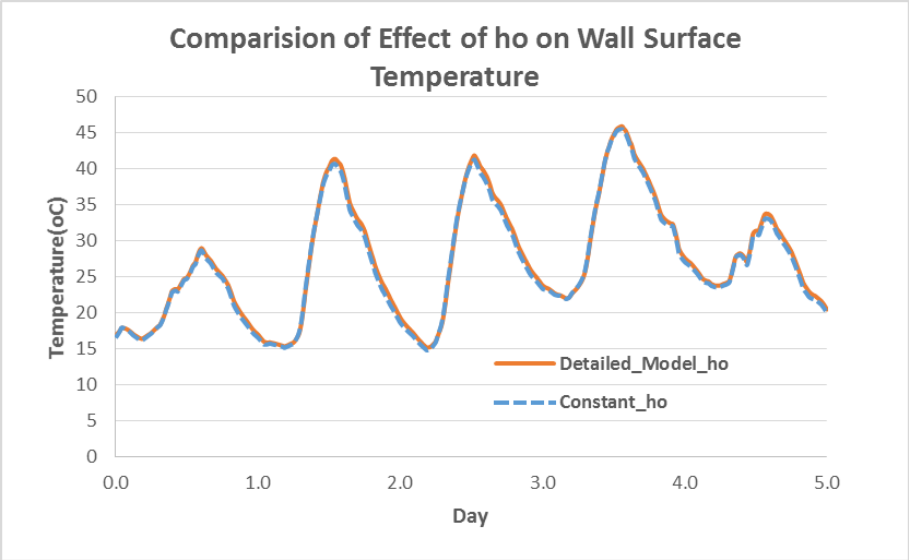

Figure 17: Comparison of constant and variable outdoor convective heat transfer on wall surface temperature

The assumption of constant inside and outside heat transfer coefficients make all the external walls to be exposed to similar boundary condition except for the radiation heat sources. Thus the individual walls can be merged together to result a lumped wall with the following physical properties

$$C_L = \sum_{i=1}^{n} C_i \quad (99)$$

$$R_L = R_1 = R_n \quad (100)$$

Where C- is thermal capacitance (J/k), R is thermal resistance (K/wm^2) and subscripts L, i and n stands for lumped, individual wall and number of sides of a zone with similar wall types.

The shortwave and long wave radiation heat gain by each surface is added to get the total radiation heat exchange by the lumped wall.

$$Q_{sw/lw} = \sum_{i=1}^{n} Q_{sw/lw,i} * A_i \quad (101)$$

Where $Q_{sw/lw}$ total short wave or long wave radiation absorbed by the lumped surface, $Q_{sw/lw,i}$ is short wave or long wave radiation absorbed by individual surfaces, A_i is area corresponding to each individual surfaces.

The shortwave radiation incident on the outside surface is the summation of direct and diffuse radiations. For a surface with a particular orientation it can be calculated as(ASHRAE 2009)

$$Q_{sw} = Q_{sw,dir} + Q_{sw,dif} \quad (102)$$

$$Q_{sw,dir} = I_b cos\theta \frac{S_s}{S} \quad (103)$$

$$Q_{sw,dif} = I_s F_{ss} + I_g F_s \quad (104)$$

Where Q_{sw} is short wave radiation incident on a surface (w/m^2), $Q_{sw,dir}$ is direct short wave radiation (W/m^2), $Q_{sw,dif}$ is diffuse short wave radiation (w/m^2), θ angle of incidence of the sun's rays (deg), S is area of the surface (m^2), S_s is sunlit area (m^2), I_b is intensity of direct radiation (W/m^2), I_s is intensity of sky diffuse radiation(W/m^2), I_g is intensity of ground reflected diffuse radiation (W/m^2), F_{ss} is angle factor between the surface and the sky and F_{sg} is angle factor between the surface and the ground.

One of the major factors affected by wall lamping is the total heat gain/loss due to long wave radiation since each surface will have a different surface temperature that is resulted due to different shortwave radiation absorbed. The long wave heat exchange per unit area for external surface can be given by (Walton 1983).

$$q''_{LWR} = \varepsilon\sigma F_{gnd}\left(T_{gnd}^4 - T_{surf}^4\right) + \varepsilon\sigma F_{sky}\left(T_{sky}^4 - T_{surf}^4\right) + \varepsilon\sigma F_{air}\left(T_{air}^4 - T_{surf}^4\right) \quad (105)$$

Where q''_{LWR} is long wave radiation exchange (W/m^2), ε is surface emissivity, σ is Stefan- Boltzmann constant (5.67e-8W/m^{2}k^4), T is temperature(k),F_{gnd} view factor of wall surface to ground surface temperature, F_{air} is view factor between wall surface and air temperature, F_{sky} is view factor sky temperature. The long wave view factors to ground and sky are calculated using the expression (Walton 1983)

$$F_{gnd} = 0.5(1 - cos\emptyset) \quad (106)$$

$$F_{sky} = (0.5(1 + cos\emptyset))^{3/2} \quad (107)$$

$$F_{air} = 0.5(1 + cos\emptyset)(1 - \sqrt{0.5(1 + cos\emptyset)}) \quad (108)$$

Where ϕ is the tilt angle of the surface (90^o for vertical surfaces). In equation 105 the ground surface temperature is assumed to be the same as the air temperature(EnergyPlus 2012).

Lumped wall long wave radiation heat gain is compared against summation of long wave radiation heat gain of each individual walls as shown in Figure 18. The result shows that there is considerable difference. But the effect of long wave radiation on the wall surface temperature is outwaited by shortwave radiation incident on the surface and it has very small effect on the surface temperature. Figure 19 shows comparison of lumped wall external surface temperature against weighted average external surface temperature of the individual walls. It is evident from the figure that the difference is very small and the assumption of wall lumping is valid, especially for models that doesn't require very detailed analysis like the one used for optimal control designs.

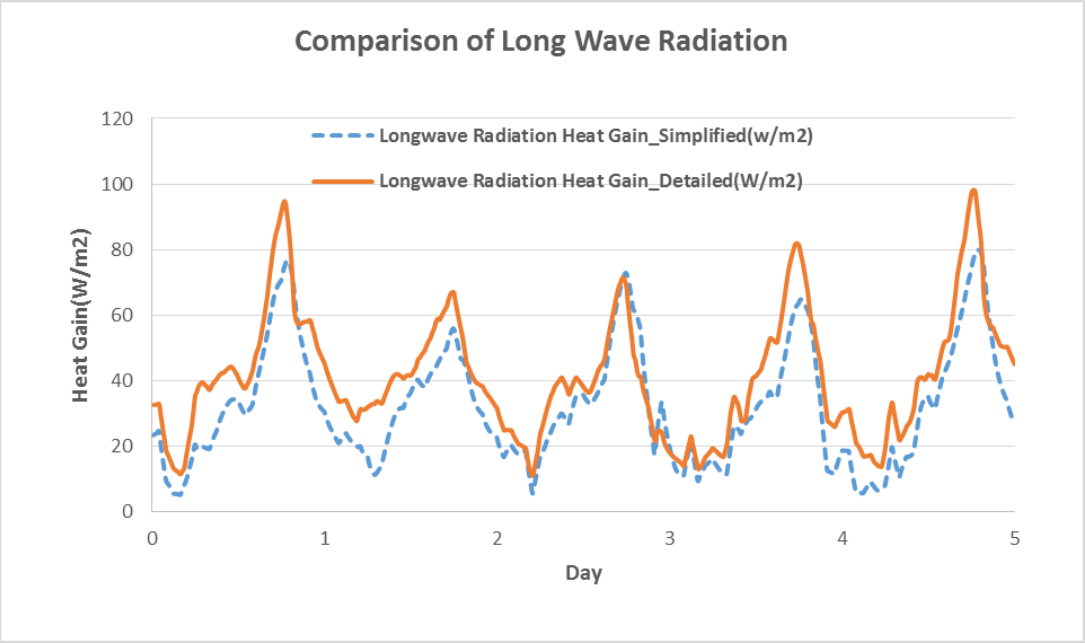

Figure 18: Comparison of effect of wall lumping on surface long wave radiation heat gain

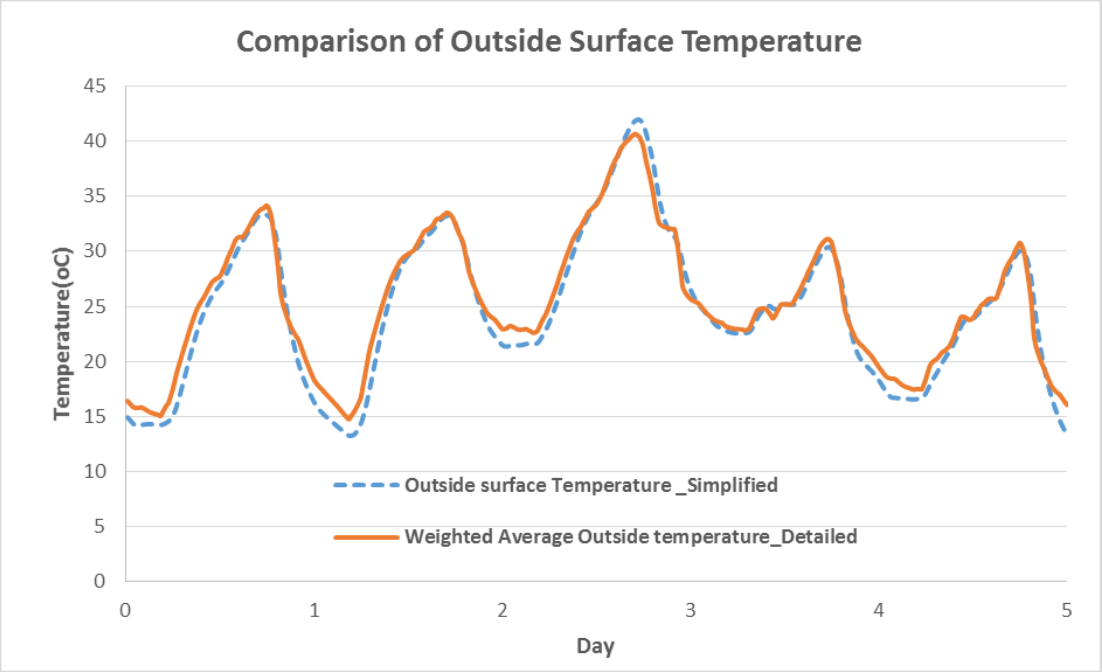

Figure 19: Comparison of effect of long wave radiation difference on wall surface temperature

4.5.2 Simplified Model for Shortwave Radiation absorbed by Internal Surfaces

Once short wave radiation is transmitted through the window, it should be absorbed by different surfaces of the particular zone before it starts to affect the room thermal condition. Determination of portions of the total transmitted radiation absorbed by these different surfaces is quite complicated and it involves the relative positions and orientations of the surfaces from the source window.

Short wave radiation absorbed by building wall internal surface is the summation of radiation transmitted through fenestration and radiation from electric lighting. Different treatment is needed for those two contributing factors due to the fact that radiation thorough fenestration is a function of orientation while radiation from internal sources is not. Determination of the portion of to the total shortwave radiation absorbed by different absorbing surfaces of a zone is complex and the development effort is high especially for buildings with many zones with source windows located in different orientations. In this research simplified parametric equations are

developed using data from EnergyPlus simulation of the same building (Equation 109). For the parametric identification process, the factors affecting the magnitude of the shortwave radiation absorbed were identified first which include intensity of outside solar radiation, transmittance of the fenestration surface, total fenestration area, area of the internal surface, absorptivity of internal surface and relative orientation of the fenestration and internal surface.

$$\boldsymbol{Q_{sw,int} = (a * Q_{sw,trans} + b * Q_{l,rad}) A_{is}\, \alpha_{is}} \qquad \textbf{109}$$

$$\boldsymbol{Q_{sw,trans} = \left(Q_{sw,dir} * \tau_{dir} + Q_{sw,dif} * \tau_{dif}\right) * A_W} \qquad \textbf{110}$$

Where $Q_{sw,int}$ is heat gain on internal surface due to shortwave radiation absorbed from solar radiation and electric lighting (W), $Q_{sw,trans}$ is short wave radiation transmitted through fenestration (W), $Q_{l,rad}$ is the radiation portion of the lighting energy (W), $\boldsymbol{Q_{sw,dir}}$ is direct short wave radiation (W/m2), $Q_{sw,dif}$ is diffuse short wave radiation (W/m^2) ,A_{is} is area of internal surface (m^2), Aw is area of the short wave radiation source window (m^2), τ_{dir} is direct transmittance of the fenestration material (details shown in "window model" section), τ_{dif} is diffuse transmittance of the fenestration material, α_{is} is absorption of the internal surface and *a* and b are constants to be identified based on measured data or simulation results from detailed models. The accuracy of the above approach is compared with results from detailed model (EnergyPlus model) for internal wall surface and the result is shown in Figure 20.

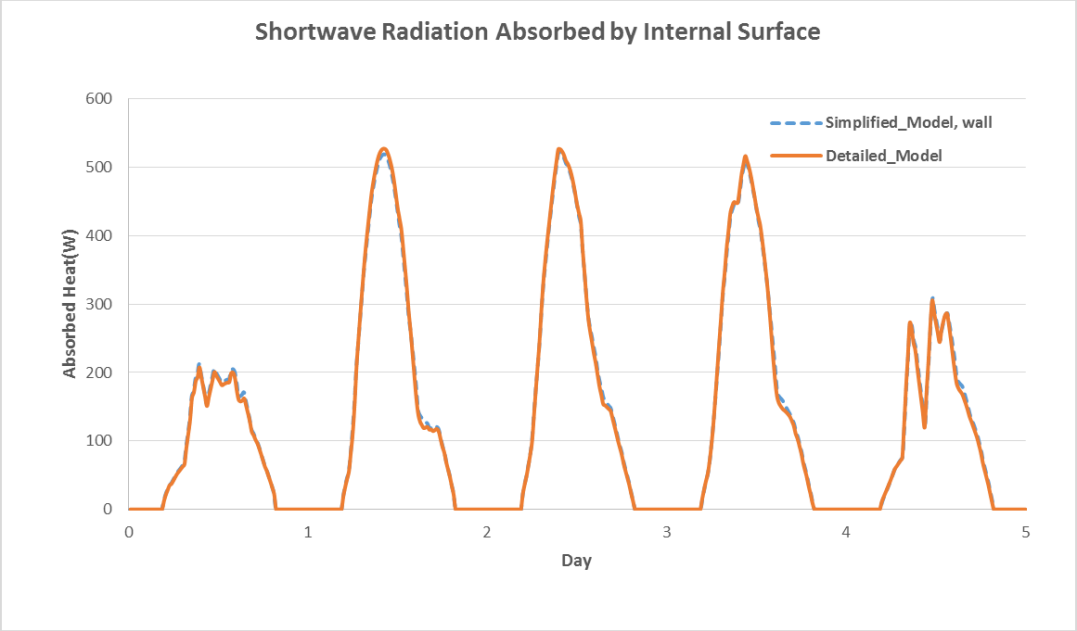

Figure 20: Comparison of solar shortwave radiation absorbed by building internal surface

4.5.3 Simplified Model for Zone Illuminance from Solar Radiation

Besides affecting thermal condition of a building, transmitted solar radiation affects the lighting level of the building. From lighting control point of view, the lighting level at a reference plane has to be determined so that appropriate lighting dimming can be applied to maintain the required illuminance. Finding the proportion of total transmitted illuminance falling on a reference plane involves consideration of view factor of the reference plane relative to each source of illumination. To help the computation, a simplified parametric equation is developed that only requires a one-time computation of the values from detail models like EnergyPlus model. This help to determine the illuminance level without considering the detailed physical phenomena. Based on simulated result a single parameter, g_f, can be determined that can capture the geometric effect on the proportion of illuminance on a reference plane and it can be given by

$$Illum_{ref} = gf * Illum_{trans} \quad (111)$$

Where $Illum_{ref}$ is the illuminance level at a reference level (lux), $Illum_{trans}$ is total transmitted illuminance through window (lux) and gf is the geometric factor used to map transmitted illuminance to illuminance at a reference level.

The above approach is tested for a specific reference point and the comparison between simplified and detailed model (EnergyPlus) is shown in Figure 21

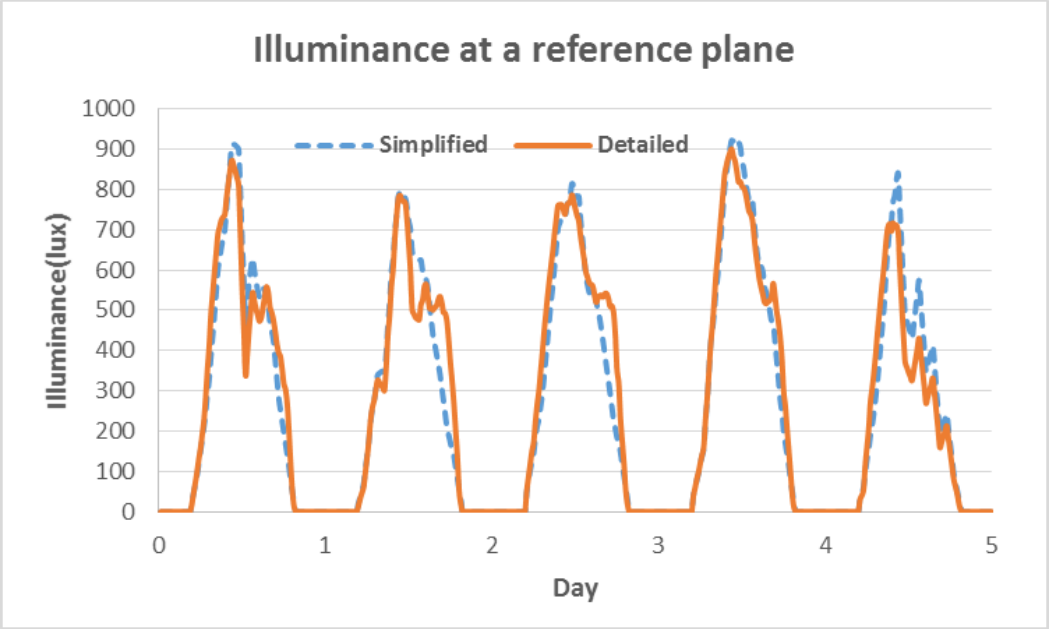

Figure 21. Comparison of illuminance level at a reference plane in a zone

4.6 Combined Building Model Verification

Before implementation of the simplified reduced model for MPC application, combined model verification is done against a more detailed model. In this research detailed EnergyPlus model is used as a virtual building for model verification. The building zone temperature computed using simplified models discussed in the previous sections is compared against an EnergyPlus model with no HVAC system to

see the accuracy of the building envelope system heat transfer and the result is shown Figure 22. The figure shows the simulation results for typical winter and summer days and it confirms that the simplified model predict the zone temperature in a good accuracy (±0.75^{o}C).

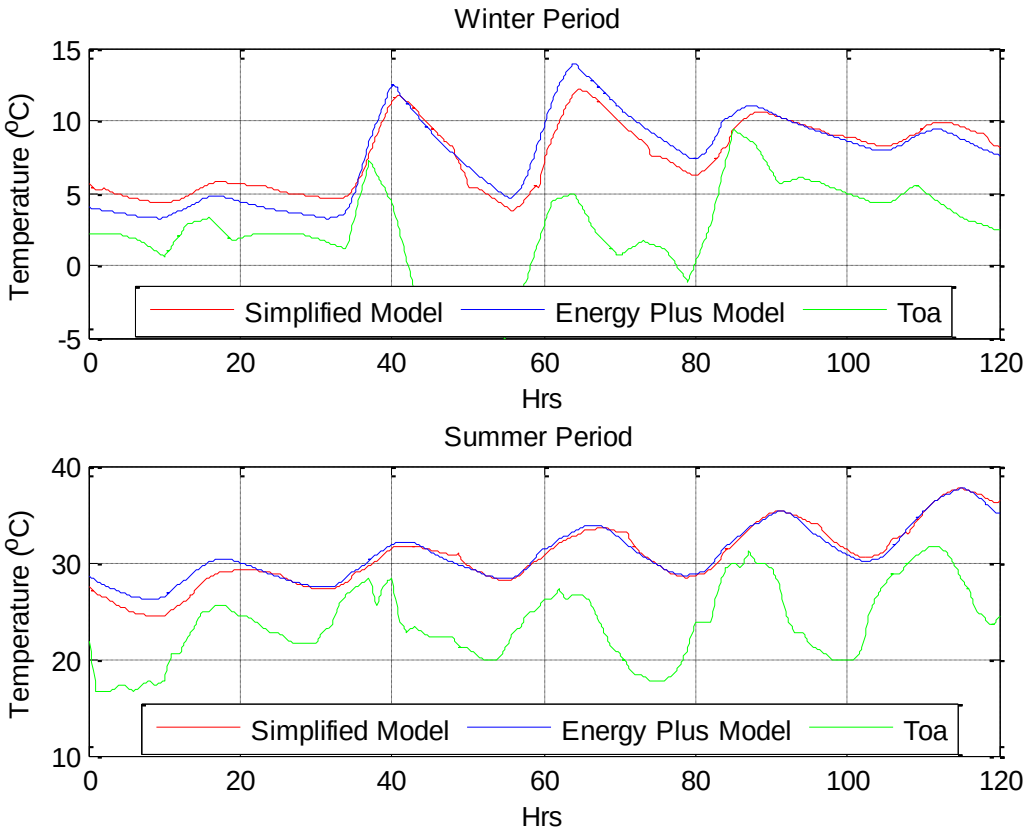

Figure 22. Zone temperature comparison between simplified and detailed model.

Besides the building model, some of the component models used in the MPC model are different from the baseline EnergyPlus models which result some difference during prediction for the whole building simulation including the HVAC system. These include models for cooling/heating coil and radiant panels. The whole building simulation results from MPC model and EnergyPlus model are compared using the

following parameters: Room temperature, relative humidity, PMV value and indoor CO2 concentration and the results are shown below.

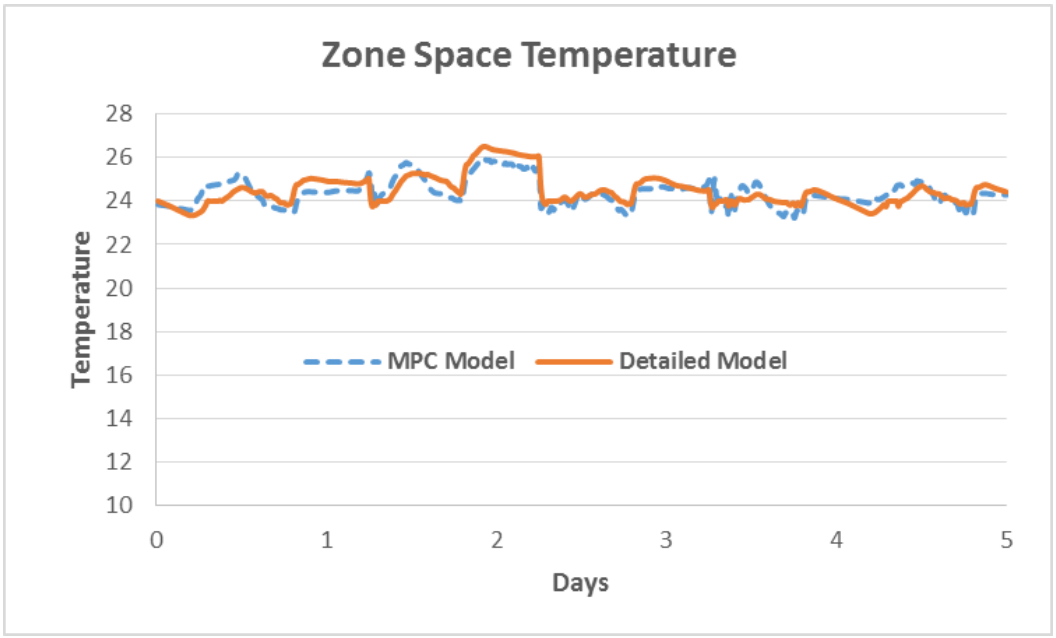

Figure 23. Comparison of zone air temperature

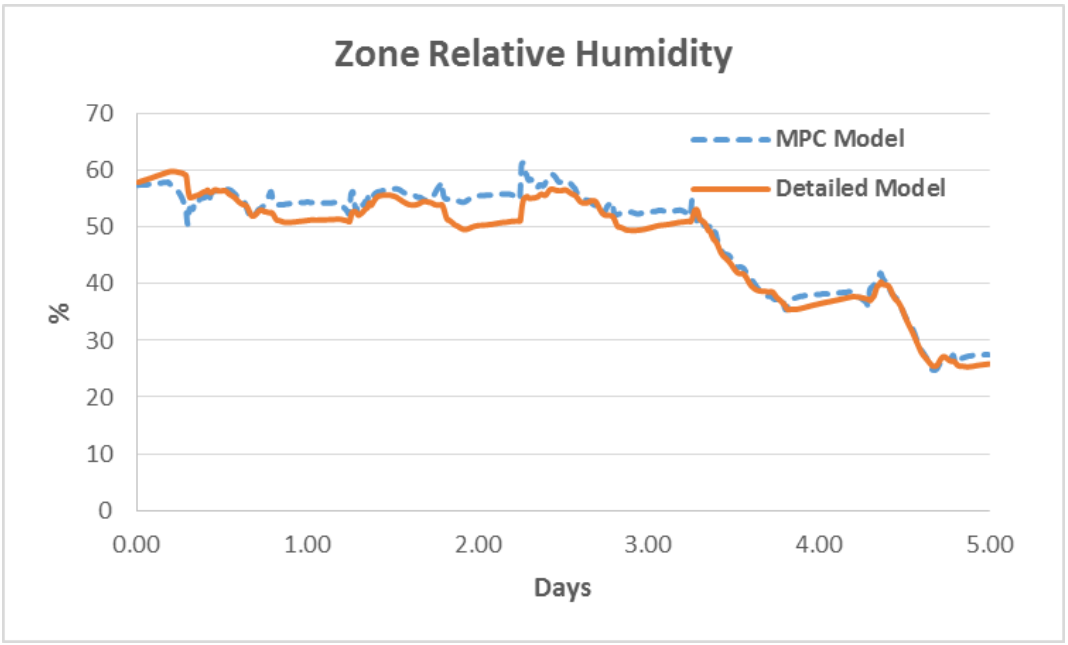

Figure 24. Comparison of zone air relative humidity

Figure 23 and Figure 24 show comparison of zone temperature and relative humidity for five days during summer. It is evident from the plot that there is a difference of

±1°C for temperature and ±5% for relative humidity between the simplified and detailed model. For control purpose this is a reasonable accuracy since the error is dumped by the use of actual temperature and relative humidity form the building as a feedback at each time step. The variation shown is mainly due to the assumption of a different radiant panel model which mainly controls the zone heating and cooling process as well as simplified models for capturing the heat transfer analysis and the length of discretization time used. A good accuracy can be obtained with small discretization time interval but it could potentially compromise the computation time needed. Figure 25 shows comparison of thermal comfort condition in terms of predicted mean vote (PMV). The observed temperature and relative humidity shown in the previous figures (Figure 23 and Figure 24) affect the zone PMV calculation and the comparison shows a maximum difference of ±0.2 between the detailed model and the MPC model.

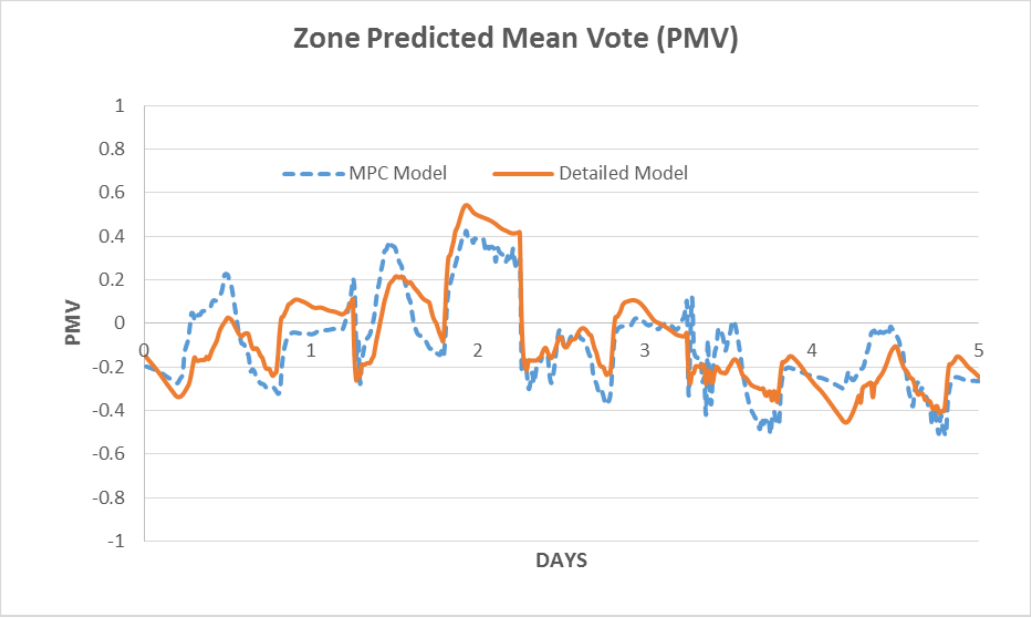

Figure 25. Zone thermal comfort interms of Predictive Mean Vote (PMV)

Besides room thermal comfort conditions, room contaminant (CO_2) concentration comparison is done and is given in Figure 26. The MPC model uses a similar contaminant model like the detailed EnergyPlus model and the result confirms its accuracy. The approach used for CO2 can be extended to other critical contaminates for the purpose of critical contaminant based demand control ventilation design.

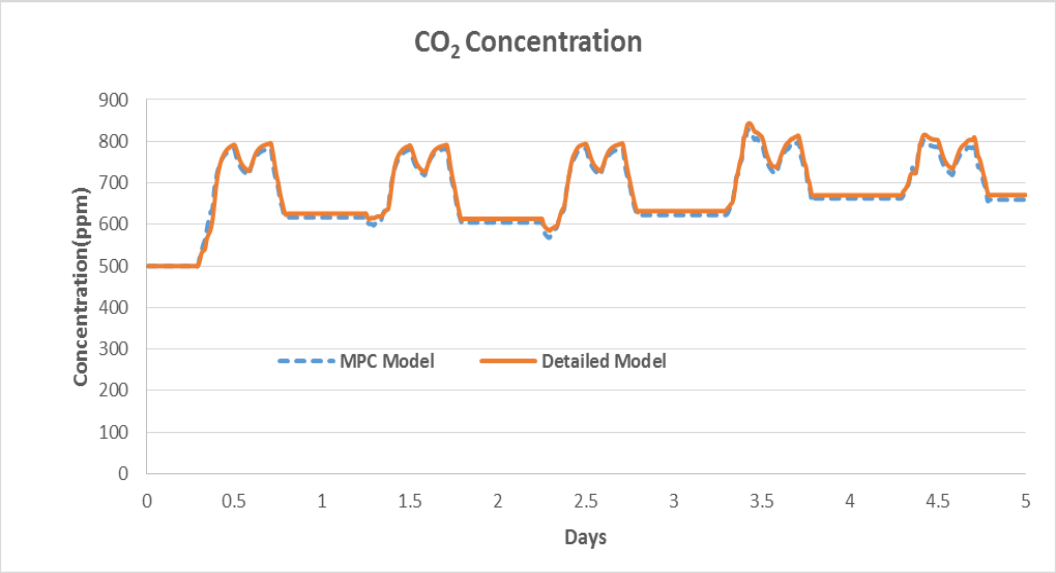

Figure 26: Room CO_2 concentration

In summary the previous whole building models available are either too simplified which are only used for the consumption of concept proving or too complicated which are not suitable for online optimization strategies like MPC. The models developed in this research are well simplified and at the same time address all the possible disturbances affecting the indoor environment quality in terms of thermal comfort, lighting and contaminants. As clearly shown in the comparison figures, the accuracy of the simplified models are reasonable and can be used for control purpose. It should be noted that in Model Predictive control strategy, at each time step zone conditions including temperature, humidity, lighting and contaminant concentration are feed to

the MPC while the MPC generates the next step control parameters depending on the received feedback and future prediction. The use of actual sensor values as a feedback gives the MPC the opportunity to damp model errors from propagating from previous steps across the entire prediction horizon.

5 EVALUATION OF MODEL PREDICTIVE CONTROL

5.1 Introduction

The ability of MPC to use models that can predict future disturbances and optimize the system in response to these disturbances enable it to have a superior performance compared to other control strategies. To investigate the potential benefits of MPC for building system both in terms of better IEQ and energy efficiency, various control strategies using MPC are considered and compared with their counterpart without MPC through a full scale building case study.

5.2 Simulation Conditions

For the case study, detailed EnergyPlus model of Center of Excellence (COE) building located in Syracuse, NY is used as a virtual test bed. The case building model satisfies requirements set by the DOE reference model (Deru et al. 2011) for commercial building. The simulation conditions used for the reference building are discussed below.

Thermal comfort conditions:

The thermal comfort requirements for the baseline building are set based on ASHRAE Standard 55. The standard set comfort conditions based on acceptance of the space by at least 80% of the occupants. For heating period the standard requires a dry bulb temperature between 20^{o}C to 23.5^{o}C with a typical winter clothing of 0.8 to 1.2clo. During cooling periods, the dry bulb temperature is required to be between 22.5^{o}C and 26^{o}C with clothing 0.35 to 0.6 clo. For the case study building, 21^{o}C and 24^{o}C are assumed as heating and cooling set points respectively. ASHRAE standard 55

does not put any limit on the relative humidity, but ISO7730 requires it to be between 30 and 70%. The same relative humidity limit is used for the baseline building.

The case building control strategies are also simulated with PMV (Predicted Mean Vote) as a thermal comfort measure and their performances were compared against those with thermal comfort control based on temperature and RH measurements. The parameters used for the case building in terms of thermal comfort are summarized in Table 9

Table 9: Constraints for thermal comfort parameter values

	Summer	Winter	Reference Standard
Temperature(^{o}C)	<=25	>=21	ASHRAE 55
Relative Humidity (%)	30≤RH≤65	30≤RH≤65	ASHRAE 62.1 , ISO 7730
PMV	<=0.5	>=-0.5	ASHRAE 55
Clothing(clo)	0.5	1	ASHRAE 55
Air Speed(m/s)	0.1	0.1	ASHRAE 55

Ventilation condition:

The minimum ventilation rate for the case building model was determined based on ASHRAE 62.1. Based on the standard, for an HVAC system with dedicated outdoor air system like the case building used, the total outdoor air intake air flow V_{ot}, can be computed using 112.

$$\boldsymbol{V_{ot} = \frac{\sum_{i=1}^{n}\left(R_p P_z + R_a A_z\right)}{E_z}} \qquad \textbf{112}$$

Where R_a outdoor airflow rate required per person ($m^3/s.m^2$) ($0.0003 m^3/s.m2$ for office), R_p is outdoor airflow rate required per person (m^3/s) (0.0025 m3/s for office), A_z zone floor area (m^2), p_z is zone population, the largest number of people expected to occupy the zone, E_z is zone air distribution effectiveness and

n is total number of conditioned zones. *Ez* is 1 for ceiling supply if warm air less than 8°C above space temperature. In the case building, the fresh air is supplied with a temperature close to the space temperature and thus air distribution effectiveness of 1 is used in this research.

Occupant, lighting and HVAC system schedule.

The occupant, lighting and HVAC system schedules used for the case building simulation are based on ASHRAE 90.1 recommendation for office building. The schedules used are summarized in Table 10.

Table 10: Recommended schedules for occupancy, lighting and HVAC system for baseline building according to ASHRAE 90.1

Hour of Day (Time)	Schedule for Occupancy			Schedule for Lighting			Schedule for HVAC System		
	Percent of Maximum Load			Percent of Maximum Load					
	Wk	Sat	Sun	Wk	Sat	Sun	Wk	Sat	Sun
1 (12-1 am)	0	0	0	5	5	5	Off	Off	Off
2 (1-2 am)	0	0	0	5	5	5	Off	Off	Off
3 (2-3 am)	0	0	0	5	5	5	Off	Off	Off
4 (3-4 am)	0	0	0	5	5	5	Off	Off	Off
5 (4-5 am)	0	0	0	5	5	5	Off	Off	Off
6 (5-6 am)	0	0	0	10	5	5	Off	Off	Off
7 (6-7 am)	10	10	5	10	10	5	On	On	Off
8 (7-8 am)	20	10	5	30	10	5	On	On	Off
9 (8-9 am)	95	30	5	90	30	5	On	On	Off
10 (9-10 am)	95	30	5	90	30	5	On	On	Off
11 (10-11 am)	95	30	5	90	30	5	On	On	Off
12 (11-12 pm)	95	30	5	90	30	5	On	On	Off
13 (12-1 pm)	50	10	5	80	15	5	On	On	Off
14 (1-2 pm)	95	10	5	90	15	5	On	On	Off
15 (2-3 pm)	95	10	5	90	15	5	On	On	Off
16 (3-4 pm)	95	10	5	90	15	5	On	On	Off
17 (4-5 pm)	95	10	5	90	15	5	On	On	Off
18 (5-6 pm)	30	5	5	50	5	5	On	On	Off
19 (6-7 pm)	10	5	0	30	5	5	On	Off	Off
20 (7-8 pm)	10	0	0	30	5	5	On	Off	Off
21 (8-9 pm)	10	0	0	20	5	5	On	Off	Off
22 (9-10 pm)	10	0	0	20	5	5	On	Off	Off
23 (10-11 pm)	5	0	0	10	5	5	Off	Off	Off
24 (11-12 am)	5	0	0	5	5	5	Off	Off	Off

Ceiling radiant panels mass flow rate

The case building uses series of ceiling radiant panels as main source of space heating and cooling. The mass flow rate of the water supplied to each radiant panel is controlled by the actuators based on the required room temperature condition. To avoid condensation on the panel surfaces, chilled water temperature at the ceiling radiant panels are maintained well above the dew point of each zone. Currently the set point temperature of the chilled water supply for the radiant panels is 16.7^{o}C.

Supply air temperature set point

The supply air from the air handling unit (AHU) is primarily designed for ventilation and to maintain the required room relative humidity. The set point temperature for the supply air temperature is 17^{o}C and 22^{o}C for summer and winter periods respectively.

Window blind angle set point

The case building is equipped with a double glass window with operable blind between the glasses. The blind angle is automatically adjusted to make a good use of the daylight. In line with this the lighting system has an automatic dimming capability and lux sensor in which the lighting can be dimmed depending on the level of the lux at the reference point. 500 lux is used as a set point for zone reference point's illuminance level while the windows blind angle are allowed to change based on the lighting and cooling/heating requirement.

5.3 Control Strategies Performance Comparison

The operation stability and possible energy saving from HVAC system highly depend on its control strategy. Apart from maintaining the set points assigned for it, a good control system should be stable and avoid abrupt control input changes to increase the

service life of the electrical and mechanical equipments in the system. In this research, the performance of different HVAC system control strategies using PID and MPC controllers are investigated in terms of providing the required comfort level as well as their energy consumption in doing so. The baseline control strategy is configured to mimic the existing control strategy in the case building. The comparison is done based on Syracuse weather data and the model is simulated for representative days in winter (12/01 - 12/05) and summer (07/10- 07/14). The outdoor conditions for the representative days are shown in Figure 27.

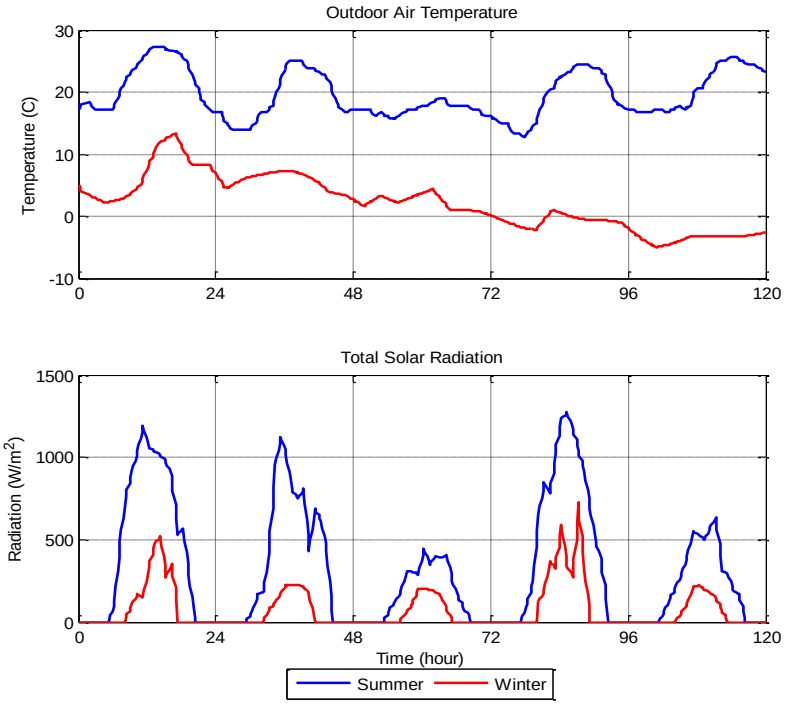

Figure 27. Outdoor air temperature and solar radiation.

5.3.1 Temperature Based Control Strategy

In this section, a PID and MPC controls based on zone temperature and relative humidity is discussed. Static schedule shown in Table 10 is used for calculating cooling loads from internal heat sources including occupants, lightings and electrical equipments. The optimized control variables used in this case are outdoor air flow

rate, supply air temperature and ceiling radiant panel flow rates to each zone. In the case of PID based control, constant temperature and flow rate are used for the supply air while chilled water and hot water flow rates are modulated using a PID controller based on the feedback temperature from each zone. Constant flow rate is used for supply air owing to the fact that the system is dedicated outdoor air system and the supply fan in the AHU is designed to handle only the ventilation requirement of the building. A set point temperature of 22^{o}C and 17^{o}C were used for supply air temperature during heating and cooling periods respectively. These set points are taken from the case building set points.

Unlike the PID controller, the MPC controller was allowed to choose any combination of the control inputs as long as the desired conditions are met. During evaluation of these optimized inputs, the physical limitations of the system as well as limitations in control inputs (maximum and minimum) are introduced as constraints to ensure convenient and stable operation of the system. More importantly the MPC predicts the combined effect of the individual control variables on the overall performance of the system unlike PID which responds to the given set point irrespective of the system performance.

Simulation results of space comfort conditions and the corresponding control inputs based on the two control methods (PID and MPC) for a representative summer and winter days are shown in Figure 28 through Figure 35. During the simulation, the temperature set points were allowed to vary between 21^{o}C and 25^{o}C during occupied hours and it is relaxed to between 10^{o}C and 30^{o}C during unoccupied hours.

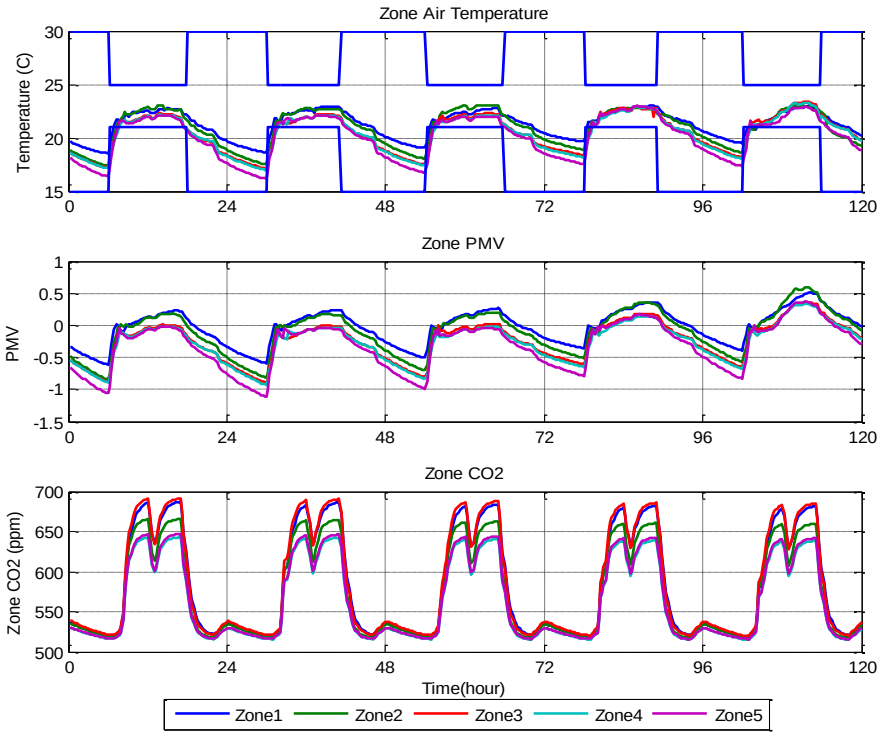

Figure 28. Zone comfort conditions - PID controller, winter

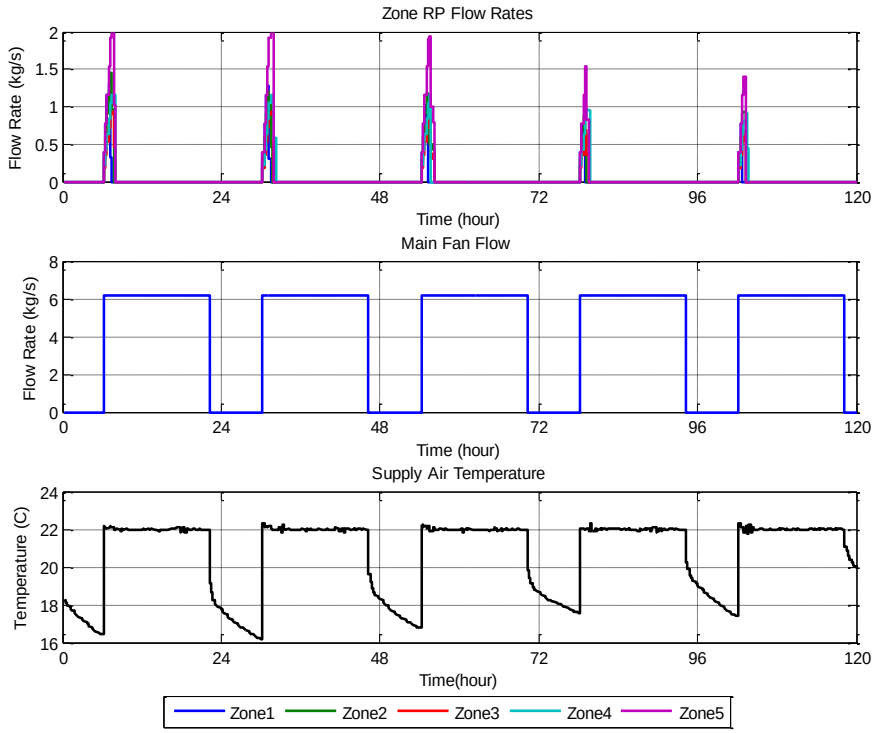

Figure 29. Control inputs -PID controller, winter

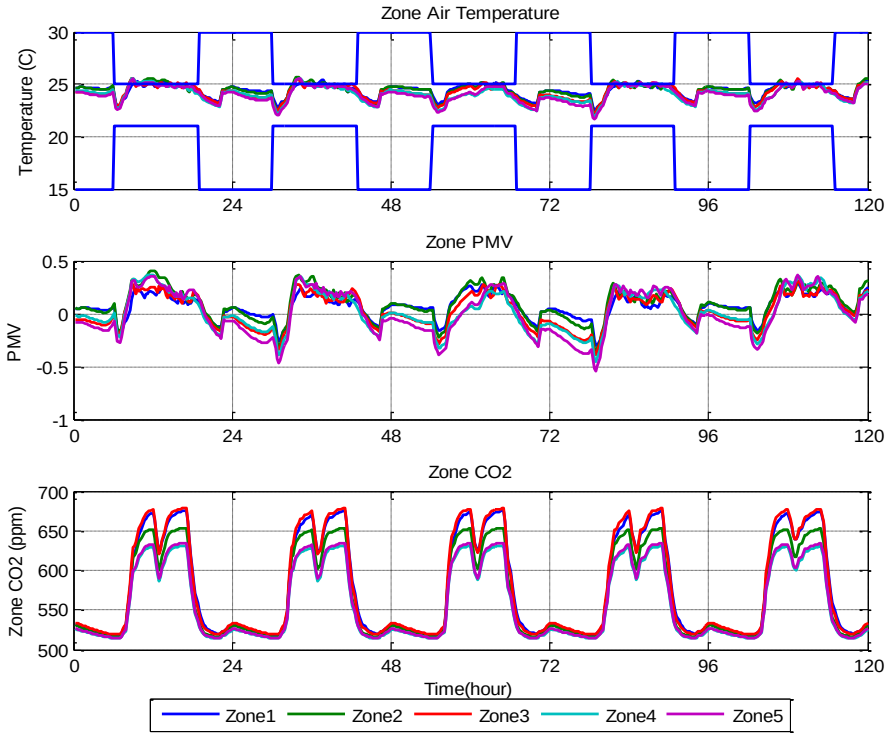

Figure 30. Zone comfort conditions - PID controller, summer

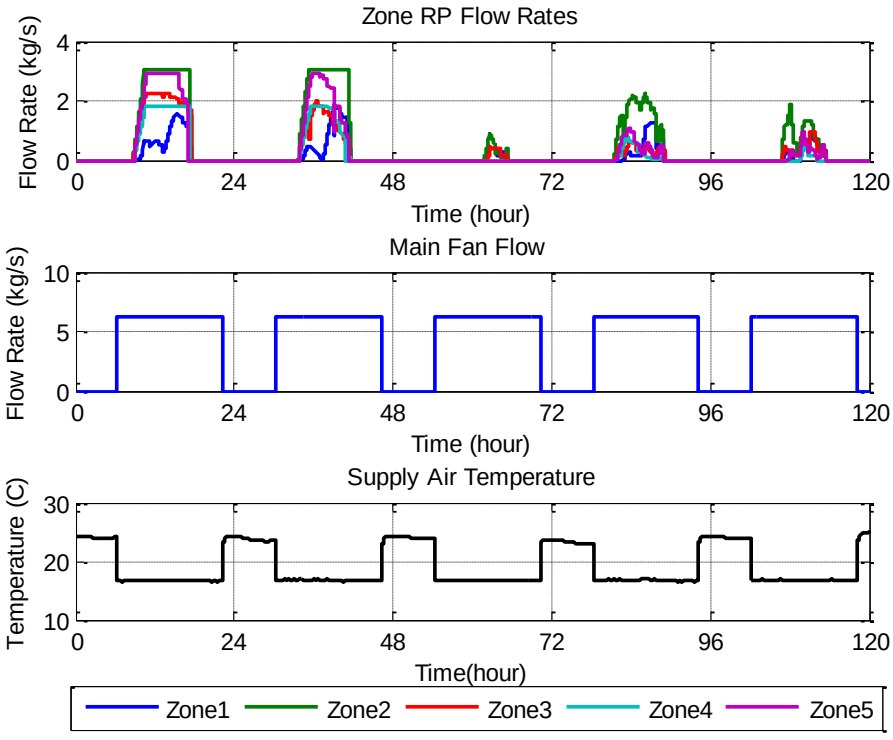

Figure 31. Control inputs - PID controller, summer

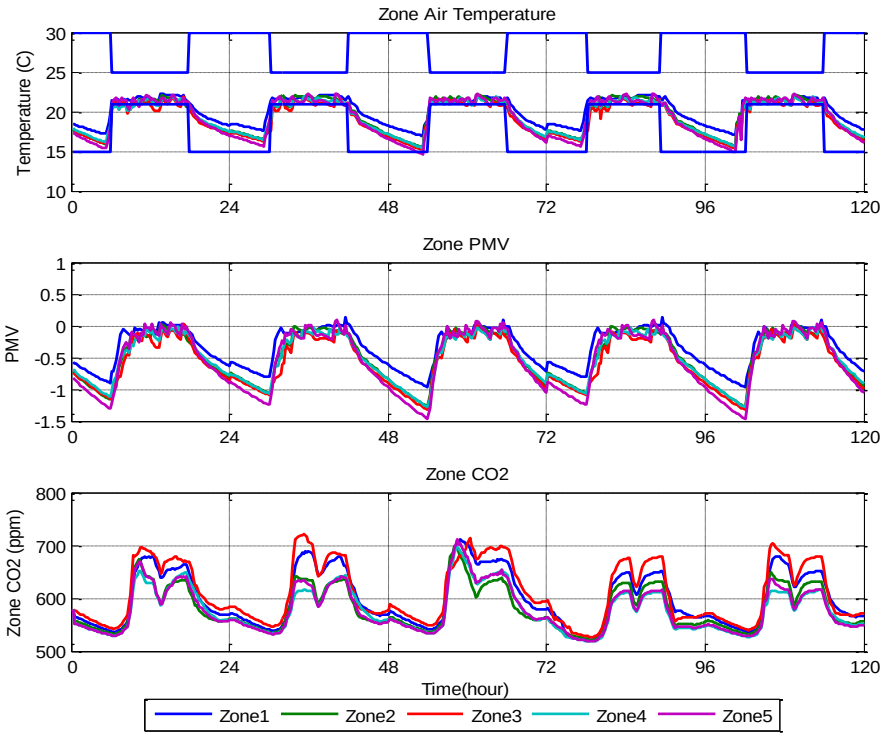

Figure 32. Zone comfort conditions - MPC controller, winter

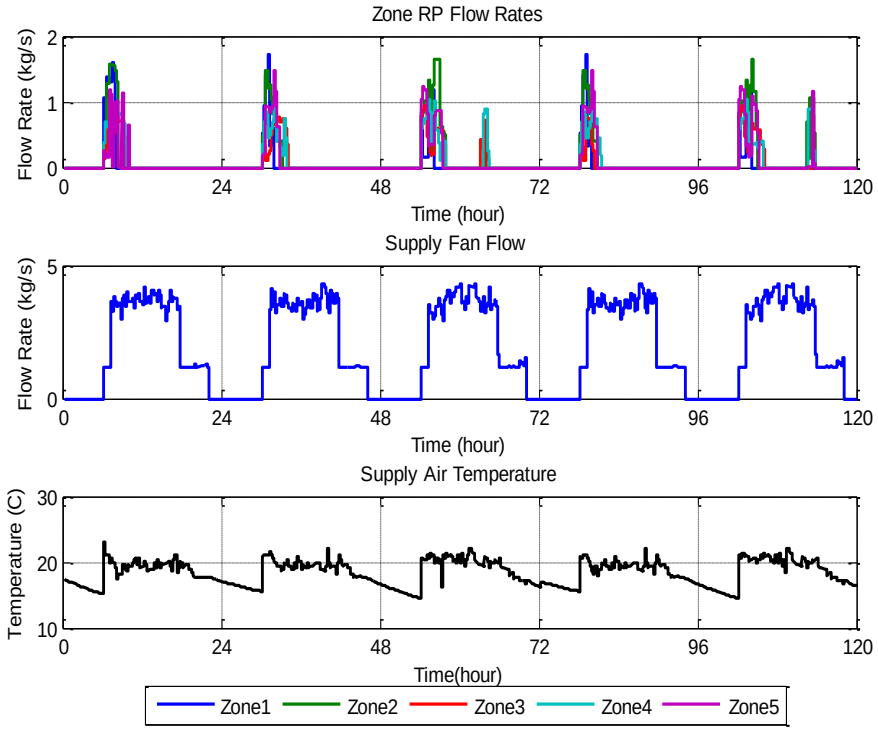

Figure 33. Control inputs - MPC controller, winter

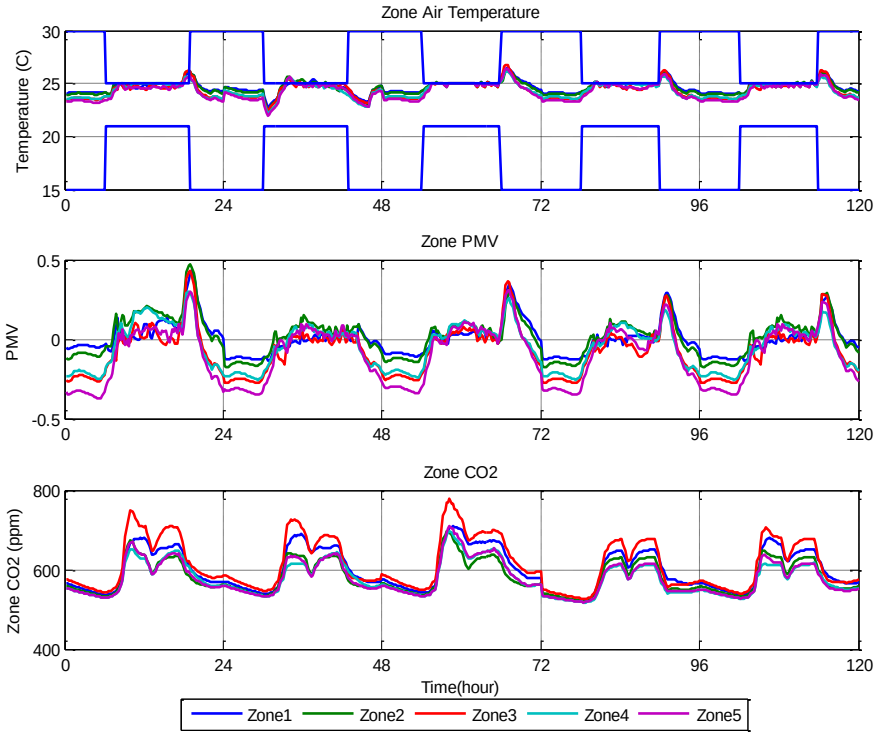

Figure 34. Zone comfort conditions - MPC controller, summer

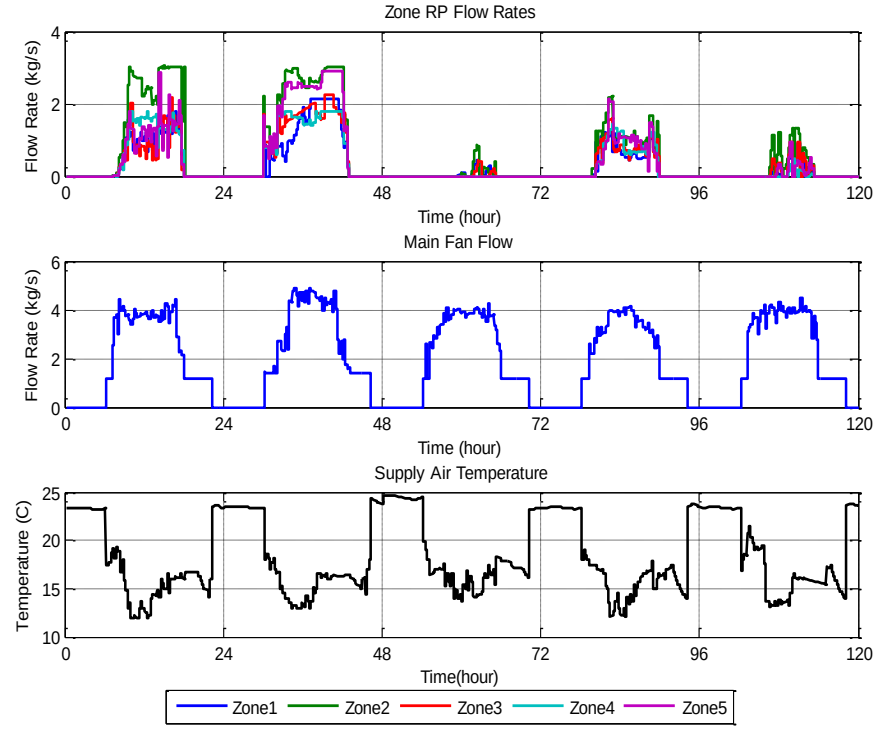

Figure 35. Control inputs - MPC controller, summer

The comparative energy savings obtained from MPC against conventional PID control for the simulation periods are shown in Figure 36. In both cases (summer and winter) the MPC had a superior performance with a total energy saving of 12.7% and 2% respectively. In addition to energy saving, the MPC controller had superior performance in terms of thermal comfort in the winter period in which the PID controller was unable to meet the required temperature in the early hours of occupancy. Due to the ability of MPC to predict future operation disturbances including operation schedule, it was able to start the system earlier before actual occupancy of the building. Even though this helps the system to avoid thermal discomfort during early hours, it also limits the possible energy saving at 2%. Another reason for the small energy saving is that most of the energy spending during winter was to treat the air needed for ventilation and no big energy saving opportunity was available which makes the MPC and PID controller to consume relatively similar amount of energy.

The MPC controller was using a relatively less outdoor air both during winter and summer. It also uses a relatively lower supply air temperature during summer which helps it to utilize the outdoor air to offset some cooling demand. The supply temperature during winter is also observed to be lower than the baseline. This is because of the fact that the lower supply air temperature was enough to maintain the required temperature during occupied hours as shown in Figure 32. These operations resulted lower fan energy and relatively higher chilled/hot water pump energy due to increased flow of water to the radiant ceiling panels Figure 36.

In regards to indoor air quality, both controllers were able to maintain the indoor CO_2 concentration level well below the acceptable limit of 1200 ppm. Apart from the temperature conditions, the PMV of each zone was simulated and the results show that it was close to zero both during summer and winter periods which indicates another opportunity for energy saving. The PMV range can be relaxed up to -0.5 during winter and 0.5 during summer. The next case study below shows a control strategy using PMV instead of temperature to compare the actual energy saving by relaxing the PMV to the above limits.

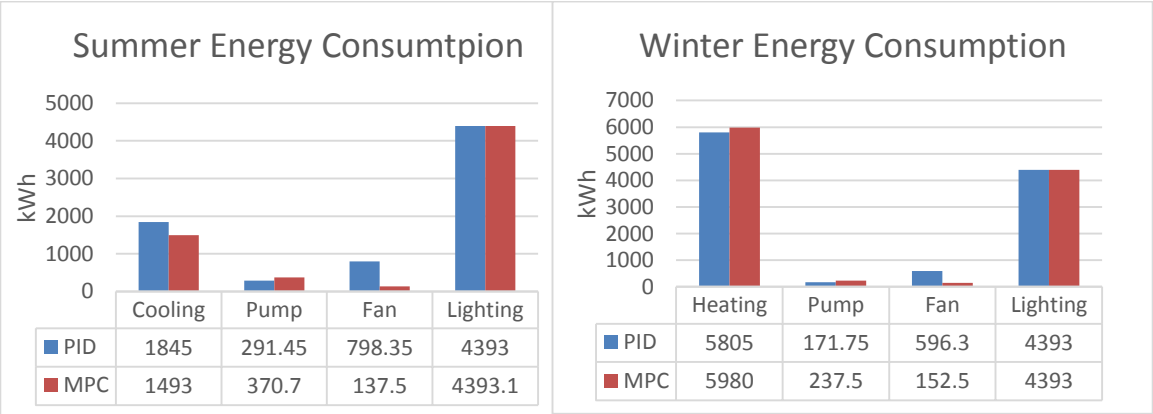

Figure 36. Typical summer and winter period energy consumptions

5.3.2 PMV Based Control Strategy

This section investigates the energy saving potential of a building control strategy in which the people thermal comfort condition is monitored using PMV. PMV combines environmental parameters (air temperature, radiant temperature, air velocity and relative humidity) and personal parameters (activity level and clothing insulation) to define thermal comfort. For PMV calculation, the radiant temperature is assumed to be equal to zone air temperature. Due to the fact that PID controller is a single input single output

(SISO) controller by nature, it cannot be used to control zone comfort based on PMV which involves nonlinear combination of the six parameters mentioned above. MPC on the other hand is a multiple input and multiple output (MIMO) controller and it is best suited for PMV based control. During occupied hours, the PMV values were allowed to vary between -0.5 and 0.5 according to the recommendation by ASHRAE 55. Accordingly the optimization problem considers these boundaries as constraints while trying to minimize the overall energy consumption by the HVAC system. During winter, even if the PMV was allowed to drop to -0.5, it never was at this value during occupied period due to considerable amount of heat gains from people, lighting, electrical equipments and solar radiation. As a result not much difference in energy saving was observed between the temperature and PMV based MPC control for the representative winter days (Table 11). During summer the MPC controller was able to relax the PMV values to 0.5 during occupied hours. As a result the room temperature was increased to around 26.5^{o}C during the same period.

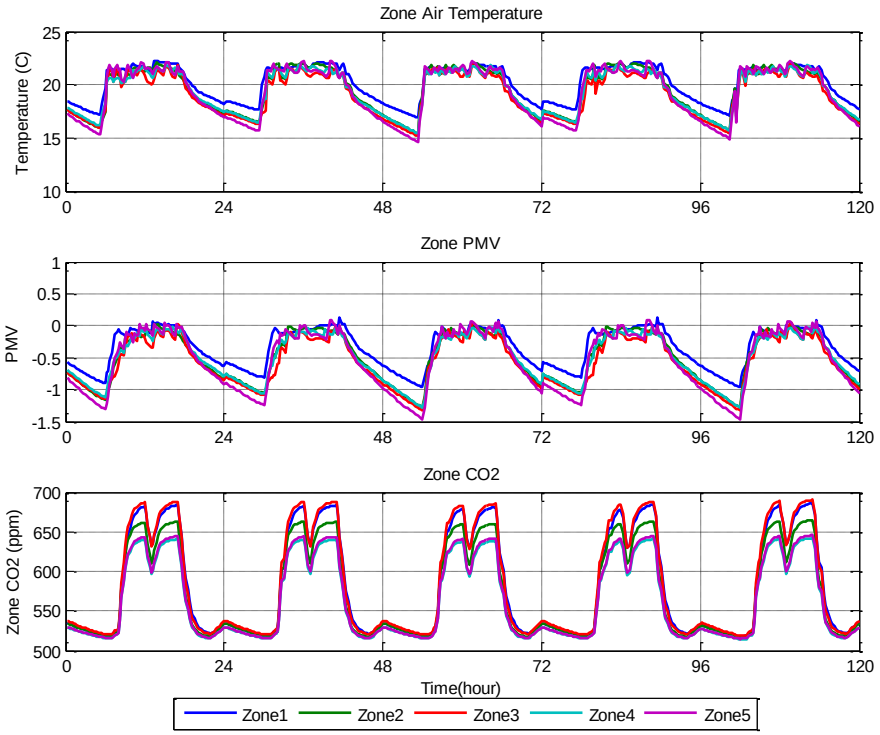

Figure 37. Zone conditions – PMV based MPC controller, winter

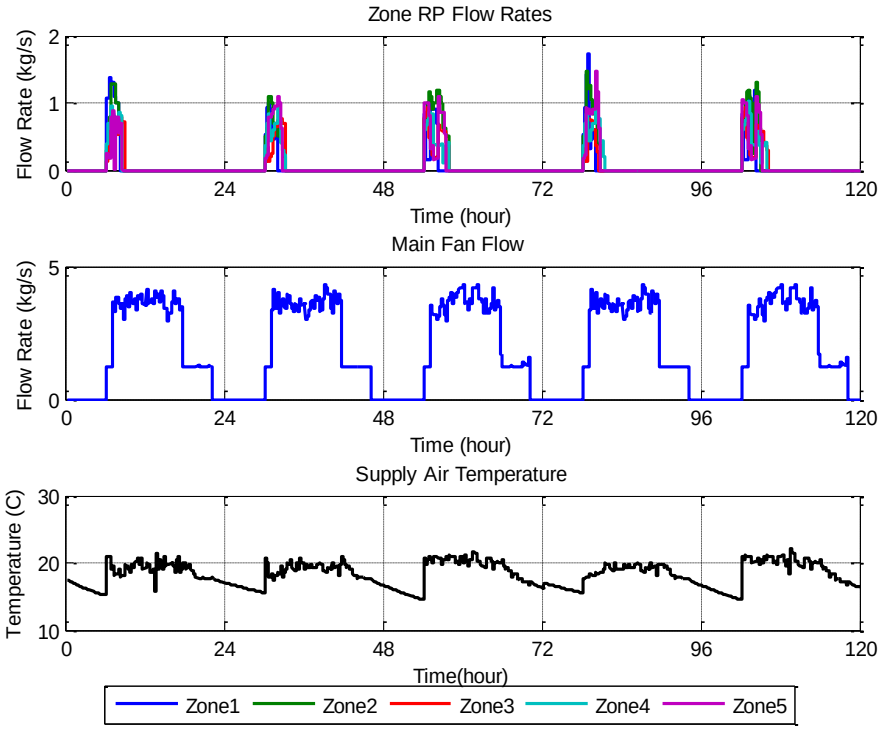

Figure 38. Control inputs - PMV based MPC controller, winter

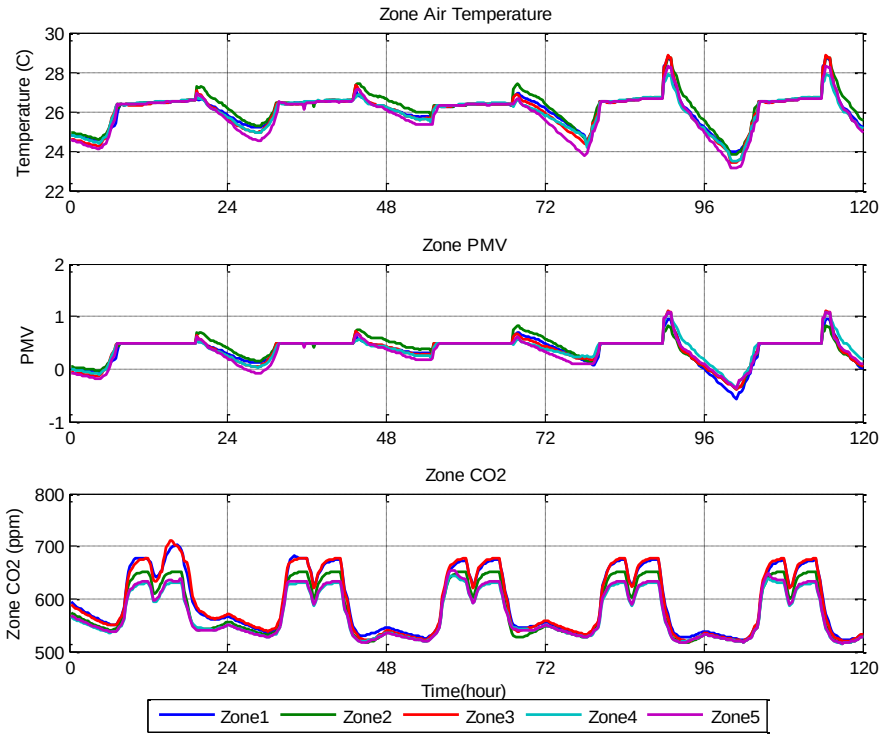

Figure 39. Zone Conditions – PMV based MPC controller, summer

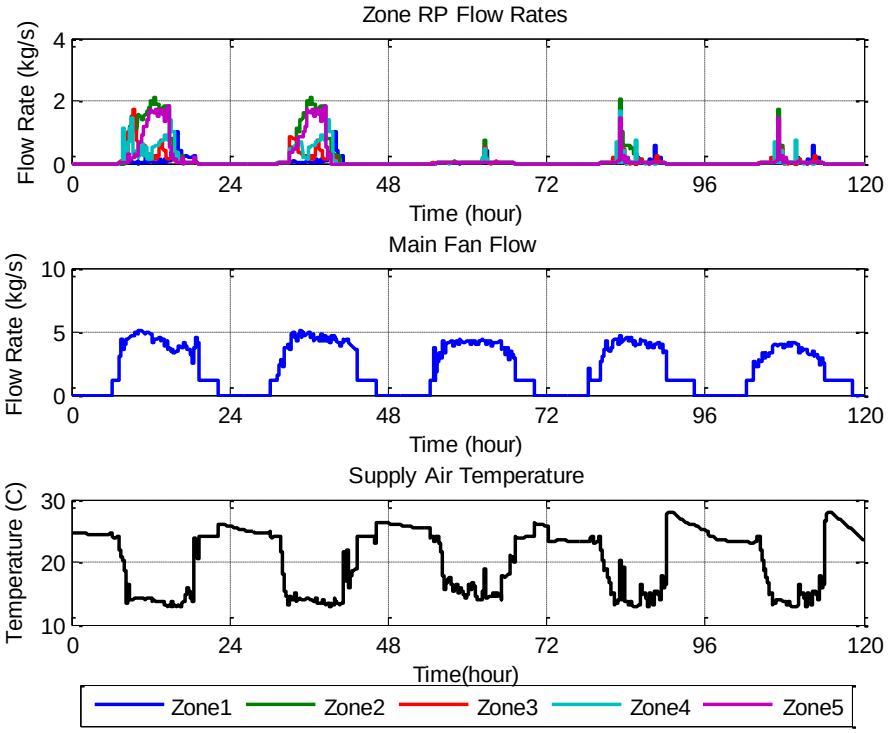

Figure 40. Controlled inputs - PMV based MPC Controller, summer

The resulting energy consumptions compared to the temperature based PID and MPC controllers for summer and winter periods are summarized in Table 11. During summer the PMV based MPC controller resulted in 13.4% and 3.5 % more energy saving compared to the temperature based PID and MPC based controllers discussed in 5.3.1. Similarly during winter, the PMV based controller resulted 1.9 % and 0.2 % energy saving compared to the temperature based PID and MPC based controller discussed in 5.3.1. The 1.9 % extra energy saving obtained from PMV based MPC is achieved due to reduction of hot water to the radiant ceiling panels and heating coils during early hours of occupancy and fan power due to reduced mass flow.

Table 11. Energy consumption comparison between temperature based and PMV based controllers.

	Summer			Winter		
	PID (Temp)	MPC (Temp)	MPC(PMV)	PID (Temp)	MPC (Temp)	MPC(PMV)
Heating (kWh)	-	-	-	5805	5980	5854
Cooling (kWh)	1845	1493	1230	0	0	0
Pump (kWh)	291	371	239	172	248	271
Fan (kWh)	798	138	310	596	153	236
Lighting	4393	4393	4393	4393	4393	4393
Total (kWh)	**7328**	**6394**	**6172**	**10966**	**10774**	**10755**
PMV % Saving	**15.8**	**3.5**		**1.9**	**0.2**	

5.3.3 Demand Control Ventilation (DCV) Based on Room Temperature Control

Demand control ventilation is one of the advanced approach for ventilation control in which it is possible to automatically reduce the minimum outdoor air intake below its design rates when the actual occupancy of spaces served by the system is less than design occupancy. In this section, energy performance of DCV based PID control strategy is investigated and compared with MPC controller. The CO_2 concentration in each zone was continuously monitored as a surrogate for occupancy measurement. Instead of using the design ventilation rate for the entire occupied hours as shown in

the baseline case (5.3.1), the controller was allowed to modulate the ventilation rate from zero to maximum depending on ventilation requirement based on floor area and number of occupants according to ASHRAE 62.1 and the allowable CO_2 level. The CO_2 level limit used was 1200ppm in each zone assuming the outdoor air CO2 concentration to be 500ppm. The performances of the DCV controller in terms of thermal comfort and energy saving during summer and winter are shown in Figure 41 through Figure 44. This strategy helps the system to modulate the outside air flow based on the people occupancy schedule and hence provide extra saving in fan energy and also reduce the energy required for treating the outdoor air.

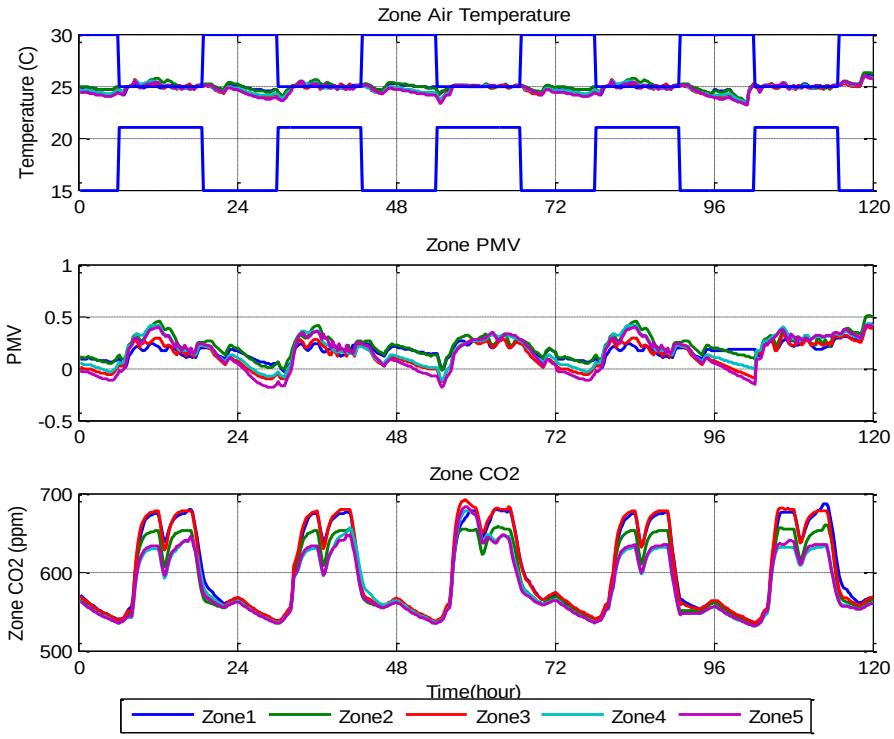

Figure 41. Zone comfort conditions - PID controller, summer (DCV)

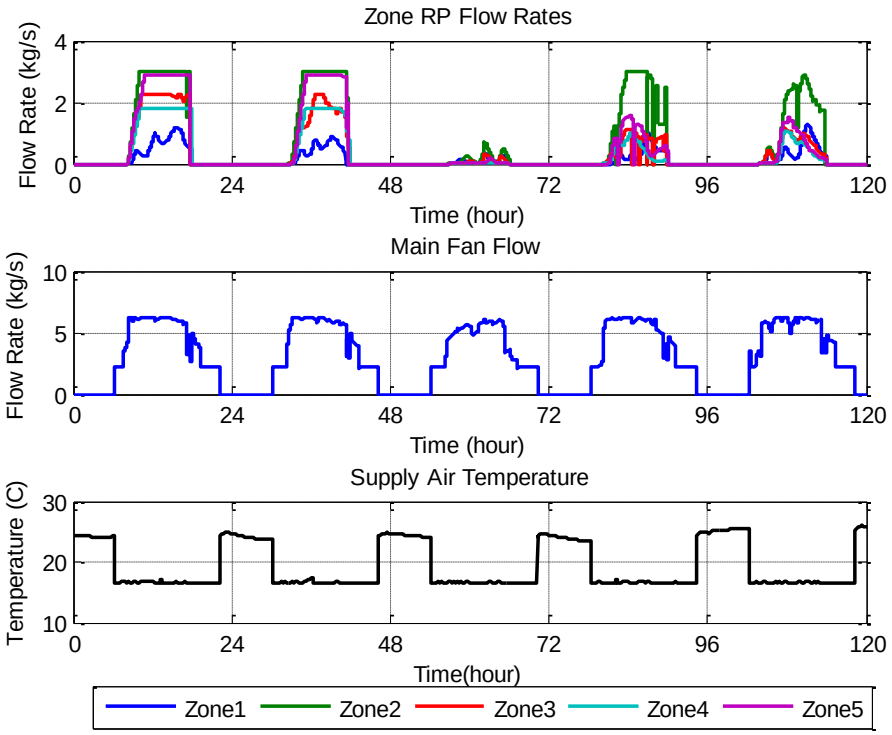

Figure 42. Control inputs -PID controller, summer (DCV)

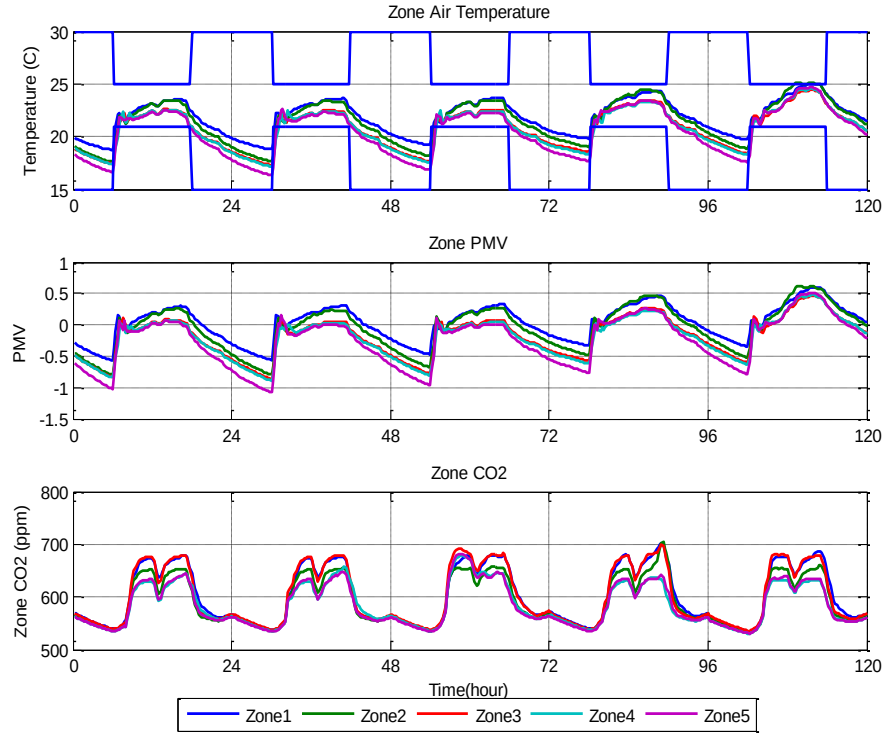

Figure 43. Zone comfort conditions -PID controller, winter (DCV)

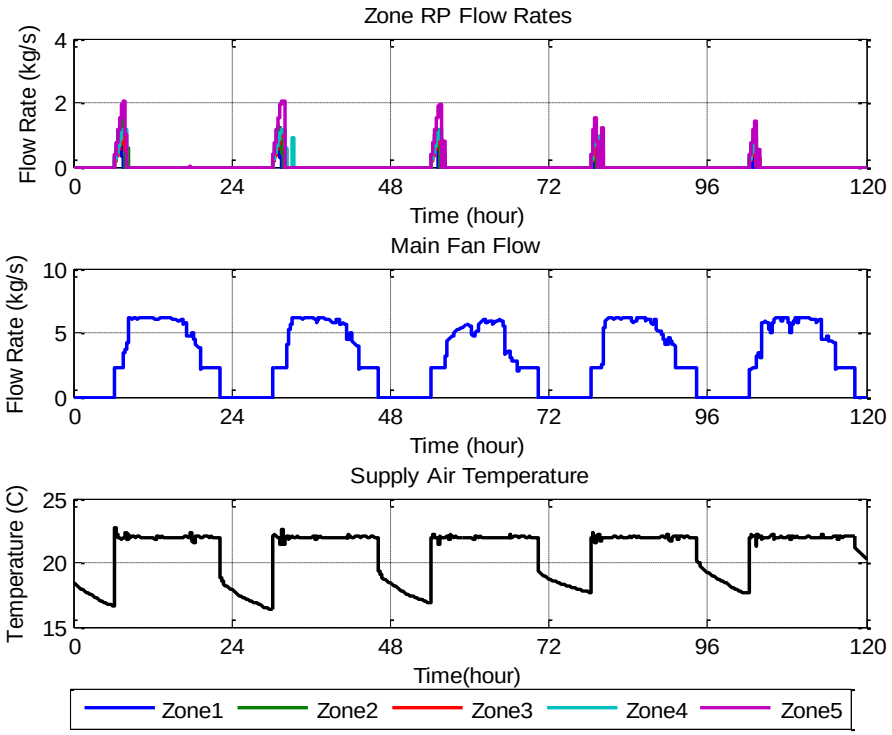

Figure 44. Control inputs - PID controller, winter (DCV)

The energy savings from DCV based control compared to the baseline temperature based control and MPC controller is summarized in Table 12. The DCV based control strategy using PID shows an energy saving of 9.9 % during summer and 4.7 % during winter compared to the baseline PID control strategy discussed in 5.3.1. The DCV based strategy used reduced outdoor air flow rate based on the occupancy schedule and this resulted a considerable energy saving on the supply fan and heating/cooling coils. The MPC strategy discussed in 5.3.1 is DCV by nature since the controller is allowed to search through all the allowable control limits including ventilation while satisfying the constraint limit on the state variables. Comparing the temperature based MPC with PID based DCV controller strategy, the MPC was able to save 3.2 % more energy during summer and used extra 3% energy during winter. The MPC was using more energy compared to DCV because of the fact that it was starting operation before actual occupancy of the building to avoid thermal discomfort

during early hours of occupancy. Comparison of the PMV based MPC to that of the DCV based PID control resulted a 12.8% energy reduction during summer and 2.9% more energy consumption during winter.

Table 12. DCV energy saving summary

	Summer				Winter			
	PID (Temp)	PID (DCV)	MPC (Temp)	MPC (PMV)	PID (Temp)	PID (DCV)	MPC(Temp)	MPC(PMV)
Heating (kWh)	-	-	-	-	5,805	5,700	5,980	5,854
Cooling (kWh)	1,845	1,673	1,493	959	-	-	-	-
Pump (kWh)	291	337	371	263	172	166	238	271
Fan (kWh)	798	200	138	145	596	195	153	236
Lighting (kWh)	4,393	4,393	4,393	4,393	4,393	4,393	4,393	4,393
Total (kWh)	**7,328**	**6,603**	**6,394**	**5,761**	**10,966**	**10,454**	**10,763**	**10,755**
Saving Compared to PID(Temp)		**9.9**	**12.7**	**21.4**		**4.7**	**1.9**	**1.9**
MPC Saving Compared to DCV			**3.2**	**12.8**			**-3.0**	**-2.9**

5.3.4 Temperature Based Control with Integrated Window and Lighting Control

Lighting contributes to 14% of energy consumption in commercial buildings. Most of the energy from lighting will be dissipated to the surrounding in the form of heat and this will add extra cooling load to the building during summer while it helps to heat the surrounding air/ building envelope during winter. The daylight energy that is properly harnessed can reduce the energy consumption for lighting as well as for HVAC system. The case building uses integrated window blind and lighting controls and the extra energy saving that can be obtained from using integrated MPC controller is simulated in this section. The integrated lighting and window blind models used for the MPC controller are discussed in section 4.2.3. In addition to the control variables used in the previous cases (outdoor air flow, supply air temperature and chilled water flow to the ceiling radiant panels), lighting level and window blind angle are added as new control variables. For each zone, two work plane reference points were defined to monitor the illuminance level. The illuminance levels in each

zone were included as constraints of the optimization problem in addition to the room thermal comfort requirements. The EnergyPlus model used to run the base cases is upgraded to include the integrated window blind system with the window blind slant angles controlled by an optimized schedule obtained from the MPC output. A lighting level of 500 lux at the working space is used as the minimum allowable illuminance level in each zone during occupied hours. The result was compared against the baseline case (5.3.1) which has no lighting and window control. Advanced control strategies using PMV is also simulated and presented in case 5.3.5. The physical properties of the integrated window blind used in this case study are summarized in Table 13.

Table 13. Window blind properties

`	Unit	Value
Slat width	m	0.013
Slat separation	m	0.013
Slat thickness	m	0.001
Slat conductivity	w/m-k	0.9
Blind to glass Distance	m	0.5
Blind Position	-	Between Glasses
Front and back side slat bea	-	0.8
Front and back side slat diff	-	0.8

The amount of solar energy admitted to the building envelope depends on the relative position of the sun throughout the day as well as the window blind angle. The variation of the window system (blind and glazing) transmittance over the day is shown in Figure 45.

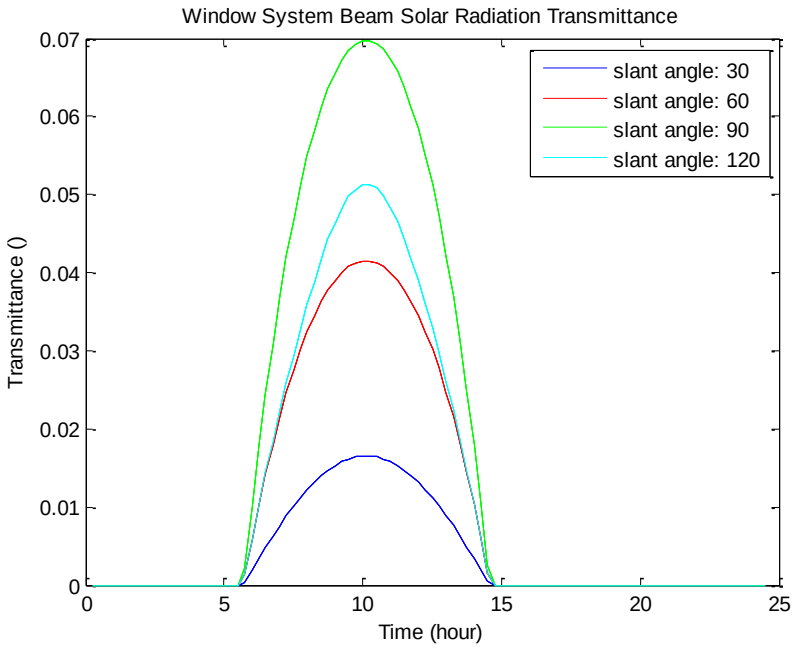

Figure 45. Window system beam solar radiation transmittance

The simulation results for summer period are shown in Figure 46 through Figure 49. The window blind control and the corresponding lighting control based on the required illuminance level resulted a big reduction in cooling load during summer which intern resulted in a big energy saving compared to the other control strategies with no lighting and blind control. Figure 49 shows that the solar radiation during mid-day was providing the illuminance level (>500lux) needed without lighting from electricity. As a result the dimming factor around mid-day was zero for all zones except zone 2.

In addition the glare index from the transmitted solar radiation was lower than the recommended value of 22 (EnergyPlus 2012) throughout the simulation day (Figure 49). The window blind was controlled according to the intensity of the available solar radiation. The window blinds were opened wide to let more sunlight during early hours and closed during mid-day to minimize the cooling load due to solar radiation.

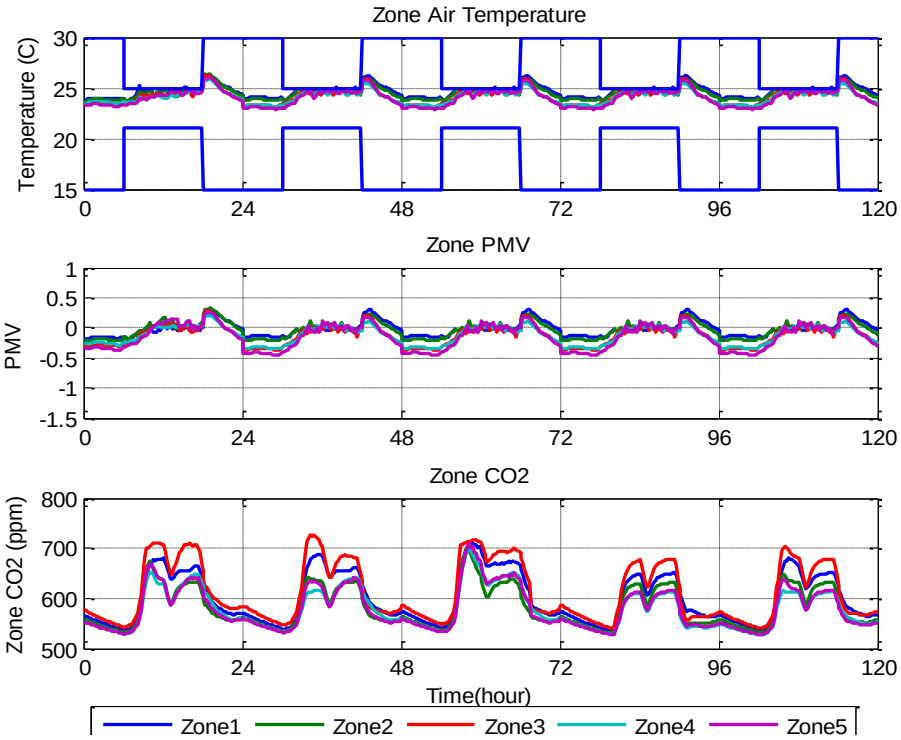

Figure 46. Zone conditions - MPC controller with integrated blind and lighting control, Summer

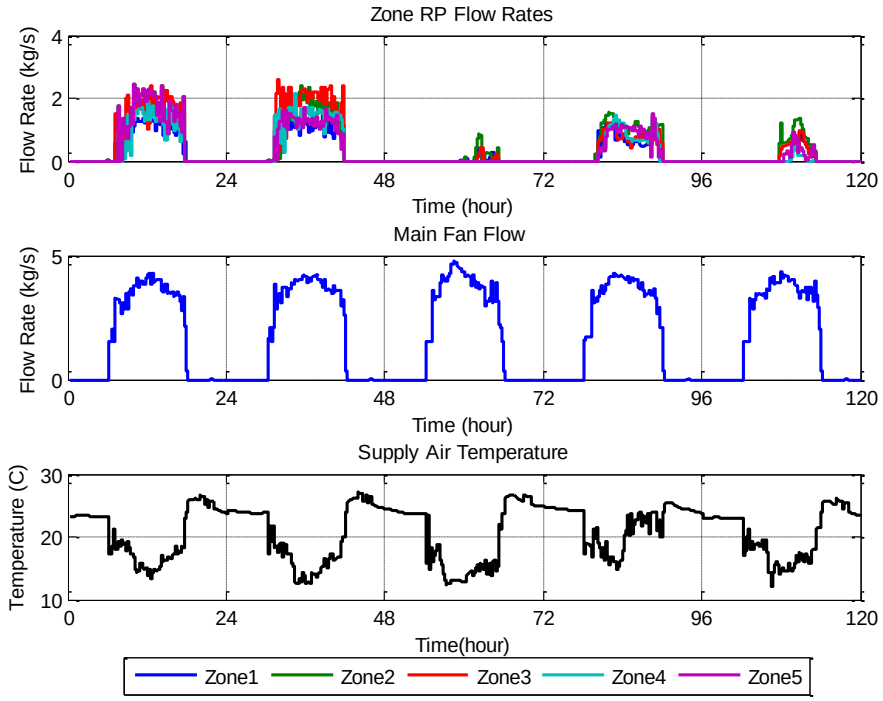

Figure 47. Control inputs for MPC controller with integrated blind and lighting control, summer

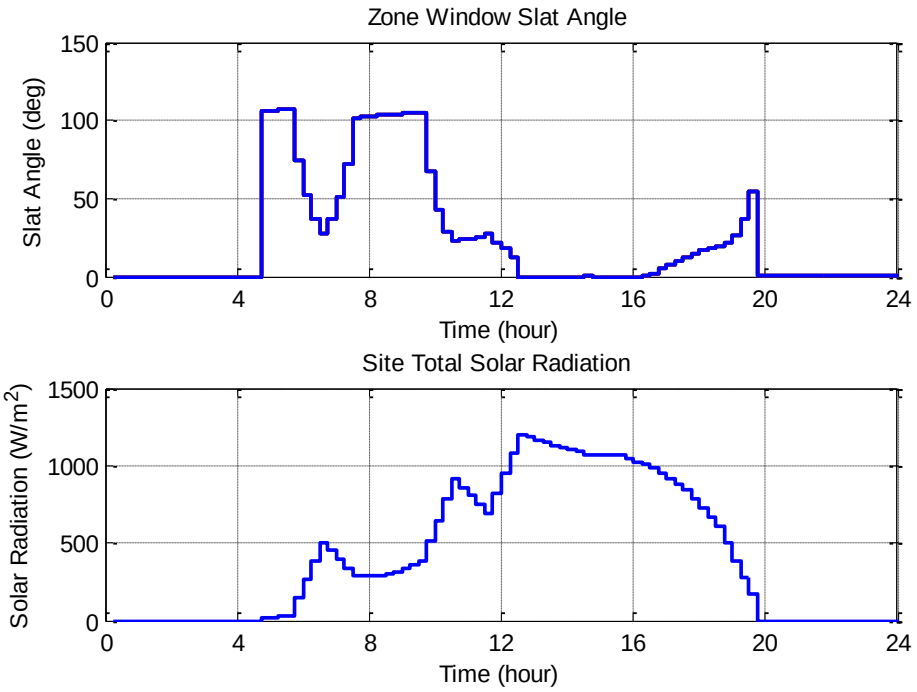

Figure 48. Variation of window slat angle with solar radiation, summer

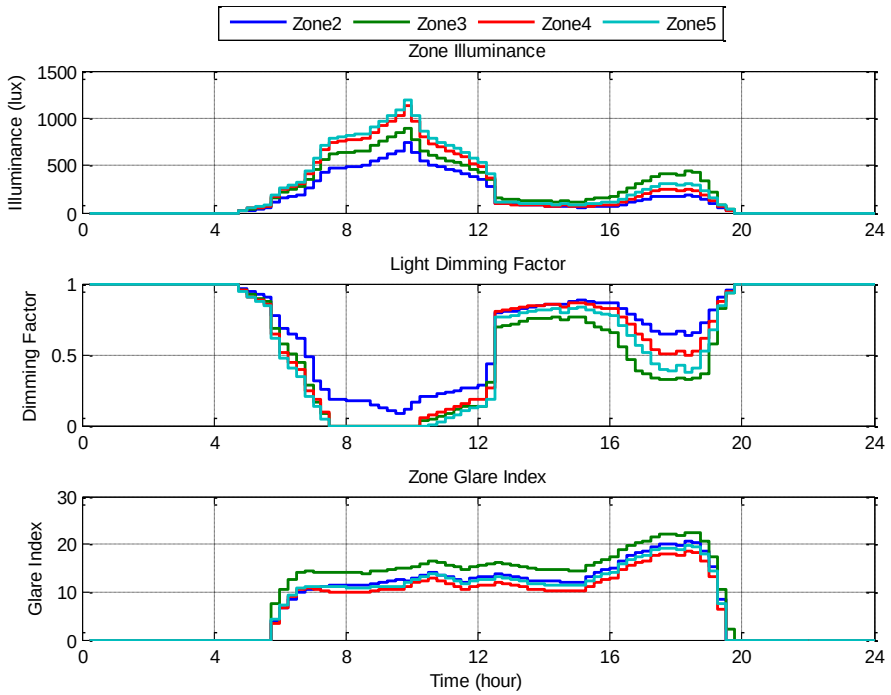

Figure 49. Integrated window and lighting control, summer

Similar to the summer case, the performances of the MPC controller using integrated window and lighting control for winter period are shown in Figure 50 through Figure 53. Not much difference was observed between the zone condition and control inputs of the temperature based MPC controllers with and without integrated window blind and lighting controls except a slight increase in hot water flow to the ceiling radiant panels in the later case. The variation of optimized window blind angle variation with solar radiation for a representative winter day is shown in Figure 52. During morning and late afternoon hours the solar intensity was relatively low and the window blind was wide open (90 Deg) to late more solar energy in to the building while a reduction in blind angle was observed during midday when the solar intensity was above ~ 150W/m^2. Accordingly most of the transmitted solar energy is used to offset the energy demand for lighting to provide the required illuminance level at the reference working plane as indicated in Figure 53.

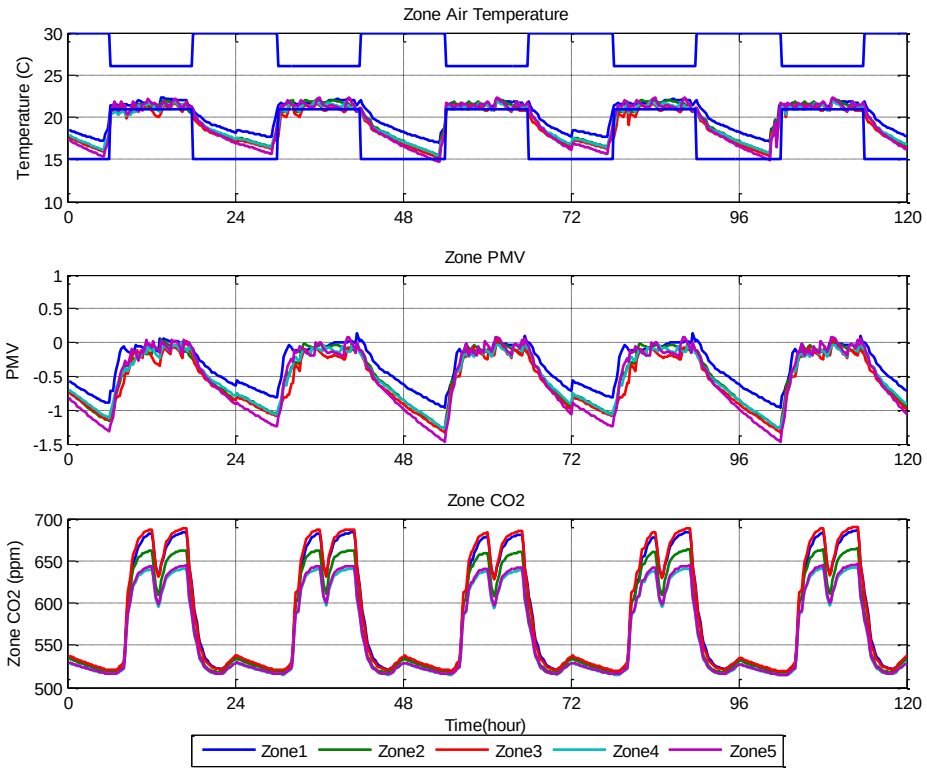

Figure 50. Zone conditions - MPC controller with integrated blind and lighting control, winter

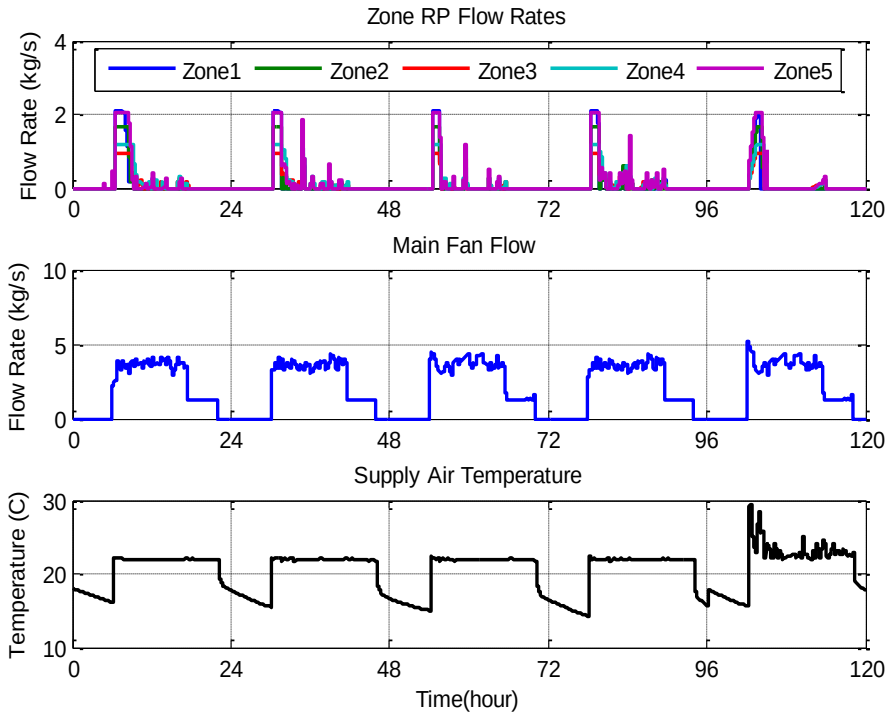

Figure 51. Control inputs - MPC controller with integrated blind and lighting control, winter

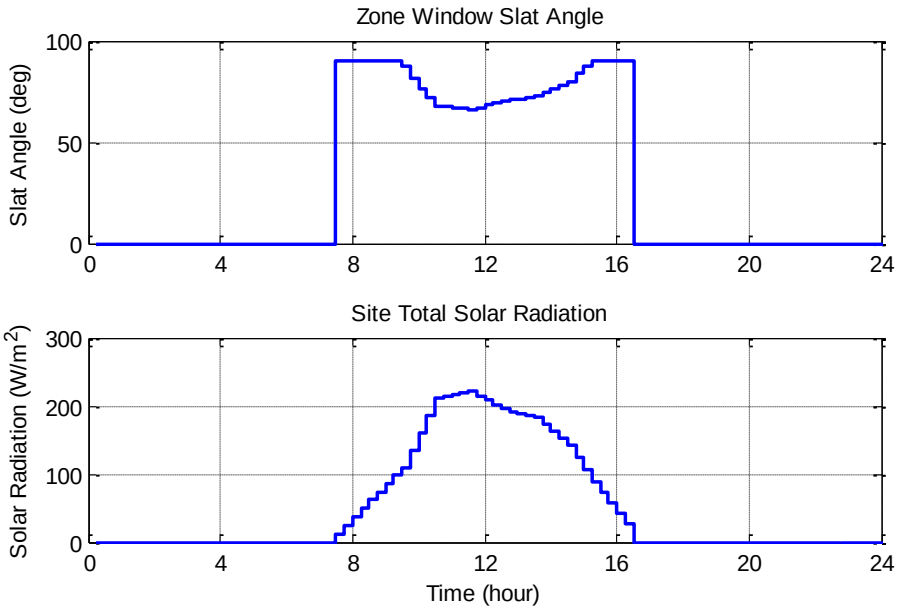

Figure 52. Variation of widow slat angle with solar Radiation, winter

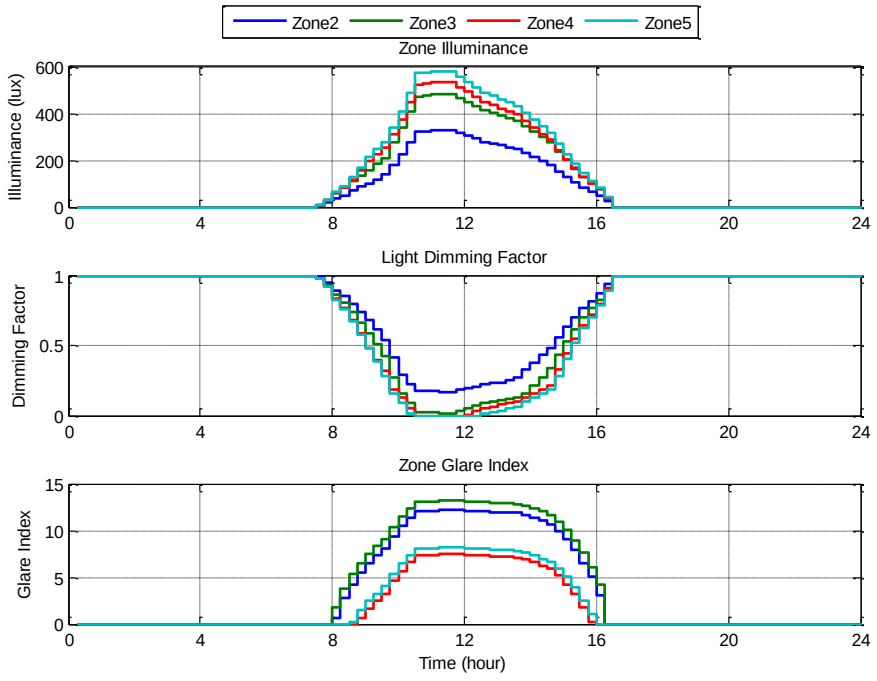

Figure 53. Integrated window and lighting control, winter

The energy consumption of MPC with integrated window blind and lighting control is compared against the baseline temperature based PID controller and temperature based MPC controllers is shown in Figure 54. The figure shows

comparison of energy consumption for five representative winter and summer days. The energy consumption by cooling and lighting show a considerable reduction as a result of lighting dimming and optimized window blind control during summer periods. This control strategy resulted 37% energy saving compared to the baseline temperature based PID control strategy and 28% energy saving compared to the temperature based MPC control strategy without integrated window blind and lighting control during summer period. During winter period, the lighting control resulted in a reduction in lighting energy consumption which in turn resulted in a slight increment in energy consumption for heating. But the integrated control strategy resulted in a net saving of 8% and 6.5% compared to the temperature based PID control and MPC control without window and lighting control respectively during winter period.

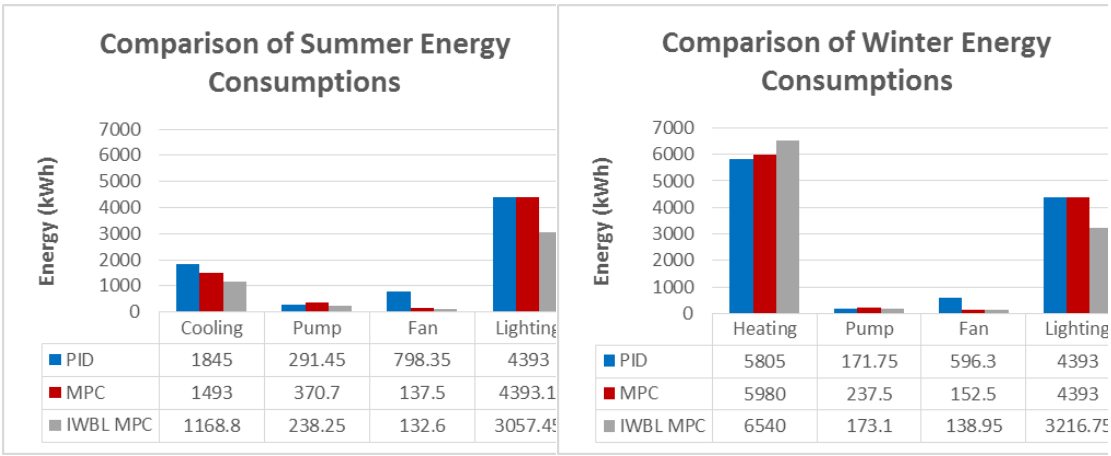

Figure 54. Energy consumption comparison of MPC with integrated window blind and lighting (IWBL) control

5.3.5 PMV Based Control with Integrated Window Blind and Lighting Control.

In this section performance of a PMV based MPC controller with integrated window blind and lighting control is investigated. Similar to section 5.3.2, the PMV value was allowed to vary between -0.5 and 0.5 during occupied hours. The optimization portion of the MPC controller aims at decreasing the total energy consumption of the HVAC and lighting system while maintaining the constraints (comfort and lighting levels). In both winter and summer, a relatively dry air condition during the simulation periods helps to relax the zone temperature requirements and as a result considerable energy was saved compared to the temperature based control strategy discussed in section 5.3.4. The zone comfort conditions were similar to the PMV based control strategy presented in section 5.3.2. The window blind angle positions as well as the corresponding illuminance level in each zone for summer and winter periods are shown in Figure 55 through Figure 58. In both periods considerable lighting energy was saved as indicated by the dimming factor. A dimming factor of 1 means all the lighting comes from electricity while 0 means all the lighting comes from solar radiation. The glare index was also below the allowable limit of 22.

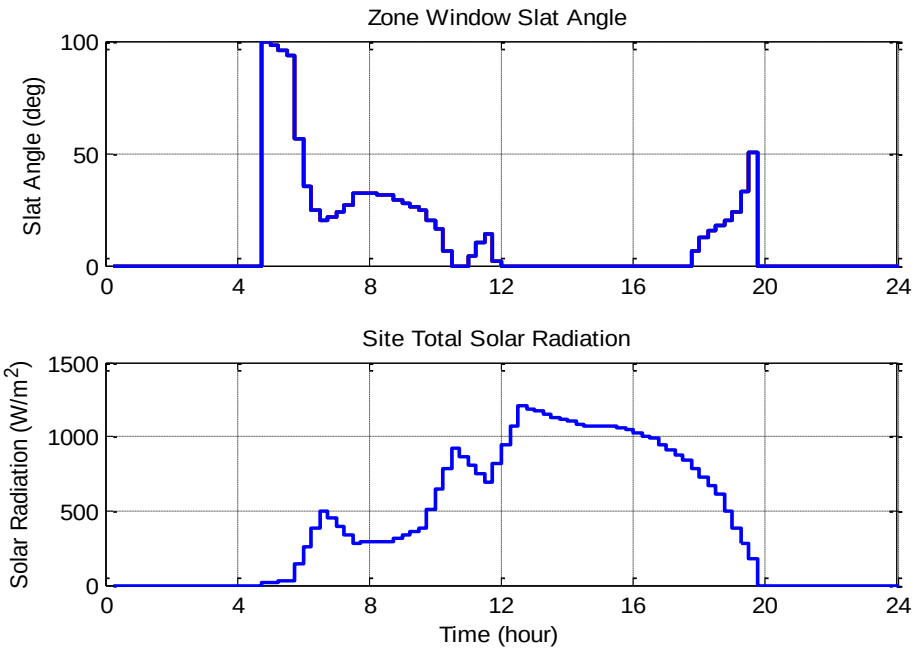

Figure 55. Variation of widow slat angle with solar radiation, summer

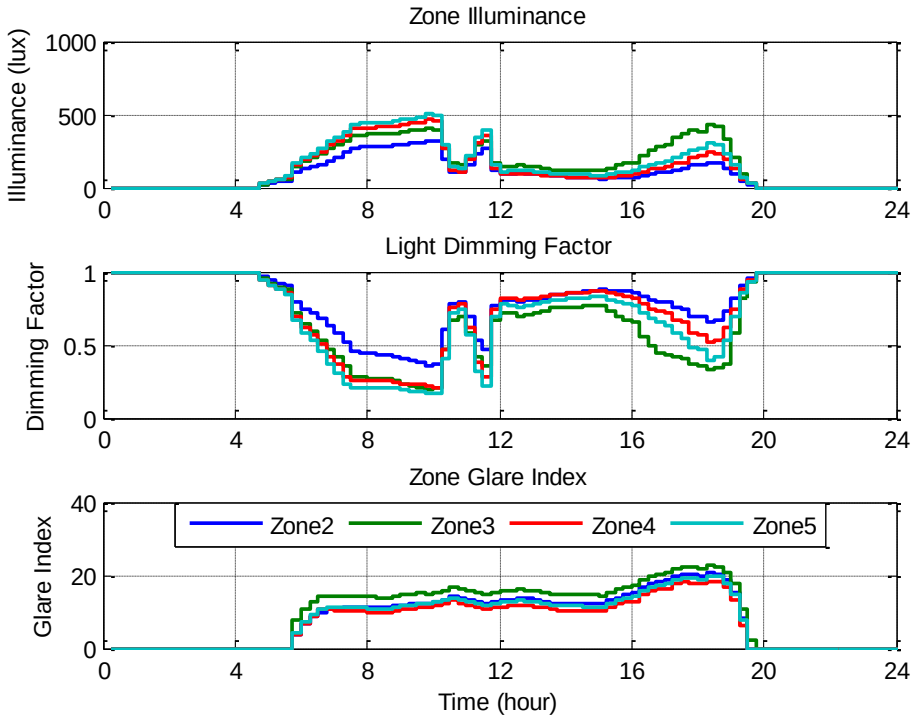

Figure 56. Integrated window and lighting control, summer

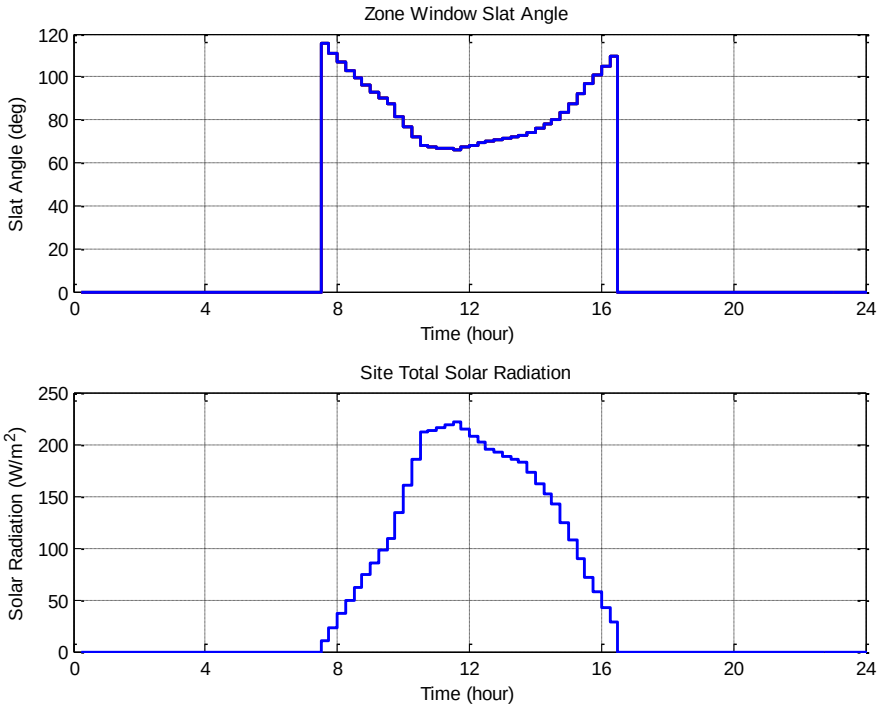

Figure 57. Variation of widow slat angle with solar radiation, winter

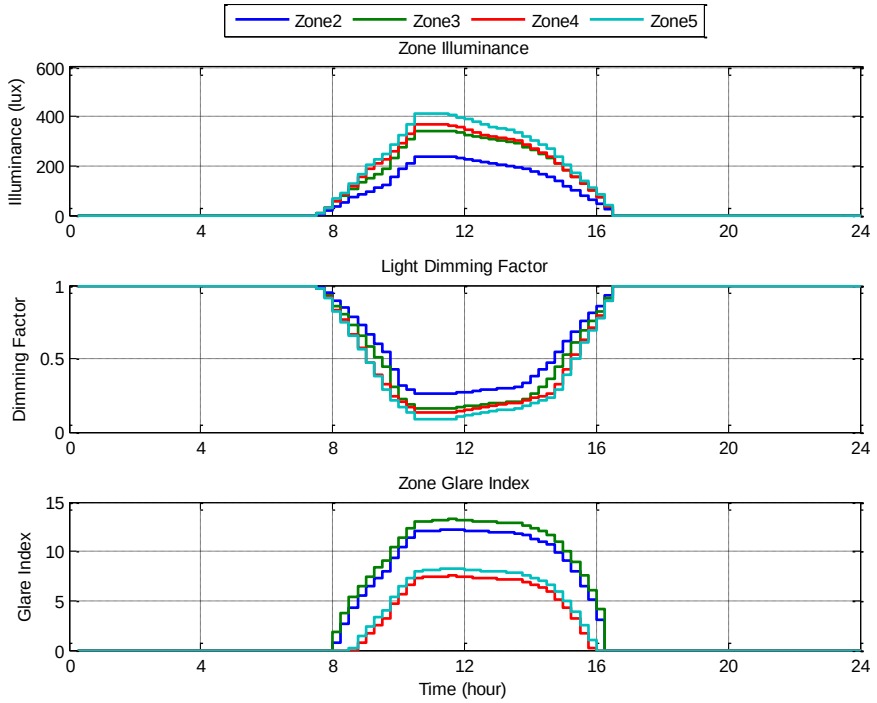

Figure 58. Integrated window and lighting control, winter

The energy consumption of PMV based MPC with integrated window blind and lighting control is compared against the baseline temperature based PID controller and PMV based MPC controllers and the result is summarized in Figure 54. The figure shows comparison of energy consumption for five representative winter and summer days. The energy consumption by cooling and lighting show a considerable reduction as a result of lighting dimming and optimized window blind control during summer periods. During summer period, this control strategy resulted in 48% energy saving compared to the baseline temperature based PID control strategy and 33.9% energy saving compared to the PMV based MPC control strategy without integrated window blind and lighting control. During winter period, the lighting control resulted a reduction in lighting energy consumption which in turn resulted a slight increment in energy consumption for heating. But the integrated control strategy resulted in a net saving of 9.1% and 7.4% compared to the temperature based PID control and PMV based MPC control without window and lighting control respectively during the same period.

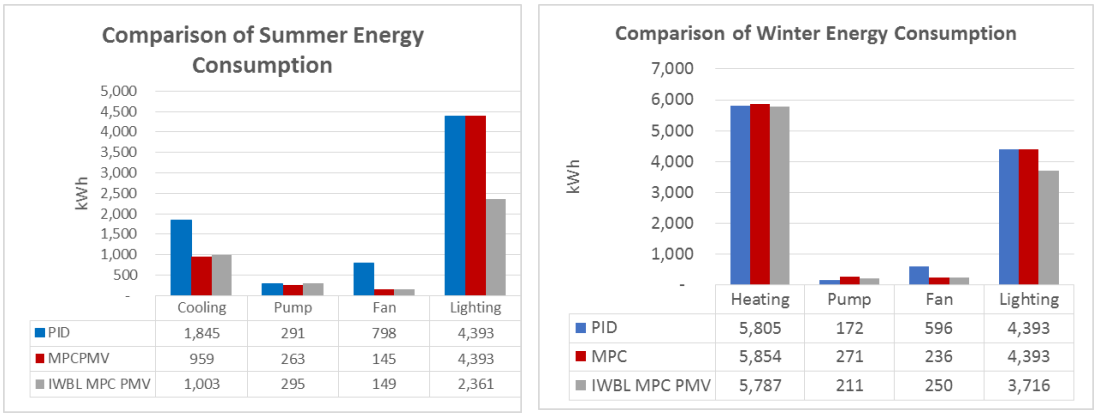

Figure 59. Energy consumption comparison of MPC with integrated window blind and lighting (IWBL) control

5.4 Summary

In this chapter performance of MPC was evaluated using different control strategies for winter and summer periods. Supply air mass flow rate, supply air temperature and chilled water/ hot water flow to the ceiling radiant panels were used as the controlled inputs. In all cases compared, the MPC controllers shows a superior performance compared to the baseline control cases used.

As discussed in the MPC section of this research one major advantage of using MPC in building HVAC control system is its ability to incorporate multiple objective functions and constraints in an easy way. This helps to insure stable operation of the system and in most cases comparable or better performance than the conventional control system using local controllers.

In the case of temperature based control, the MPC resulted a big saving compared to the baseline control strategy. The reason for the big saving was the relatively high energy saving in the fan energy as a result of varying the air mass flow rate based on occupancy instead of keeping it constant during the entire occupancy time. Besides the observed energy saving, the MPC also showed superior performance in terms to thermal comfort during winter period. One of the advantage of MPC over conventional controllers is its ability to integrate disturbance model which helps it to take anticipatory control action rather than corrective control. As a result of the prediction of occupancy schedule ahead of the actual occupancy, the MPC controller was able to start heating early which helps to avoid human discomfort at early hours of occupancy.

It should also be noted that MPC by nature has a cost function that can incorporate multiple objectives. Depending on the particular application and purpose of the

building different waiting factors can be assigned for the multiple objectives (example energy saving and thermal comfort). In this research comfort condition was given priority than energy and for that reason it was included as a constraint of the MPC controller instead of a cost function so that it will be maintained during all operation time.

Another advantage of MPC is its convenience for using predictive mean vote (PMV) for zone comfort. Even if PMV is believed to be a more comprehensive way of defining thermal comfort, it is not yet implemented in most buildings because of the fact that involves multiple parameters which makes it difficult for conventional controllers which are single input single output (SISO) controllers. Because of the fact that PMV is a multiple input multiple output (MIMO) controller, it is convenient for applying PMV based thermal comfort control and the simulation result shows a considerable energy saving form this strategy compared to the temperature based control.

In addition to the control inputs considered above, integrated widow blind and lighting control were added to evaluate the extra benefit from blind and lighting control. Currently most advanced buildings use lighting and window blind control strategies. The most advanced control strategy is using closed loop integrated lighting and window blind control which responds to the required illuminance level at the working plane (Mukherjee et al. 2010). Use of MPC gives extra benefit of using the integrated lighting and window blind control by incorporating the heating or cooling requirement of the building in addition to the required illuminance level. In this research optimal blind angle position was determined by considering the cooling/heating load as well as illuminance level and the result shows considerable energy saving.

In summary, we were able to prove that MPC can be applied in a system level and its performance was superior both in terms or energy and thermal comfort. Applying this strategy across the globe can bring tremendous energy globally and helps the effort to reduce greenhouse gas emission. The only concern for implementation of this method in a real building is the challenge of getting reliable component models and the associated development effort. Developing a library of robust and simplified component models that can be used for different buildings can considerably reduce the development effort and the models and the approaches developed here can be used for the implementation.

6 A NOVEL ENERGY EFFICIENT DEMAND BASED VENTILATION SYSTEM FOR CRITICAL CONTAMINANT AND OVERALL IAQ CONTROL

6.1 Introduction

People in the United States spend approximately 90% of their time indoors (Klepeis, Tsang, and Behar 1996). Indoor air quality (IAQ) has profound effects on the health and human performance. To achieve acceptable IAQ, combinations of the following actions are essential: contaminant source control, proper ventilation, humidity management and adequate filtration. Besides maintaining acceptable IAQ, it is also necessary to keep the associated energy consumption and costs as low as possible. In this research effort has been made to develop an energy - efficient ventilation strategy that is capable of controlling the concentration levels of multiple contaminants typically found in indoor air.

Often there is a conflicting effect between remedies taken to reduce contaminants of indoor and outdoor origins. Introducing outdoor air can dilute concentrations of contaminants with indoor sources and at the same time it can increase the concentrations of contaminants originated from outdoor sources. To avoid such conflicting effects the ventilation system should be smart enough to monitor both indoor and outdoor air quality.

Most traditional ventilation systems provide fixed Minimum outdoor air flow based on design capacity and this could result in loss of energy or discomfort when the building operates in off design conditions. To circumvent this problem, Demand Control Ventilation (DCV) can be used for resetting minimum outdoor air ventilation rate based on occupancy. Most DCV systems use indoor CO2 concentration level as a

means to control outdoor air flow rate due to its direct association with presence of occupants. In real indoor environment, several pollutants which have serious health effect also co-exist. Various studies have shown associations of IAQ and human performance in addition to the potential health risks associated with poor indoor air quality(Wargocki, Wyon, and Fanger 2000). Researchers estimate the potential gain of productivity through improved indoor air quality to be from 20 to 160 Billion Dollar in US considering only office workers (Fisk, 2002).

To address this problem, a ventilation strategy based on critical contaminants is proposed. The strategy considers multiple contaminants of concern with indoor and outdoor sources. A Matlab/SIMULINK model is developed to evaluate the effects of the proposed strategy on IAQ and energy consumption.

6.2 Contaminants of Concern and Indoor Air Quality

Four commonly available indoor air contaminants were selected for the study: Toluene, Formaldehyde, PM2.5 and CO2 (used as a surrogate for occupant-generated pollutants). Toluene is selected as a representation of the total volatile organic compound (TVOC) level as it is commonly used as a reference compound for TVOC quantification. Formaldehyde is considered because of the high health risk associated with it even at very low concentration level. PM2.5 is considered due to its high seasonal and geographical variation of concentration in outdoor air and it is a good candidate to demonstrate performance of the proposed control strategy in different geographical location. Generation rate and allowable indoor concentrations of the four contaminants considered are summarized in Table 1.

Assuming mass flow rate of supply and return air to be equal in each zone, indoor air contaminant concentration over time can be given by

$$\rho V_r \frac{dC_i}{dt} = \dot{m}_{sys}(C_{sys} - C_i) + \dot{m}_{inf} C_o - \dot{m}_{exf} C_r + S_r - k_d C_i \quad (113)$$

Where C_i is zone contaminant concentration (kg/m^3), C_o is outdoor air contaminant concentration (kg/m^3), ρ is density of air (kg/m^3) , Vr is zone volume (m^3), $\dot{m}_{sys}$ is zone mechanical ventilation rate (kg/s), $\dot{m}_{inf}$ is infiltration mass flow rate (kg/s) , $\dot{m}_{exf}$ is exfiltration mass flow rate (kg/s), S is contaminant source generation(kg/m^3/s), k_d is contaminant rate of deposition on surface(kg/s) and C_{sys} is the mixture of outdoor air and return air concentrations with the proportion which depends on the damper opening u_m

$$C_{sys} = u_m C_o + (1 - u_m) C_i \quad (114)$$

To account for the flow due to infiltration (v_{inf}) and exfiltration (V_{exf}), ASHRAE 90.1 baseline infiltration/exfiltration rate of 31m^3/hr.m^2 is used. In addition to the contaminant simulation model, building thermal model is developed to the evaluate effect of the proposed control strategy on overall energy consumption and thermal comfort. Energy balance for indoor air is given by equation 115 .

$$M_i C_p \frac{DT_i}{dt} = m_{sys,i} c_p (T_s - T_i) + Q_{sensible,i} \quad (115)$$

Where M_i is zone air mass (kg), C_p is specific heat of air (kJ/kg.K), Ti is zone air temperature (^{o}C), m_{sys} is mass flow rate of supply air (kg/s), T_s is supply air temperature (^{o}C) and $Q_{sensible}$ is the total sensible heat which is comprised of convective heat gains from surrounding opaque surfaces of the building envelope, internal heat gains, windows and infiltration.

6.3 Model Description

A five zone building model equipped with Variable Air Volume (VAV) with reheat system in each zone is used for the simulation. A SIMULINK model is

developed to simulate contaminant concentration and indoor air temperature of each zone. Nonlinear regression algorithm was used to identify parameters used in using simulation results from an EnergyPlus model of the same building.

6.4 Baseline Ventilation

To compare potential benefits of the newly proposed ventilation strategy, a base line ventilation system using ASHRAE 62.1 min ventilation requirement is developed. For the baseline ventilation, the design minimum outdoor air flow rate is calculated using:

$$\boldsymbol{v_{ot} = \frac{D\sum_{i=1}^{n} R_p P_z + \sum_{i=1}^{n} R_a A_z}{E_v}} \qquad 116$$

Where D is occupant diversity ratio, R_p is outdoor airflow rate required per person (m^3/s), Ra is outdoor airflow rate required per unit area ($m^3/s.m^2$), p_z is zone population, the largest number of people expected to occupy the zone, A_z is zone floor area (m^2) and the ventilation efficiency, E_v the ventilation efficiency which can be determined from Table 6.3 of ASHRAE 62.1 based on the maximum value of primary air fraction z_p

$$\boldsymbol{Z_p = \frac{R_p P_z + R_a A_z}{E_z V_{pz}}} \qquad 117$$

Where E_z is the zone distribution effectiveness and V_z is minimum primary air flow through VAV to each zone (m3/s). Based on equation 116 the design outdoor air flow rate, V_{ot}, is calculated to be 40% of the summation of the minimum CFM set points of the VAVs in each zone. For the baseline ventilation system, the split range

sequencing control strategy (S. Wang and Xu 2002) shown in Figure 60 is implemented to switch ventilation modes during heating and cooling operations. In this control strategy, difference between actual supply air temperature and its set point is used for temperature control by modulating heating coil valve, cooling coil valve and the fresh air damper. The fresh air damper will be kept at its minimum position when the system is in the heating mode or when the fresh air temperature is higher than the return air temperature.

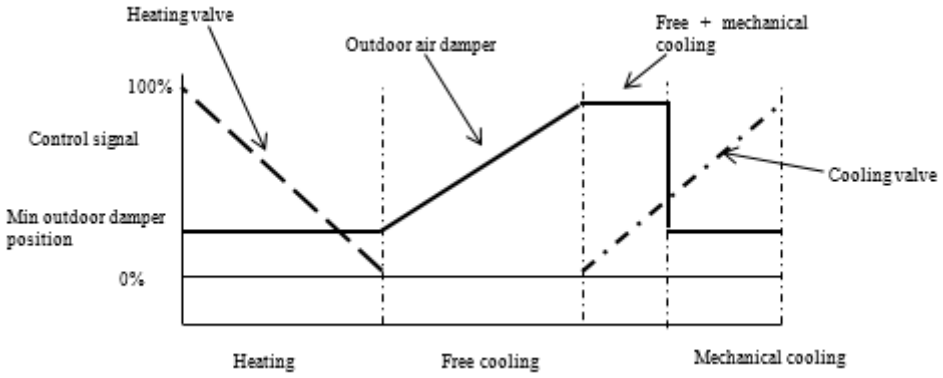

Figure 60. Split range control strategy

6.5 Proposed Control Strategy

The proposed strategy uses temperature and contaminant information from each zone to control outdoor air damper position unlike the baseline strategy that uses only temperature information. There are two modes of operation for the contaminant based control strategy depending on which contaminant source, indoor or outdoor, is dominating. When outdoor contaminant level exceeds a value that has a potential to result a concentration level which is higher than the permissible concentration level at steady state, outdoor air damper will be kept at minimum position based on ASHRAE 62.1 so that the control requirements for pollutants of indoor origin are satisfied. The damper is kept at the minimum position with the assumption that the filter of the air

handling unit (AHU) has a capacity to maintain required permissible indoor concentration at design minimum outdoor air ventilation rate. To reduce the impact of limiting outdoor air damper at its design minimum position on compromising the use of free cooling, contaminant-based strategy will only be activated one hour before the building is occupied and will be disabled when the building is not occupied. If indoor concentration limit is more than the permissible value even with minimum outdoor ventilation rate due to deterioration of the filter, the system will generate alarm for filter replacement. Outside air contaminant level that can result the indoor concentration to exceed the allowable indoor concentration level at steady state, Co_{ss}, can be obtained from equation 113 and is given by

$$Co_{ss} = \frac{\left(k_v + k_d - pk_v(1 - u_m) - \frac{\dot{V}_{inf}}{V_i}\right) c_{ss} - s_i}{pk_v u_m + \frac{\dot{V}_{inf}}{V_i}} \qquad 118$$

In times when there are dominating indoor contaminant sources, demand controlled ventilation (DCV) strategy based on critical contaminant concentration will be used. Figure 61 shows DCV control strategy. The controller takes maximum value of each contaminant from each zone and compares them with their permissible value. The one with maximum deviation from its permissible value will be used as a critical contaminant to control outdoor air minimum damper position. To avoid different scaling of contaminants, each contaminant deviation is normalized using its permissible value.

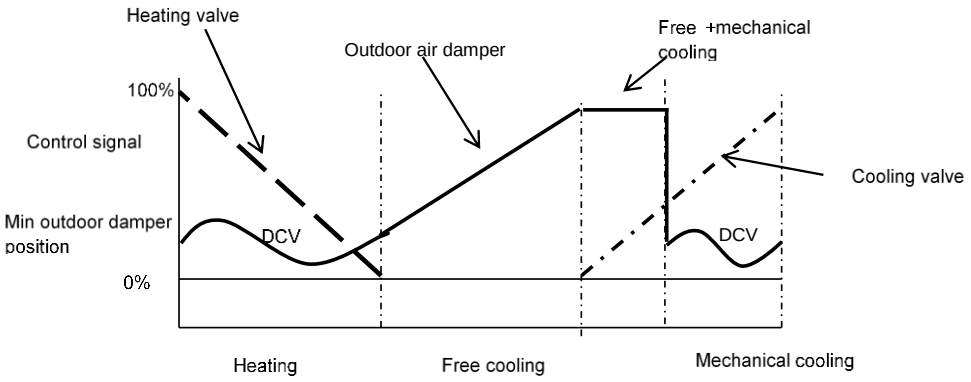

Figure 61. Split range sequencing control strategy with DCV

DCV's ability to automatically adjust minimum damper position depending on room contaminant concentration saves energy by avoiding energy that would otherwise be lost to treat extra air introduced to the building when it is partially occupied. When indoor contaminant sources are strong, the system might require more outdoor air proportion than the baseline to dilute contaminants concentration. This will ensure good IAQ at the cost of extra energy that would not be possible using baseline ventilation system. When the contaminant levels are in acceptable range, the amount of outdoor air ventilation is determined by thermal comfort requirement of the building. Implementation of the control logic discussed above in Simulink is shown in Figure 62.

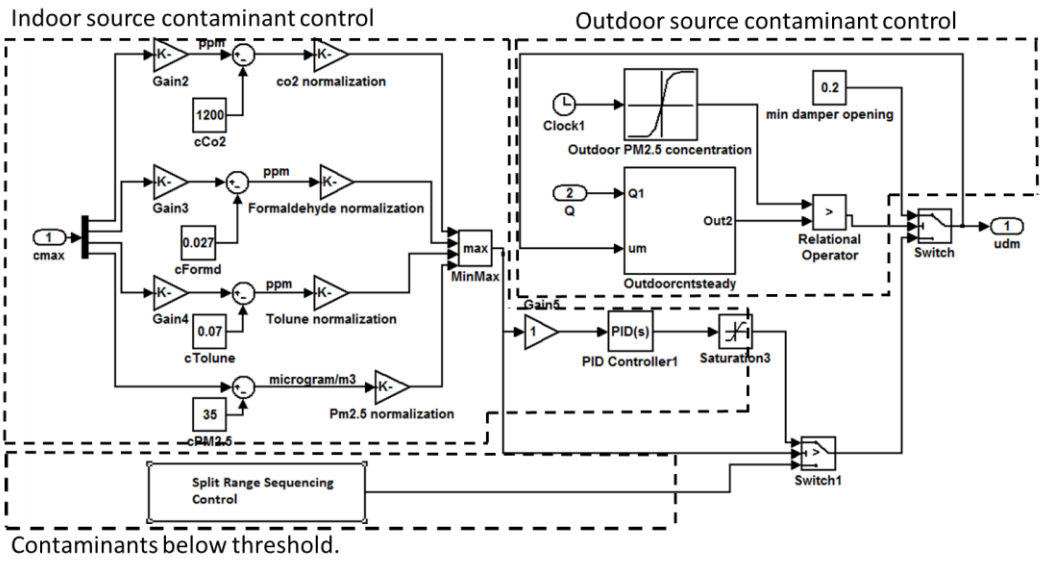

Figure 62. Implementation of the proposed control in simulink

6.6 Results and Discussion

The performance of the proposed control strategy is checked taking two different base cases and the results are discussed below

CASE I

Minimum outdoor ventilation rate based on ASHARE62.1 requirement is used as a baseline for comparison in case I. According to the procedure recommended by the standard, the minimum outdoor ventilation rate for the case building is found to be 40% of the minimum total primary air required by the building VAV system. The percentage energy savings obtained from the proposed ventilation strategy for the four selected cities are given in Table 14.

For Syracuse, Huston and Fairbanks, the proposed control strategy results in a considerable energy saving besides maintaining the required IAQ. It is also observed that there is a slight increment in energy consumption for Los Angeles. This is because of the fact that the outdoor air temperature condition in Los Angles is

favorable for free cooling(Economizer cycle) and the proposed control strategy limit the use of outdoor air when its contaminant concentration has a capacity to exceed the allowable indoor concentration level. As can be seen in Figure 63the outdoor PM2.5 concentration level is above the permissible indoor PM2.5 level, i.e. 35µg/m^3, and the proposed control strategy forced the system to use minimum outdoor air instead of free cooling and this resulted in increased energy consumption.

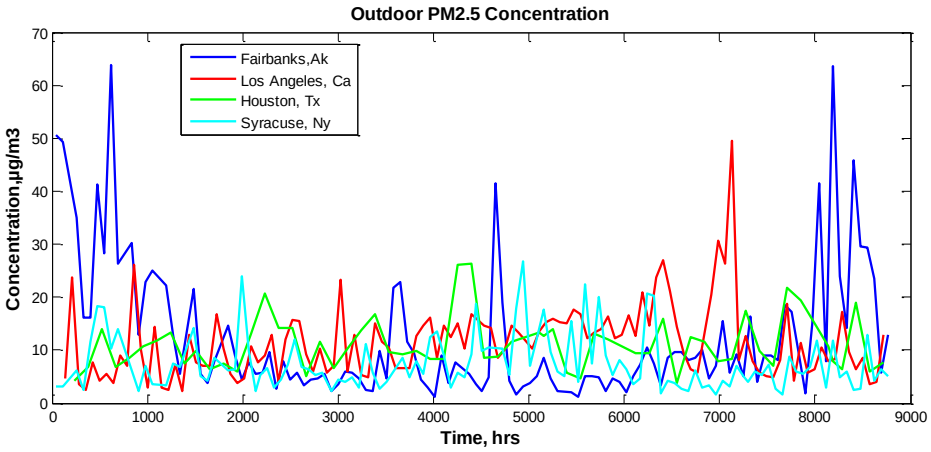

Figure 63. Annual PM2.5 outdoooor air PM2.5 concentration

CASE II

Case II use minimum outdoor air ventilation rate based on LEED requirement as a baseline ventilation. LEED require 30% more ventilation than ASHRAE 62.1. Based on LEED standard the minimum outdoor ventilation required for the case building is 50% of the minimum primary air required by the VAV system.

To compensate for the energy consumption due to increased ventilation rate, heat recovery system is added in the simulation model. The comparison of the annual energy saving of the proposed control strategy against the baseline ventilation is given in Table 14.

In general, compared to case I, the energy saving obtained by the proposed control strategy for case II is less. This is because of the fact that the presence of heat recovery saves a considerable energy that would be required for heating especially for cities with strong winter conditions like Syracuse and Fairbanks. A relatively higher saving is obtained for Huston because of its relatively strong summer condition compared to the other cities.

Table 14. Summary of energy saving from proposed strategy compared to baseline cases

Case 1: Baseline Ventilation based on ASHRAE 62.1				
	Syracuse,NY	Houston,TX	Los Angeles,CA	Fairbanks,AK
% Energy saving	8	47	-0.03	23
Case 2: Baseline Ventilation based on LEED				
% Energy saving	0.83	17	0.03	-0.018

The simulation result also shows that besides energy saving, indoor air concentrations of all the contaminants were in their permissible range for the entire simulation period of 1 year for both cases. To clearly show the profiles of contaminants, a sample of the case I simulation results for the first five days of January for Fairbanks, AK weather is shown in Figure 64 and Figure 65. Since outdoor temperature was low during the simulation period, the outdoor damper was kept at its minimum for the baseline, Figure 64, and concentration levels for Formaldehyde and Toluene remained constant due to the fact that air flow rate was constant. For the proposed strategy, Figure 65, profiles of Formaldehyde and Toluene depended on the amount of outdoor air admitted which varied throughout the simulation period depending on how the DCV changed the damper position. CO_2 level increased during occupied hours and was in its permissible limit in both cases.

It should be noted that the savings obtained could be reduced if the outdoor air quality is bad because of the fact that the strategy gives priority for IAQ. To demonstrate

this, the same building was simulated for reduced filter efficiency of 10% from 60% for Fairbanks weather (2010) where there was a big variation in outdoor PM2.5 concentration. The result is shown in Figure 66**.** It is evident from the figure that the outdoor air had its picks in mid-summer and early winter. During these times, indoor concentration was observed to be above permissible indoor concentration of 35 $\mu g/m^3$ for the baseline case since it did not have a means to adjust the ventilation rate based on outdoor concentration. But the proposed control strategy was able to maintain the permissible value all the time by limiting the inflow of outdoor air based on the quality of outdoor air. As a result the saving was reduced to 16% from its original value of 23% shown in case I.

To quantify the additional energy consumption resulted from consideration of multiple contaminants, the proposed control strategy is compared with a CO_2 based DCV. The result shows that there is insignificant difference (0.0001% in average) between the two with the proposed strategy using relatively more energy. This is because of the fact that assumed indoor generation rates for Formaldehyde and Toluene based on results from EPA BASE study(EPA_BASE 2006) are below the allowable indoor concentration limits and the ventilation rate is almost governed by CO_2 except at times where the outdoor PM2.5 concentration is high. This is a good indication that the proposed control strategy is as good as conventional DCV systems in terms of energy saving with superior performance in terms of maintaining IAQ.

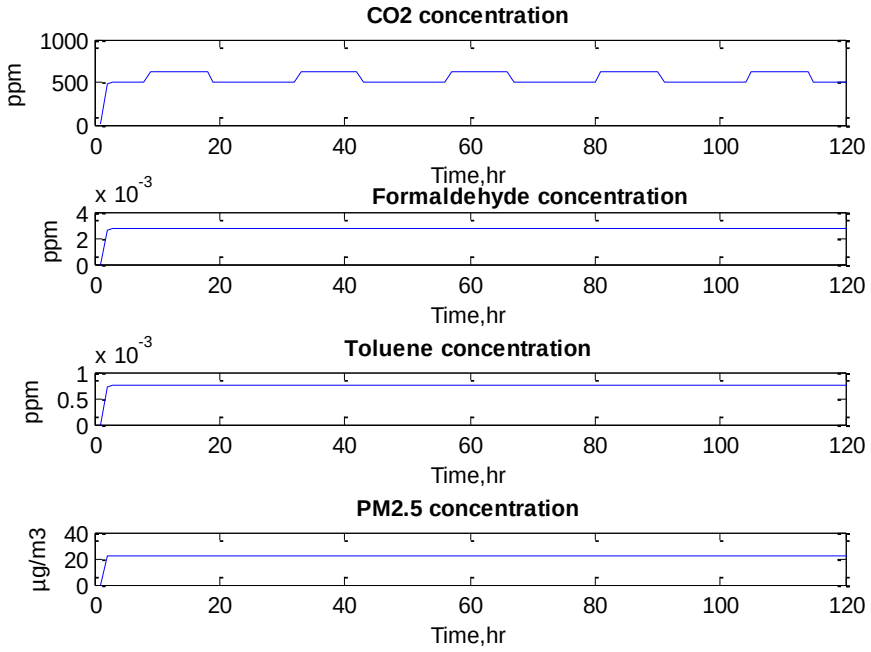

Figure 64 . Contaminant concentrations for five days in January for Fairbanks: baseline

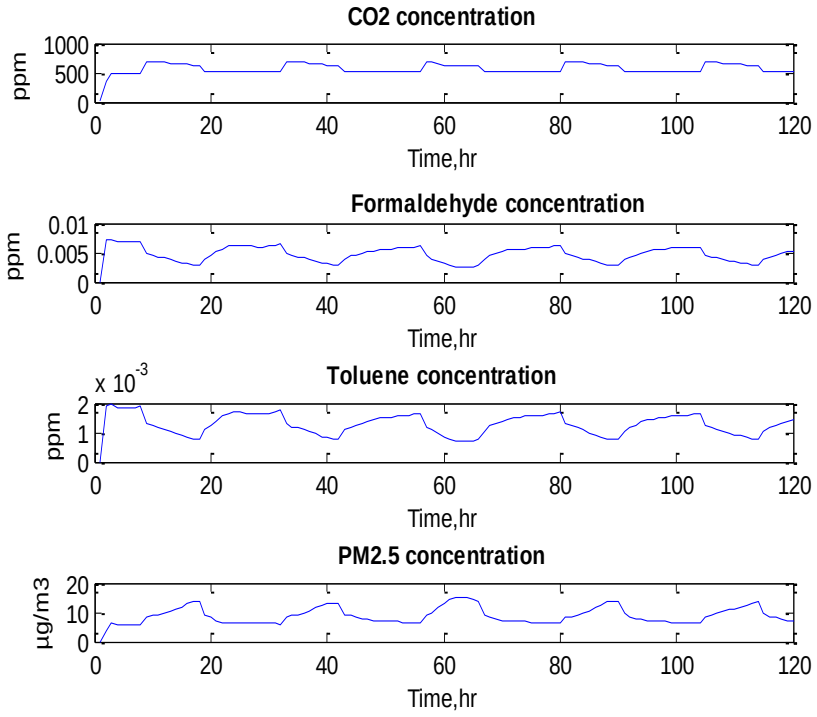

Figure 65 . Contaminant concentrations for five days in January for Fairbanks: proposed method

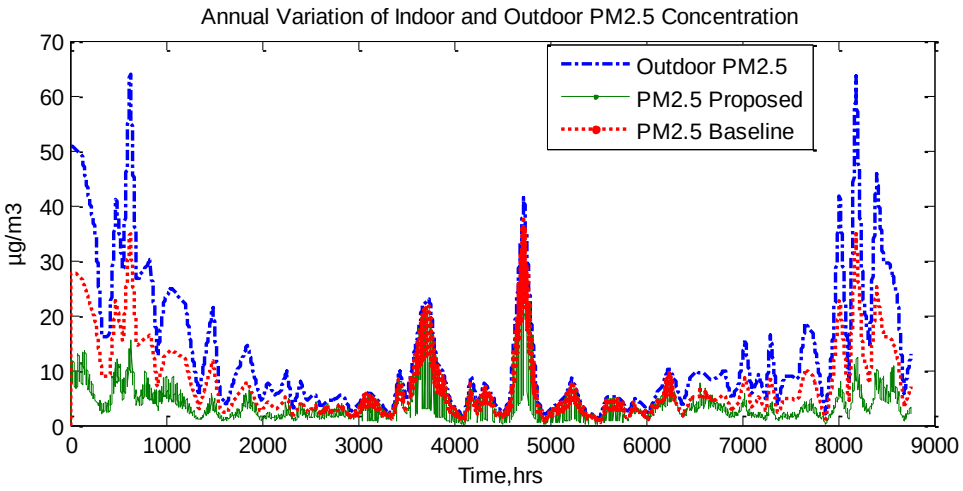

Figure 66. Annual variations of indoor and outdoor PM2.5 concentration

6.7 Conclusions

In summary, the proposed control approach gives extra advantage of checking concentration of multiple indoor air contaminants and adjusting the outdoor air ventilations accordingly. So far only demand based control strategy based on CO2 is implemented in building ventilation control and depending on the building purpose and application, this strategy could result bad result where there are other dominating indoor contaminants and in that case the proposed control strategy could result a better IAQ.

In addition to the IAQ control, the energy saving potential of this approach was compared with ventilation strategies with no DCV capabilities that use minimum outdoor air ventilation rate based on ASHRAE 62.1 recommendation and LEED requirement which suggest 30% more ventilation rate with addition of heat recovery system. The result indicates that the possible energy saving depends on the geographical location of the building.

One major concern related to the proposed approach is the availability of reliable sensors and associated costs related to sensors and system upgrade. With sensor costs getting cheaper over time, it is probable that it can be applied to buildings system in the near future. At this point in time, the proposed approach can be a good candidate for facilities that are very sensitive to pollutants like hospitals and other high tech research facilities

7 CONCLUSION AND DISCUSSION

In US alone buildings consume 41% of the total primary energy and out of which the energy needed for heating, ventilation, air conditioning and lighting take the big portion. Recently more and more buildings are starting to deploy building management system (BMS) to ease the process of performance monitoring and analysis. This also makes it easy to develop and deploy advanced control strategies that can improve energy efficiency as well as Indoor Environmental Quality (IEQ) of the building.

This dissertation develops and demonstrates the methods and approaches to implement a model - based advanced control system called Model Predictive Control (MPC) in a real building. Previous related works were mainly focused on concept proofing instead of real application in a full scale building. In this research, application of MPC for a real building was investigated. Major findings include:

1) MPC controller involves the development of component models and definition of an objective function based on which optimized control inputs are determined. During the development of the MPC controller, simplified but sufficiently accurate component models were developed and used. In addition, methods were developed to simplify the building model so that the computation time and related development effort can be reduced. Detailed models from the EnergyPlus software were used to verify the approaches used and the results indicated comparable accuracy of the simplified model as compared to the detailed models.
2) A detailed framework for implementation of MPC in a full scale building is developed. Each of the component models as well as the MPC controller were developed in Matlab environment and co-simulation strategy was used to integrate

the controller with the detailed building model which is developed in EnergyPlus. The co-simulation tool used is MLE+ tool and it has a capacity to talk to Building Management Systems (BMS) that support BACnet communication protocol. Thus the developed MPC controller can talk to actual building controllers using BACnet.

3) Some of the component models involved in the MPC controller in this study were nonlinear and local optimization techniques instead of global optimizers were used to minimize the computation time needed. Rule based approaches were implemented to assign initial values for the control inputs to avoid unacceptable local optimum points.
4) The performances of the MPC controller for various thermal comfort and ventilation strategies were investigated. The cases investigated included MPC for temperature based comfort control, MPC for PMV based control, MPC with integrated window blind and lighting control for comfort control based on temperature and PMV. In all the cases its performance was compared with baseline control system using Proportional, Integrator and Derivative (PID) controller. All the comparison results indicated that considerable energy could be saved by applying MPC to a building system. Energy saving as high as 48% was possible using the MPC with integrated window blind and lighting control. In addition to energy saving, the MPC controllers also showed superior performance in terms of maintaining zone comfort.
5) A new critical contaminant based demand control ventilation strategy was also proposed and its performance was compared to conventional ventilation strategies based on ASHRAE 62.1 and LEED. The result indicated superior performance in terms of maintaining the required indoor air quality year round. The strategy is

specifically useful for buildings exposed to strong outdoor or indoor contaminant sources. The currently available demand controlled ventilation strategy only considers CO2 concentration to modulate the minimum outside air ventilation and it can result in poor air quality where there are other contaminants with strong indoor or outdoor sources.

To facilitate the process of implementation of the MPC in different types of buildings, the following topics are recommended for research.

1) One of the big challenges in the application of MPC in real building is developing component models and the related development effort. To minimize this, a library of commonly available HVAC and building component models is required. This research was mainly focused on dedicated outdoor air system with ceiling radiant panels.Component models for other HVAC systems need to be developed. In line with this Lawrence Berkeley National Laboratory (LBNL) has already started building component models using MODELICA software platform. Using library of models can minimize the development effort considerably.
2) In this research, the MPC was focused on the air handling unit side and radiant ceiling panels. More energy can be saved if the plant loops are included in the MPC. As an extension of this research, it is worth considering MPC including the heat pump and boiler loops.
3) In this dissertation, the radiant mean temperature was assumed to be the same as the zone temperature. This assumption is proved to be applicable in most buildings (Walikewitz et al. 2015). But the effect of this assumption on the overall thermal comfort (PMV) should be further studied for building systems that use radiant ceiling panel for heating and cooling. The fact that most

ceiling radiant panels have considerable area with an elevated temperature during winter and relatively lower temperature during summer may affect the room PMV considerably.

4) We were not able to check the developed MPC controller in the case building since it was an occupied building and the MPC was only checked and simulated using detailed model of the building using EnergyPlus. In the future, it is worth checking the developed method using a test building with BACnet capability.

5) The proposed critical contaminant based demand control ventilation strategy used Proportional Integral and Derivative (PID) control. The MPC version of this IAQ control strategy can be developed in the future to further improve its energy efficiency.

REFERENCES

Anthony, Kelman, and Borrelli Francesco. 2011. "Bilinear Model Predictive Control of HVAC System Using Sequential Quadratic Programming." *18th IFAC World Congress*, 9869–74. Milano, Italy: International Federation of Automatic Control (IFAC).

Antoulas, A.C, and D.C Sorensen. 2001. "Approxmiation of Large_scale Dynamical Systems: An Overview." *International Journal of Applied Mathematics and Computer Science* 11 No 5: 1093–1121.

ASHRAE. 2009. *ASHRAE handbook:Fundamentals*. Atlanta, Ga.: American Society of Heating, Refrigerating and Air-Conditioning Engineers. http://www.knovel.com/web/portal/browse/display?_EXT_KNOVEL_DISPLAY_bookid=2554.

ASHRAE. 2012. *ASHRAE Handbook: Fundamental - Panel Heating and Cooling*. ASHRAE Handbook: HVAC Systems and Equipment. Atlanta, GA: American Society of Heating Refrigration and Air conditioning Engineers.

ASHRAE Standard 55-2013. 2013. *Thermal Environment Condition For Human Occupancy*. Atlanta, GA: American Society of Heating Refrigration and Air conditioning Engineers.

ASHRAE Standard 62.1. 2007. *Ventilation for Acceptable Indoor Air Quality*. Atlanta, GA: American Society of Heating, Refrigerating and Air-Conditioning Engineers.

Athienitis, A. K., and A. Tzempelikos. 2002. "A Methodology for Simulation of Daylight Room Illuminance Distribution and Light Dimming for a Room with a Controlled Shading Device." *Solar Energy* 72 (4): 271–81.

Biao Sun, P. B. Luh, Qing-Shan Jia, Ziyan Jiang, Fulin Wang, and Chen Song. 2013. "Building Energy Management: Integrated Control of Active and Passive Heating, Cooling, Lighting, Shading, and Ventilation Systems." *IEEE Transactions on Automation Science and Engineering* 10 (3): 588–602. doi:10.1109/TASE.2012.2205567.

Camacho, E.F, and C Bordons. 2003. *Model Pridictive Control*. London: Springer-Verlag.

Carols E., Garcia, Prett David M., and Morari Manfred. 1989. "Model Predictive Control: Theory and Practice -a Survey." *International Federation of Automatic Control*.

Casas, W., and G. Schmitz. 2005. "Experiences with a Gas Driven, Desiccant Assisted Air Conditioning System with Geothermal Energy for an Office Building." *Energy and Buildings* 37 (5): 493–501. doi:10.1016/j.enbuild.2004.09.011.

Cassola, Federico, and Massimiliano Burlando. 2012. "Wind Speed and Wind Energy Forecast through Kalman Filtering of Numerical Weather Prediction Model Output." *Applied Energy* 99 (November): 154–66. doi:10.1016/j.apenergy.2012.03.054.

Chandan, Vikas. 2010. "Modeling and Control of Hydronic Building HVAC Systems." University of Illinois. http://www.ideals.illinois.edu/handle/2142/16204.

Chen, T. Y. 2002. "Application of Adaptive Predictive Control to a Floor Heating System with a Large Thermal Lag." *Energy and Buildings* 34 (1): 45–51.

Chow, T. T., G. Q. Zhang, Z. Lin, and C. L. Song. 2002. "Global Optimization of Absorption Chiller System by Genetic Algorithm and Neural Network." *Energy and Buildings* 34 (1): 103–9.
CIE 85. 1989. "Technical Report: Solar Spectral Irradiance." Comissioin Internationale de l'Eclairage. http://www.a1pdf.com/cie-0851989-p-314197.html.
Claridge, D. E., and B. Abushakra. 2001. "Accounting for the Occupancy Variable in Inverse Building Energy Baselining Models." In *Proceedings of the International Conference for Enhanced Building Operations (ICEBO)*. http://repository.tamu.edu/handle/1969.1/5161.
Coblenz, C.W, and P.R Achenbach. 1963. "Field Measurment of Ten Electrically - Heated Houses." *ASHRAE Transactions*, 358–65.
COMNET. 2010. *Commercial Building Energy Modeling Guidelines and Procedures*. Commerical Energy Services Network.
Conroy, Christopher, and Mumma Stanley. 2001. "Ceiling Radiant Cooling Panel as a Viable Distributed Parallel Sensible Cooling Technology Integerated with Dedicated Outdoor Air Systems." *ASHRAE Transactions* 107.
Deng, Kun, Prabir Barooah, Prashant G. Mehta, and Sean P. Meyn. 2010. "Building Thermal Model Reduction via Aggregation of States." In *American Control Conference (ACC), 2010*, 5118–23. http://ieeexplore.ieee.org/xpls/abs_all.jsp?arnumber=5530470.
Deru, Michael, Kristin Field, Daniel Studer, Kyle Benne, Brent Griffith, Paul Torcellini, Bing Liu, Mark Halverson, Dave Winiarski, and Michael Rosenberg. 2011. "US Department of Energy Commercial Reference Building Models of the National Building Stock." http://digitalscholarship.unlv.edu/renew_pubs/44/?utm_source=digitalscholarship.unlv.edu%2Frenew_pubs%2F44&utm_medium=PDF&utm_campaign=PDFCoverPages.
Dong, Ming, Dong Yang, Yan Kuang, David He, Serap Erdal, and Donna Kenski. 2009. "PM2.5 Concentration Prediction Using Hidden Semi-Markov Model-Based Times Series Data Mining." *Expert Systems with Applications* 36 (5): 9046–55. doi:10.1016/j.eswa.2008.12.017.
D.Q.Mayne. 2001. "Control of Constrained Dynamic Systems." *European Journal of Control* 7 (2-3).
Emmerich, S.J., J.W. Mitchell, and W.A. Beckman. 1994. "Demand-Controlled Ventilation in a Multi-Zone Office Building." *Indoor and Built Environment* 3 (6): 331–40. doi:10.1177/1420326X9400300607.
EnergyPlus. 2011. "Getting Started with EnergyPlus." DOE.
EnergyPlus. 2012. "EnergyPlus Engineering Reference." US department of Energy(DOE).
EPA_BASE. 2006. "U.S. Environmental Protection Agency Building Survey and Evaluatoin (BASE) Study Volatile Organic Compound Data Workbook." US Environmental Protection Agency.
Erickson, Varick L., Miguel Á Carreira-Perpiñán, and Alberto E. Cerpa. 2011. "OBSERVE: Occupancy-Based System for Efficient Reduction of HVAC Energy." In *Information Processing in Sensor Networks (IPSN), 2011 10th International Conference on*, 258–69. IEEE. http://ieeexplore.ieee.org/xpls/abs_all.jsp?arnumber=5779043.
Fanger, P.O. 1973. *Thermal Comfort*. New York: McGraw_Hill Book Company.

Fisk, William J. 2002. "How IEQ Affects Health, Productivity." *ASHRAE Journal-American Society of Heating Refrigerating and Airconditioning Engineers* 44 (5): 56–60.
Frauke, Oldewurtel. 2011. "Stochastic Model Predictive Control for Energy Efficient Building Climate Control." Germany: ETH Zurich.
Freire, Roberto Z., Gustavo H.C. Oliveira, and Nathan Mendes. 2008. "Predictive Controllers for Thermal Comfort Optimization and Energy Savings." *Energy and Buildings* 40 (7): 1353–65. doi:10.1016/j.enbuild.2007.12.007.
Frontczak, Monika, and Pawel Wargocki. 2011. "Literature Survey on How Different Factors Influence Human Comfort in Indoor Environments." *Building and Environment* 46 (4): 922–37. doi:10.1016/j.buildenv.2010.10.021.
Ge, Gaoming, Fu Xiao, and Xinhua Xu. 2011. "Model-Based Optimal Control of a Dedicated Outdoor Air-Chilled Ceiling System Using Liquid Desiccant and Membrane-Based Total Heat Recovery." *Applied Energy* 88 (11): 4180–90. doi:10.1016/j.apenergy.2011.04.045.
Goswami, D. 1986. "VAV Fan Static Pressure Control with DDC." *Heating, Piping and Air Conditioning* 58(12): 113–17.
Gouda, M.M, S Danaher, and C.P Underwood. 2002. "Builidng Thermal Model Reduction Using Nonlinear Constrained Optimization." *Builiding and Environment* 37: 1255–65.
Gowri, Krishnan, David W. Winiarski, and Ronald E. Jarnagin. 2009. *Infiltration Modeling Guidelines for Commercial Building Energy Analysis*. Pacific Northwest National Laboratory USA. http://ibpsa-boston.com/minutes/IBPSAboston-presentations_2011-09-16_Gowri.pdf.
Gruber, Peter, Markus Gwerder, and Jürg Tödtli. 2001. "Predictive Control for Heating Applications." In *CLIMA 2000 World Congress, Nápoles, Setembro*, 15–18. http://www.sysecol2.ethz.ch/OptiControl/Lit/Grub_01_Proc-ClimaNapoli2001_ID469.pdf.
Henderson, David E., Jana B. Milford, and Shelly L. Miller. 2005. "Prescribed Burns and Wildfires in Colorado: Impacts of Mitigation Measures on Indoor Air Particulate Matter." *Journal of the Air & Waste Management Association* 55 (10): 1516–26.
IDAE. 2009. *Acceptance Conditions of Alternative Procedures to LIDER and CALENER*. Spain: Institute of Diversification and saving of Energy.
ISO 7730. 2005. "Moderate Thermal Environments--Determination of the PMV and PPD Indices and Specification of the Conditions for Thermal Comfort."
ISO 15099:2003. n.d. *Thermal Performance of Windows, Doors and Shading Devices- Detailed*.
Jeong, Jae-Weon, and Stanley A Mumma. 2004a. "Simplified Cooling Capacity Estimation Model for Top Insulated Metal Ceiling Radiant Cooling Panels." *Applied Thermal Engineering* 24 (14-15): 2055–72. doi:10.1016/j.applthermaleng.2004.01.017.
Jeong, Jae-Weon, and Stanley A Mumma. 2004b. "Simplified Cooling Capacity Estimation Model for Top Insulated Metal Ceiling Radiant Cooling Panels." *Applied Thermal Engineering* 24 (14-15): 2055–72. doi:10.1016/j.applthermaleng.2004.01.017.

Jonathan, Currie, and I. Wilson David. 2012. *OPTI: Lowering the Barrier Between Open Source Optimizers and the Industrial MATLAB User*.
Josephine, Lau, and Xingbin Lin. 2011. "Simulation Based Ventilation of Two CO2- Based Demand Control Ventilation Control Logic for Multiple_zone VAV System." University of Nebraska -Lincoln.
Katipamula, Srinivas, and Michael R. Brambley. 2005. "Review Article: Methods for Fault Detection, Diagnostics, and Prognostics for Building Systems—A Review, Part I." *HVAC&R Research* 11 (1): 3–25.
Klepeis, Neil E., Andy M. Tsang, and Joseph V. Behar. 1996. "Analysis of the National Human Activity Pattern Survey (NHAPS) Respondents from a Standpoint of Exposure Assessment." *Final Rpt EPA*. http://exposurescience.org/pub/reports/NHAPS_Report1.pdf.
Lai, Joseph H.K., and Francis W.H. Yik. 2009. "Perception of Importance and Performance of the Indoor Environmental Quality of High-Rise Residential Buildings." *Building and Environment* 44 (2): 352–60. doi:10.1016/j.buildenv.2008.03.013.
LaVerne, W.Salhoff, and Gregory D.Salhoff. 1998. Window Shade System with Multiple , Sequentially Connected Window Shading Elements. United states Patent 5735328, filed 1996 1996, and issued 1998.
Lu, Jiakang, Tamim Sookoor, Vijay Srinivasan, Ge Gao, Brian Holben, John Stankovic, Eric Field, and Kamin Whitehouse. 2010. "The Smart Thermostat: Using Occupancy Sensors to Save Energy in Homes." In *Proceedings of the 8th ACM Conference on Embedded Networked Sensor Systems*, 211–24. ACM. http://dl.acm.org/citation.cfm?id=1870005.
Mahdavi, Ardeshir. 2008. "Predictive Simulation-Based Lighting and Shading Systems Control in Buildings." *Building Simulation* 1 (1): 25–35. doi:10.1007/s12273-008-8101-4.
McQuiston, F.C, J.D Parker, and J.D Spittler. 2000. *Heating, Ventilating and Air Condiioning Analysis and Design, Fifth Edition*. New York: John Wiley.
Moore, Brian J, and D. Scott Fisher. 2003. "Pump Differential Pressure Setpoint Reset Based on Chilled Water Valve Posistion." *ASHRAE Transactions* 109(1): 373–79.
Mukherjee, Satyen, Dagnachew Birru, Dave Cavalcanti, Eric Shen, Maulin Patel, Yao-Jung Wen, and Sushanta Das. 2010. "Closed Loop Integrated Lighting and Daylighting Control for Low Energy Buildings." *Proceedings of the 2010 ACEEE*, 252–69.
Murdoch, J.B. 1985. *Illumination Engineering-From Edison's Lamp to the Laser*. New York: Macmillan Publishing Inc.
Nassif, N. 2011. "CO2-Based Demand-Controlled Ventilation Control Strategies for Multi-Zone HVAC Systems." http://repository.tamu.edu/handle/1969.1/128800.
Nassif, Nabil, Stanislaw Kajl, and Robert Sabourin. 2005. "Simplified Model-Based Optimal Control of VAV Air-Conditioning System." In *Proceedings of the 9th IBPSA Conference (International Building Performance Simulation Association), August*, 15–18. http://www.ibpsa.org/proceedings/BS2005/BS05_0823_830.pdf.
Nghiem, Truong X., and George J. Pappas. 2011. "Receding-Horizon Supervisory Control of Green Buildings." In *American Control Conference (ACC), 2011*,

4416–21. http://ieeexplore.ieee.org/xpls/abs_all.jsp?arnumber=5990995.
Pang, Xiufeng, Prajesh Bhattacharya, Zheng O'Neill, Philip Haves, Michael Wetter, and Trevor Bailey. 2011. "Real-Time Building Energy Simulation Using EnergyPlus and the Building Controls Virtual Test Bed." *Proc. Building Simulation'11*. http://buildings.lbl.gov/sites/all/files/2011-ibpsa-bcvtb-ePlus.pdf.
Reinhart, Christoph F. 2004. "Lightswitch-2002: A Model for Manual and Automated Control of Electric Lighting and Blinds." *Solar Energy* 77 (1): 15–28. doi:10.1016/j.solener.2004.04.003.
Richalet, J., A. Rault, J. L. Testud, and J. Papon. 1978. "Model Predictive Heuristic Control: Applications to Industrial Processes." *Automatica* 14 (5): 413–28.
Rishel, J.B. 2003. "Control of Variable Speed Pumps for HVAC Water Systems." *ASHRAE Transactions* 109: 380–89.
Shih, Shou Hsing, and Chris P. Tsokos. 2008. "Prediction Models for Carbon Dioxide Emissions and the Atmosphere." *Neural, Parallel and Scientific Computations* 16 (1): 165.
Simmler, H, U Fischer, and F Winkelmann. 1996. "Solar_Thermal Window Blind Model for DOE-2." Lowerence Berkeley National laboratory.
Široký, Jan, Frauke Oldewurtel, Jiří Cigler, and Samuel Prívara. 2011. "Experimental Analysis of Model Predictive Control for an Energy Efficient Building Heating System." *Applied Energy* 88 (9): 3079–87. doi:10.1016/j.apenergy.2011.03.009.
Spittler, Jeffery D, Daniel E Fisher, and Curties O Pedersen. 1997. "The Radiant Time Series Cooling Load Calculation Procedure." *ASHRAE Transactions* vol 103 part 2.
Tzempelikos, Athanassios, and Andreas K. Athienitis. 2007. "The Impact of Shading Design and Control on Building Cooling and Lighting Demand." *Solar Energy* 81 (3): 369–82. doi:10.1016/j.solener.2006.06.015.
USDOE. 2011. *Building Energy Data Book*. Washington DC.
Van Konynenburg, Peter, Stephen Marsland, and James McCoy. 1989. "Solar Radiation Control Using NCAP Liquid Crystal Technology." *Solar Energy Materials* 19 (1): 27–41.
Walikewitz, Nadine, Britta Jänicke, Marcel Langner, Fred Meier, and Wilfried Endlicher. 2015. "The Difference between the Mean Radiant Temperature and the Air Temperature within Indoor Environments: A Case Study during Summer Conditions." *Building and Environment* 84 (January): 151–61. doi:10.1016/j.buildenv.2014.11.004.
Walton, G.N. 1983. *Thermal Analysis Research Program Reference Manual*. NBSSIR83-2655. National Bureau of standards(NIST).
Wang, Shengwei, and Xinqiao Jin. 2000. "Model-Based Optimal Control of VAV Air-Conditioning System Using Genetic Algorithm." *Building and Environment* 35 (6): 471–87.
Wang, Shengwei, and Xinhua Xu. 2002. "A Robust Control Strategy for Combining DCV Control with Economizer Control." *Energy Conversion and Management* 43 (18): 2569–88.
Wang, Yao-Wen, Wen-Jian Cai, Yeng-Chai Soh, Shu-Jiang Li, Lu Lu, and Lihua Xie. 2004. "A Simplified Modeling of Cooling Coils for Control and

Optimization of HVAC Systems." *Energy Conversion and Management* 45 (18-19): 2915–30. doi:10.1016/j.enconman.2003.12.024.
Wargocki, Pawel, David P. Wyon, and P. Ole Fanger. 2000. "Productivity Is Affected by the Air Quality in Offices." In *Proceedings of Healthy Buildings*, 1:635–40. http://senseair.se/wp-content/uploads/2011/05/1.pdf.
Westphalen, Detlef, and Scott Koszalinski. 1999. "Energy Consumption Characteristics of Commercial Building HVAC Systems. Volume II: Thermal Distribution, Auxiliary Equipment, and Ventilation." *Arthur D. Little Inc (ADLI)* 20: 33745–00.
Wetter, Michael. 2012. *Building Controld Virtual Test Bed User Manual*. Berkeley, CA: Lawrence Berkley National Laboratory.
Wilcox, Stephen, and William Marion. 2008. *Users Manual for TMY3 Data Sets*. National Renewable Energy Laboratory Golden, CO. http://www.nrel.gov/docs/fy08osti/43156.Pdf.
Willy, Bernal, Behl Madhur, X. Ngheim Troung, and Mangharam Rahul. 2012. "MLE+: A Tool for Integerated Design and Deployment of Energy Efficient Building Controls." In *$th ACM Workshop on Embeded Sensing Systems for Energy Efficiency in Buildings*. Toronto , Canada: Building Sys.
Wong, L.T., K.W. Mui, and P.S. Hui. 2008. "A Multivariate-Logistic Model for Acceptance of Indoor Environmental Quality (IEQ) in Offices." *Building and Environment* 43 (1): 1–6. doi:10.1016/j.buildenv.2007.01.001.
Yahiaoui, A., J. Hensen, L. Soethout, and D. van Paassen. 2006. "MODEL BASED OPTIMAL CONTROL FOR INTEGRATED BUILDING SYSTEMS." http://www.bwk.tue.nl/bps/Hensen/publications/06_iprc_yahiaoui.pdf.
Yuan, Shui, and Ronald Perez. 2006. "Multiple-Zone Ventilation and Temperature Control of a Single-Duct VAV System Using Model Predictive Strategy." *Energy and Buildings* 38 (10): 1248–61. doi:10.1016/j.enbuild.2006.03.007.
Yu, Yuebin. 2012. "MODEL-BASED MULTIVARIATE CONTROL OF CONDITIONING SYSTEMS FOR OFFICE BUILDINGS." Carnegie Mellon University.
Zimmermann, Gerhard, Yan Lu, and George Lo. 2011. "A SIMULATION BASED FAULT DIAGNOSIS STRATEGY USING EXTENDED HEAT FLOW MODELS (HFM) 2." In *Proceedings of Building Simulation 2011: 12th Conference of International Building Performance Simulation Association, Sydney*, 14–16. https://www.ibpsa.org/proceedings/BS2011/P_1231.pdf.

Vita

Name: Korbaga Fantu Woldekdian

Place of Birth: Wolkite, Ethiopia

Education:

Name and Location	Dates	Degree
Addis Ababa University, Addis Ababa, Ethiopia	2002-2004	M.Sc.(Mechanical Eng'g)
Bahirdar University, Addis Ababa, Ethiopia	1997-2001	B.Sc. (Mechanical Eng'g)

Employment:

Name and Location	Dates	Job Title
U&S Services Inc., Tonawanda, NY	2014-2015	HVAC Analyst
CDH Energy, Syracuse, NY	2013-2014	Project Engineer
Syracuse University, Syracuse, NY	2010-2013	Teaching Assistant
Addis Ababa University, Addis Ababa, Ethiopia	2007-2009	Lecturer
Bahir Dar University, Bahirdar, Ethiopia	2001-2006	Lecturer